

# New analytical methodologies in the study of auxin biochemistry

A Dissertation  
SUBMITTED TO THE FACULTY OF  
UNIVERSITY OF MINNESOTA  
BY

**Peng Yu**

IN PARTIAL FULFILLMENT OF THE REQUIREMENTS  
FOR THE DEGREE OF  
DOCTOR OF PHILOSOPHY

**Advisor: Jerry D. Cohen**

August, 2014

© Peng Yu 2014

## Acknowledgements

First of all, I would like to thank my advisor Dr. Jerry Cohen for his exceptional mentorship during my graduate studies. Jerry is not only the advisor in my scientific career, but also a good friend in life. I enjoyed a lot of academic freedom thanks to Jerry's trust and open mind and I had the fortune to collect eleven visas to attend conferences worldwide, which was invaluable in the growth of a young scientist. I'll always remember the times when I fiddled with pushrods and intake gasket on my car in Jerry's shop, as well as times when I took HPLC pumps and mass specs apart. I am also very grateful for the countless hours Jerry spent on revising my fellowship application, papers, and this thesis. Graduate school was definitely among the most fruitful and enjoyable times in my life so far.

Next, I would also like to thank members of my advisory committee Drs. William Gray, Adrian Hegeman, Igor Libourel, and Min Ni for their guidance and encouragement along the way. The suggestions early on in my graduate studies all proved useful later on, and the discussions during my committee meeting and individual meetings all played instrumental role in shaping my career.

I wish to extend my special thanks to Prof. Min Ni, for recruiting me into the Plant Biological Sciences graduate program. I would like to express my gratitude to the PBS program, administrative staff of the program and the Department of Plant Biology, especially our program coordinator Gail Kalli. Gail once said: "My job is to hold your hand, and make your graduate studies a success." That was five years ago, but felt like yesterday. During the past years, Directors of Graduate Studies Jane Glazebrook, Gary Muehlbauer, George Weiblen, and Cindy Tong have helped me many times at different stages.

The Department of Horticultural Science has hosted my graduate studies, during which time I had the pleasure to work with numerous outstanding scientists and staff members. Drs. Wen-Ping Chen, Xiaoyuan Yang, Xing Liu, Lana Barkawi, Paul Boswell, Mikel Roe, and Mr. Doug Brinkman provided me a lot of help with great patience, as I stumbled into a completely different field of study in a foreign language. Members of the

Cohen/Gardner/Hegeman/Boswell group were also outstanding colleagues and dear friends. In particular, I wish to acknowledge Paula Lor, an undergraduate scientist who contributed a lot of work for this dissertation, and Drs. Alison Pawlus, Dana Freund, and Nathan Tivendale for their expertise and help. The departmental staff have also provided professional administrative support throughout my career.

I shall also express my great gratitude towards Ms Jing Chen, Dr. He Huang and the Hospitality Center for Chinese who helped me settle down in Minnesota when I first came. Their kindness shall be remembered. My life in Minnesota was also accompanied with the great friendships of Mufan Guo, You Lü, Lian Lian, He Huang, Meihua Yu, Mike Wilson, Jonathan Fankhauser, Jason Kaasovic, Sam Young, Jeff Harrison, Scott Parkin, Michael Fusaro, to name just a few.

I had the great pleasure to visit Prof. Dr. Jutta Ludwig-Müller's lab at Technische Universität Dresden in the summer of 2012. Jutta and Antje Walter were very helpful and shared the research progress and vision with me. I have also attended the Proteomics Workshop organized by the Center for Mass Spectrometry and Proteomics at the University of Minnesota, and the Plant Proteomics Workshop organized by Drs. Michael Sussman, Joshua Coon, and Jean-Michel Ané, which introduced and re-introduced me to the field of mass spectrometry and proteomics.

I was also part of the Multi-Functional Agriculture and Food System fellowship program, co-sponsored by the University of Minnesota, USDA and the Monsanto Company. Drs. Donald Wyse, Nicholas Jordan, and Brett Bussler played instrumental role in setting up such a great cross-sector collaborative program. It was a great learning environment in this program and we took quite a few trips to the Monsanto Company. We were warmly welcomed and exchanged ideas on how to shape our agricultural and food systems and the landscape.

Drs. Changbin Chen and Seth Naeve provided the tomatoes and soybeans used in my studies, respectively.

My graduate funding was provided by the Department of Plant Biology, the Monsanto Fellowship, the PBS summer fellowships, and National Science Foundation (IOS 1238812). My graduate research was funded by the National Science Foundation

(IOS 0820940, 0606666, 0923960, 1238812), Minnesota Agricultural Experiment Station, and the Gordon and Margaret Bailey Endowment for Environmental Horticulture. The PBS graduate program and Microbial and Plant Genomics Institute have kindly provided me with travel grants to attend conferences. I also wish to acknowledge the Fellowship in Plant Developmental Biology I received through the Department of Horticultural Science.

Last but not least, my parents have offered me tremendous support, even they do not completely understand what I have been doing. They also showed tremendous courage and patience in letting their only child embark on a five-year long journey on the other side of the planet. I love you both.

## **Dedication**

I wish to dedicate this dissertation to the people who lost their lives fighting for peace, equality, and human rights. I also dedicate this dissertation to the people spending some of the best times in their lives in pursuit of science, knowledge, and possibly, a better future.

## Abstract

Auxin is the essential plant hormone that regulates many aspects of plant growth and development. Plants typically possess highly complex biochemical networks to regulate the homeostasis of the active hormone, through the regulation of biosynthesis, degradation, transport and conjugation. Biosynthesis, among other processes, has been of particular importance and warranted extensive studies over the decades of auxin research. A number of pathways were proposed and some enzymes potentially involved have been characterized. Stable isotope labeling and turnover studies have proven very useful in these investigative efforts. With the advancement of analytical and computational technologies, it is now feasible to concurrently analyze the turnover patterns of all the precursors in the entire auxin biosynthesis network. I devoted chapter two of the dissertation to establish LC-MS methods to concurrently quantify most of the auxin precursors and deployed different isotopic labeling strategies for turnover studies in *Arabidopsis thaliana*. Preliminary results showed that indole-3-pyruvate (IPyA) and indole-3-acetaldehyde (IAAld) were among the fastest to be labeled and a key regulatory step existed between IPyA and indole-3-acetic acid (IAA). Chapter three reported the discrepancy and the study of the amount of the total IAA determined by alkaline hydrolysis and that of the summation of all known forms of IAA conjugates in *Arabidopsis*. My results indicated that chemical artifacts induced by harsh chemical treatments were responsible for a significant portion of the unknown putative IAA conjugates. In chapter four, I described a facile way to directly survey a plant extract for its indole profile, notably IAA conjugates, based on high resolution and accurate mass (HR/AM) liquid chromatography-mass spectrometry (LC-MS). The method was successfully applied to *Glycine max*, *Solanum lycopersicum*, *Cocos nucifera*, and *Ginkgo biloba*. Together, these investigations and developments have led to an improved understanding of auxin metabolism and now provide useful tools for subsequent studies.

## Table of Contents

|  |      |
|--|------|
| List of Tables .....   | vii  |
| List of Figures .....  | viii |
| Chapter 1 Introduction: The metabolism of the plant hormone indole-3-acetic acid .....                             | 1    |
| Chapter 2 A stable isotope labeling study of the IAA biosynthetic pathways in<br><i>Arabidopsis thaliana</i> ..... | 10   |
| Chapter 3 Quantitative evaluation of IAA conjugate pools in <i>Arabidopsis thaliana</i> .....                      | 34   |
| Chapter 4 Indole metabolomics: a facile means for the identification of indolic<br>compounds .....                 | 52   |
| Chapter 5 Conclusions: Towards understanding auxin networks .....  | 82   |
| Bibliography .....   | 84   |
| Appendix .....   | 97   |

## List of Tables

|  |    |
|--|----|
| Table 1-1 Oxidation products of IAA that have been reported in plant tissues.....        | 6  |
| Table 1-2 New IAA conjugates isolated from plants since 1999.....                        | 7  |
| Table 2-1 Isoptic traces measured in the [ <sup>15</sup> N]ANT labeling experiment. .... | 22 |
| Table 3-1 Chemical conversion of glucobrassicin into IAA. ....                           | 50 |
| Table 3-2 IAA genesis during protein degradation and tissue hydrolysis .....             | 51 |
| Table 4-1 List of indolic compounds identified.....                                      | 78 |
| Table 4-2 Partial list of indolic compounds obtained from one young tomato leaf .....    | 79 |
| Table 4-3 Partial list of indolic compounds from one male ginkgo flower .....            | 80 |
| Table 4-4 Partial list of indolic compounds obtained from coconut milk sample .....      | 81 |

## List of Figures

|  |    |
|--|----|
| Figure 1-1 Currently proposed auxin biosynthetic pathways. ....  | 8  |
| Figure 1-2 Potential deactivation products of IAA.....   | 9  |
| Figure 2-1 NaB <sub>2</sub> H <sub>4</sub> derivatization based workflow for measuring auxin precursors. ....  | 27 |
| Figure 2-2 Labeling patterns of auxin precursors via ANT, Indole or Trp feeding.....   | 28 |
| Figure 2-3 Quantitative analysis of auxin precursor labeling patterns. ....  | 29 |
| Figure 2-4 CH <sub>3</sub> ONH <sub>2</sub> derivatization-based workflow of auxin precursor measurement. ....   | 30 |
| Figure 2-5 Quantitative measurement of auxin precursors by LC-MS.....  | 31 |
| Figure 2-6 [ <sup>13</sup> C <sub>6</sub> ]ANT labeling of auxin precursors. ....  | 32 |
| Figure 2-7 Minute-scale labeling patterns of IPyA and Trp following ANT application. ....  | 33 |
| Figure 3-1 Strong anion exchange fractionation of 65% 2-propanol extracts of about 20 mg <i>Arabidopsis</i> seeds. ....  | 47 |
| Figure 3-2 C18 fractionation of a protein digest and total IAA released following hydrolysis in each fraction. ....  | 48 |
| Figure 3-3 Total IAA profile measured by the differential base hydrolysis method.....  | 49 |
| Figure 4-1 Workflow of indolic compound identification from plant tissue.....  | 67 |
| Figure 4-2 Fragmentation patterns of endogenous indole-3-acetyl-aspartic acid (IA-Asp), indole-3-acetyl-glutamic acid (IA-Glu) and indole-3-acetyl-tryptophan (IA-Trp) compared with their respective standards. ....                  | 68 |
| Figure 4-3 Fragmentation pattern of endogenous N(α)-acetyl-tryptophan (Ac-Trp), N(α)-malonyl-tryptophan (Malonyl-Trp), and N(α)-succinyl-tryptophan (SA-Trp) compared with respective standards. ....                                  | 69 |
| Figure 4-4 Fragmentation patterns of endogenous N(α)-malyl-tryptophan compared with the standard. ....   | 70 |
| Figure 4-5 (a) <sup>1</sup> H NMR spectrum of the α isomer of N(α)-(S)-malyl-(S)-tryptophan methyl ester, (b) and (c) <sup>13</sup> C NMR spectra of α and β isomers of N(α)-(S)-malyl-(S)-tryptophan methyl ester, respectively. .... | 71 |
| Figure 4-6 Fragmentation patterns of endogenous <i>trans</i> -tryptophan alcohol and <i>cis</i> -tryptophan alcohol compared with their respective standard. ....  | 72 |

|   |     |
|---|-----|
| Figure 4-7 Fragmentation pattern of a synthetic peptide Phe-Gly-Gly-Phe. ....   | 73  |
| Figure 4-8 LC-MS chromatogram showing the relative abundance of indole-3-acetyl-<br>aspartic acid (IA-Asp), indole-3-acetyl-glutamic acid (IA-Glu), and indole-3-acetyl-<br>tryptophan (IA-Trp). .... | 74  |
| Figure 4-9 LC-MS chromatogram of synthetic and endogenous N( $\alpha$ )-maly-L-(S)-<br>tryptophans. ....  | 75  |
| Figure 4-10 LC chromatogram and MS/MS spectra of the four different tryptophan<br>alcohols present in soybean. ....   | 76  |
| Figure 4-11 Labeled tryptophan alcohols (Trp-OH) were not recovered after spiking in<br>[ <sup>13</sup> C <sub>11</sub> , <sup>15</sup> N <sub>2</sub> ]-labeled tryptophan. ....                     | 77  |
| <br>  |     |
| Figure A- 1 PIF4 regulates expression of the SAUR19–24 subfamily at high temperature.<br>.....  | 99  |
| Figure A- 2 Free IAA amount and expression of auxin biosynthesis genes. ....  | 101 |
| Figure A- 3 Auxin levels in wide type Arabidopsis and mutants. ....   | 103 |

## **Chapter 1 Introduction: The metabolism of the plant hormone indole-3-acetic acid**

The life of a plant is not easy. A seed has to germinate at the right time under the correct conditions and quickly grow strong enough to fend off various stresses from the surrounding environment. In its adult life, it will need to compete for resources like light and water, and defend against pathogens and herbivores, all while being immobile. One important reason that it can accomplish these daunting tasks is because plants possess a highly complex yet immediately responsive network of signal processing for job execution – through the use of plant hormones. The plant growth hormone auxin lies in the center of this regulatory network. It has a role in almost all aspects of plant growth and development. The idea of a mobile signal travelling to a different part of the plant to exert its growth effects was proposed over a century ago (Ciesielski, 1872; Darwin and Darwin, 1880). Since then, researchers have uncovered the identities of various growth hormones, with indole-3-acetic acid (IAA) being the principal auxin *in planta*. With the advent of modern molecular biology and analytical biochemistry, it was revealed that plants possess an equally complex network of auxin metabolism, involving its multi-pathway biosynthesis, deactivation through oxidation, regulation through conjugation, polar transport facilitated by specific carriers, and auxin perception and downstream responses (Woodward and Bartel, 2005). Some of these aspects of auxin biochemistry will be the topics of the subsequent chapters in this dissertation.

Given its central importance in growth and developmental regulation, the biochemical origin of IAA has been an active area of research since its discovery to be the bioactive auxin (Kögl *et al.*, 1934; Thimann, 1935). Biosynthesis is also a key means for maintaining the homeostasis of the hormone. Currently, two general classes of auxin biosynthetic pathways have been described in the literature, namely the tryptophan dependent and tryptophan independent pathways (Figure 1-1). A number of precursors have been implicated in the tryptophan dependent pathways, including indole-3-pyruvic acid (IPyA), indole-3-acetaldehyde (IAAld), indole-3-acetamide (IAM), indole-3-acetaldoxime (IAOx), and indole-3-acetonitrile (IAN). The discovery and presence of

these auxin precursors in various plants have been summarized in a recent review (Table 1 in Korasick *et al.*, 2013). The first complete IAA biosynthetic pathway – the IPyA pathway - was recently confirmed by both genetic analysis and biochemical characterization (Won *et al.*, 2011). This was accomplished after decades of active research by a number of different groups and reported in multiple publications; some of the key accomplishments leading to this pathway elucidation have been summarized (see Table 2 in Tivendale *et al.*, 2014). This pathway involves the transamination of tryptophan with a keto-acid by tryptophan aminotransferase (TAA) enzymes to produce IPyA, and the subsequent oxidative decarboxylation by YUCCA flavin-monooxygenase enzymes to produce IAA. The isotopic labeling studies described in this dissertation are consistent with and thus add further support to the idea that this is the major pathway in wild type *Arabidopsis* seedlings under normal conditions (Chapter Two). Evidence for pathways involving other precursors also have been described for various species and were the subjects of several review articles (Korasick *et al.*, 2013; Ljung, 2013; Tivendale *et al.*, 2014). Disruptions in some of these pathways have severe consequences in the normal development of the plant, for instance, the *vanishing tassel 2 (vt2)* mutation in maize results in much fewer leaves and shorter plants compared to the wild type (Phillips *et al.*, 2011), a result of drastically reduced IAA production. The tryptophan independent pathway was established on the basis of both genetic and biochemical studies (Baldi *et al.*, 1991; Wright *et al.*, 1991; Normanly *et al.*, 1993; Östin *et al.*, 1999; reviewed in Tivendale *et al.*, 2014), and indole-3-glycerol phosphate had been suggested as one possible intermediate (Ouyang *et al.*, 2000; Zhang *et al.*, 2008). Further studies of the gene(s) and possible intermediate compound(s) involved should shed more light on this topic.

Extensive quantitative analyses on auxin biosynthetic pathways have been performed in the past to learn about the kinetics of these processes, and significant insights, such as the existence of the tryptophan independent IAA biosynthesis, were gained through such analyses (reviewed in Tivendale *et al.*, 2014). With the continued advancement of analytical technologies and computational capacities, it is now possible to measure most of the metabolites involved in auxin metabolism concurrently and

construct a global view of auxin homeostasis from such studies. Part of this dissertation is devoted to exploring the analytical methods and mathematical analyses required to comprehensively study the fluxes through the various proposed auxin biosynthesis pathways. For this purpose, HR/AM LC-MS/MS methods were developed to concurrently measure most of the major auxin precursors postulated to date (Tivendale *et al.*, 2014), accompanied with stable isotope labeling strategies to trace the fluxes through these precursors from upstream compounds. Computational workflows to extract the quantitative information for statistical analyses were also established. These results are described in detail in Chapter 2.

In addition to biosynthesis, another important means to maintain the homeostasis of auxin is through deactivation (Ljung, 2013). Major mechanisms for deactivation include oxidative destruction, and reversible or irreversible conjugation to other biomolecules (Figure 1-2). Oxidative destruction through ring oxidation was first described by Reinecke and Bandurski (1981) and an enzyme preparation capable of this reaction was also partially characterized (Reinecke and Bandurski, 1988). Intermediates in this pathway are summarized by Normanly *et al.*, (2010, Figure 9), and updated in Table 1-1. Recently, the gene and an enzyme involved in this process was characterized from rice (*Oryza sativa*) (Zhao *et al.*, 2013) and evidence for its orthologs in other species was presented (Kawai *et al.*, 2014). IAA degradation through the formation of oxindole-3-acetic acid (oxIAA) likely plays key roles in the normal reproductive development of rice and possibly other plants as well, since blocking this pathway leads to aberrant seed development (Zhao *et al.*, 2013). The conjugation of IAA is another important biological process to maintain the level of the active hormone, which includes the formation of indole-3-acetyl glucose, indole-3-acetyl-myo-inositol and its sugar derivatives, and various IAA amino acid conjugates. Disruptions in the formation of these conjugates can lead to stunted growth (Rampey *et al.*, 2004), increases disease resistance (González-Lamothe *et al.*, 2012), enhanced root growth (Iyer *et al.* 2005) or improved yield (Ishimaru *et al.*, 2013). The research on IAA conjugates (also referred to as “bound auxin”) has a relatively long history starting from the first demonstration by Cholodny (1935) of unavailable or bound forms as seed auxin precursors. Subsequently, it was

shown that the majority of cellular IAA was conjugated to various biomolecules (Bandurski and Schulze, 1977; Bialek and Cohen, 1986; Epstein *et al.*, 1986; Walz *et al.*, 2002). The forms of IAA conjugates that exist in plant or formed by them and the prevalence of various IAA conjugates have been summarized by Slovin *et al.*, (1999, Table 1), and Korasick *et al.*, (2013, Table 1). Some additional compounds not reported in the previous reviews are shown in Table 1-2.

The observation that most cellular auxin is conjugated led to research efforts into characterizing this class of compounds in terms of their occurrence and broader biological significance. To date, only soybean (*Glycine max*) and corn (*Zea mays*) have been characterized in detail for their IAA conjugate profiles, primarily using classical approaches initiated several decades ago (reviewed in Slovin *et al.*, 1999). In *Arabidopsis thaliana*, the discrepancy between the amount of total IAA determined via base hydrolysis and the summation of all the known forms of IAA conjugates presented a quandary that for over a decade remained unsolved (Tam *et al.*, 2000). In this dissertation, efforts are detailed to characterize the pool of 'total IAA' (that found after strong base hydrolysis) in *Arabidopsis* using both traditional approaches and advanced methods of instrumental analysis to resolve this issue. Significant chemical artifacts resulting from harsh chemical treatments commonly employed for conjugate hydrolysis are shown to cause an overestimation of the 'total IAA' pool and these analytical issues are discussed in detail in Chapter 3.

It is clear that mysteries still remain in the full understanding of the biosynthesis and subsequent catabolism of IAA and this is partially attributable to the need for ever more sensitive analytical methods to characterize novel compounds in these processes whose concentration could be as low as, or even lower, than that of IAA. Chapter Four describes an analytical procedure suitable for the rapid identification and relative quantification of newly discovered as well as previously described indolic compounds. A quick survey of several plant species allowed the identification of some novel IAA and tryptophan conjugates. The method is based on HR/AM LC-MS, involves minimal sample preparation thus providing a relatively unbiased sampling while retaining high

sensitivity and specificity. This method will be a useful tool in the biochemical characterization of the metabolism of the plant hormone IAA, as well as other indolic compounds.

Another important aspect of auxin physiology is the perception of the hormone and subsequent cellular responses. It is now clear that the SCF<sup>TIR1</sup> complex and Aux/IAA proteins function as co-receptors for auxin and act through targeting Aux/IAAs for degradation and thus releasing the repression of AUX/IAAs on the transcriptional activity of AUXIN RESPONSE FACTORS (ARFs) which bind to the auxin responsive elements (AuxREs) in the promoter of auxin-responsive genes and ultimately activate the expression of the target genes (Chapman and Estelle, 2009; Dharmasiri *et al.*, 2005; Kepinski and Leyser, 2005; Villalobos, Luz Irina A Calderón *et al.*, 2012). There is increasing evidence pointing to a role for Auxin Binding Protein 1 (ABP1) as another potential auxin receptor, especially in light of rapid cell expansion and other quick responses upon auxin treatment (Paque *et al.*, 2014; Schenck *et al.*, 2010). In the auxin responses involving gene expression, specific genes downstream of AuxREs are expressed following auxin perception in specific tissues and are then manifest as specific auxin responses through their interaction with other cellular components. The appendix to this dissertation contains three papers to which I have contributed that relates to auxin responses.

**Table 1-1 Oxidation products of IAA that have been reported in plant tissues\*.**

| Oxidation product                                    | Plant                       | Reference                     |
|--|-----------------------------|-------------------------------|
| Oxindole-3-acetic acid (oxIAA)                       | <i>Arabidopsis thaliana</i> | Ostin <i>et al.</i> , 1998    |
|  | <i>Zea mays</i>             | Reinecke <i>et al.</i> , 1981 |
| oxIAA-Glc  | <i>Arabidopsis thaliana</i> | Kai <i>et al.</i> , 2007a     |
| 7-HO-oxIAA   | <i>Zea mays</i>             | Lewer <i>et al.</i> , 1987    |
| 7-OH-oxIAA-Glc                                       | <i>Zea mays</i>             | Nonhebel <i>et al.</i> , 1984 |
| 4-OH-oxIAA   | <i>Zea mays</i>             | Wille <i>et al.</i> , 2011    |
| oxIAA-Asp  | <i>Arabidopsis thaliana</i> | Ostin <i>et al.</i> , 1998    |
|  | <i>Solanum lycopersicum</i> | Ostin <i>et al.</i> , 1995    |
| oxIAA-Asp-N- $\beta$ -Glc                            | <i>Solanum lycopersicum</i> | Ostin <i>et al.</i> , 1995    |
| oxIAA-Asp-N- $\beta$ -Glc- $\beta$ -1,4-Glc          | <i>Solanum lycopersicum</i> | Ostin <i>et al.</i> , 1995    |
| 5-O- $\beta$ -D-glucopyranosyl 3,5-dihydroxy-2-oxIAA | <i>Oryza sativa</i>         | Tateishi <i>et al.</i> , 1998 |
| 5-O- $\beta$ -D-cellobiosyl-3,5-dihydroxy-2-oxIAA    | <i>Oryza sativa</i>         | Tateishi <i>et al.</i> , 1998 |
|  | <i>Arabidopsis thaliana</i> |                               |
| 6-OH-IA-Phe  | <i>Arabidopsis thaliana</i> | Kai <i>et al.</i> , 2007a     |
| 6-OH-IA-Val  | <i>Arabidopsis thaliana</i> | Kai <i>et al.</i> , 2007a     |

\*Also refer to Normanly *et al.*, (2010, Figure 9) for a list of IAA oxidation products up to 2005.

**Table 1-2 New IAA conjugates isolated from plants since 1999\***

| Conjugate  | Plant                         | Reference                            |
|--|-------------------------------|--------------------------------------|
| IA-Phe   | <i>Funaria hydrometrica</i>   | See Korasick <i>et al.</i> ,<br>2013 |
|  | <i>Helleborus niger</i>       |                                      |
|  | <i>Orthotrichum lyellii</i>   |                                      |
|  | <i>Oryza sativa</i>           |                                      |
| IA-Leu   | <i>Arabidopsis thaliana</i>   | See Korasick <i>et al.</i> ,<br>2013 |
|  | <i>Ceratopteria richardii</i> |                                      |
|  | <i>Physcomitrella patens</i>  |                                      |
|  | <i>Arabidopsis thaliana</i>   |                                      |
| IA-Trp   | <i>Oryza sativa</i>           | Staswick 2009                        |
|  | <i>Glycine max</i>            | Cao <i>et al.</i> , 2011             |
|  | <i>Phaseolus vulgaris</i>     | Yu <i>et al.</i> , 2014              |
| IA-IAP1  | <i>Phaseolus vulgaris</i>     | Walz <i>et al.</i> , 2002            |
| 4-Cl-IAA<br>protein                              | <i>Pisum sativum</i>          | Park <i>et al.</i> , 2010            |
| IAA protein                                      | <i>Fragaria vesca</i>         | Park <i>et al.</i> , 2006            |
| N-β-D-<br>glucopyranosyl<br>-IAA (IAA-N-<br>Glc) | <i>Oryza sativa</i>           | Kai <i>et al.</i> , 2007b            |
|  | <i>Zea mays</i>               |                                      |
| IA-N-Glc-Asp                                     | <i>Oryza sativa</i>           | Kai <i>et al.</i> , 2007b            |
| IA-N-Glc-Glu                                     | <i>Oryza sativa</i>           | Kai <i>et al.</i> , 2007b            |
| IA-4-O-<br><i>myo</i> -inositol                  | <i>Arabidopsis thaliana</i>   | Wu <i>et al.</i> , 2014              |
| IA-5-O-<br><i>myo</i> -inositol                  | <i>Arabidopsis thaliana</i>   | Wu <i>et al.</i> , 2014              |
| IA-1-O-<br><i>myo</i> -inositol                  | <i>Arabidopsis thaliana</i>   | Wu <i>et al.</i> , 2014              |
| IA-2-O-<br><i>myo</i> -inositol                  | <i>Arabidopsis thaliana</i>   | Wu <i>et al.</i> , 2014              |

\*see Slovin *et al.*, (1999) for a list of IAA conjugates up to 1999. IA: indole-3-acetyl.  
IAP1: IAA binding protein 1.

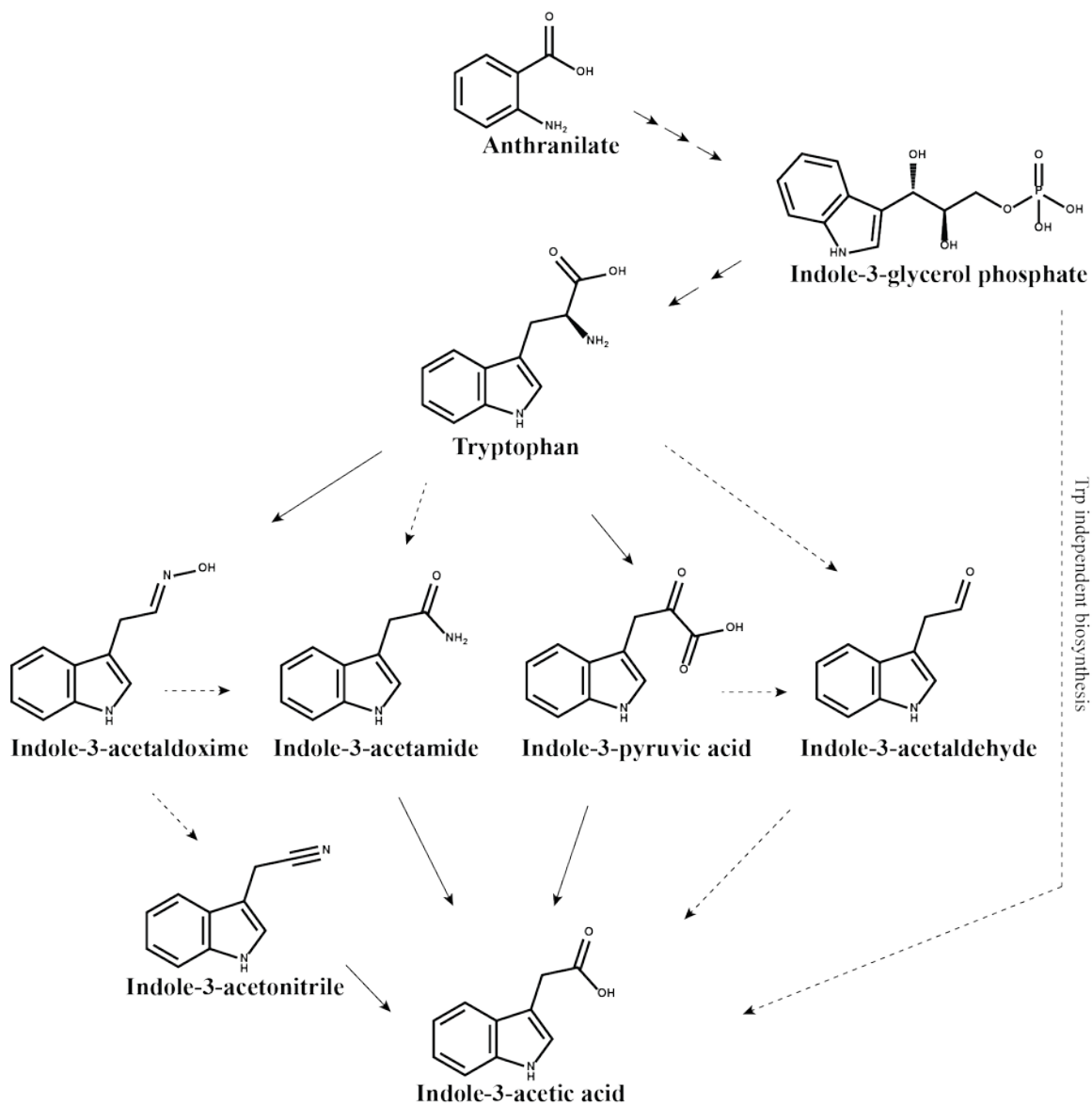


**Figure 1-1** Currently proposed auxin biosynthetic pathways. Solid arrows indicate that enzymes responsible for the reactions have been identified in at least one species, where dotted arrows indicate the enzymes remain to be discovered.

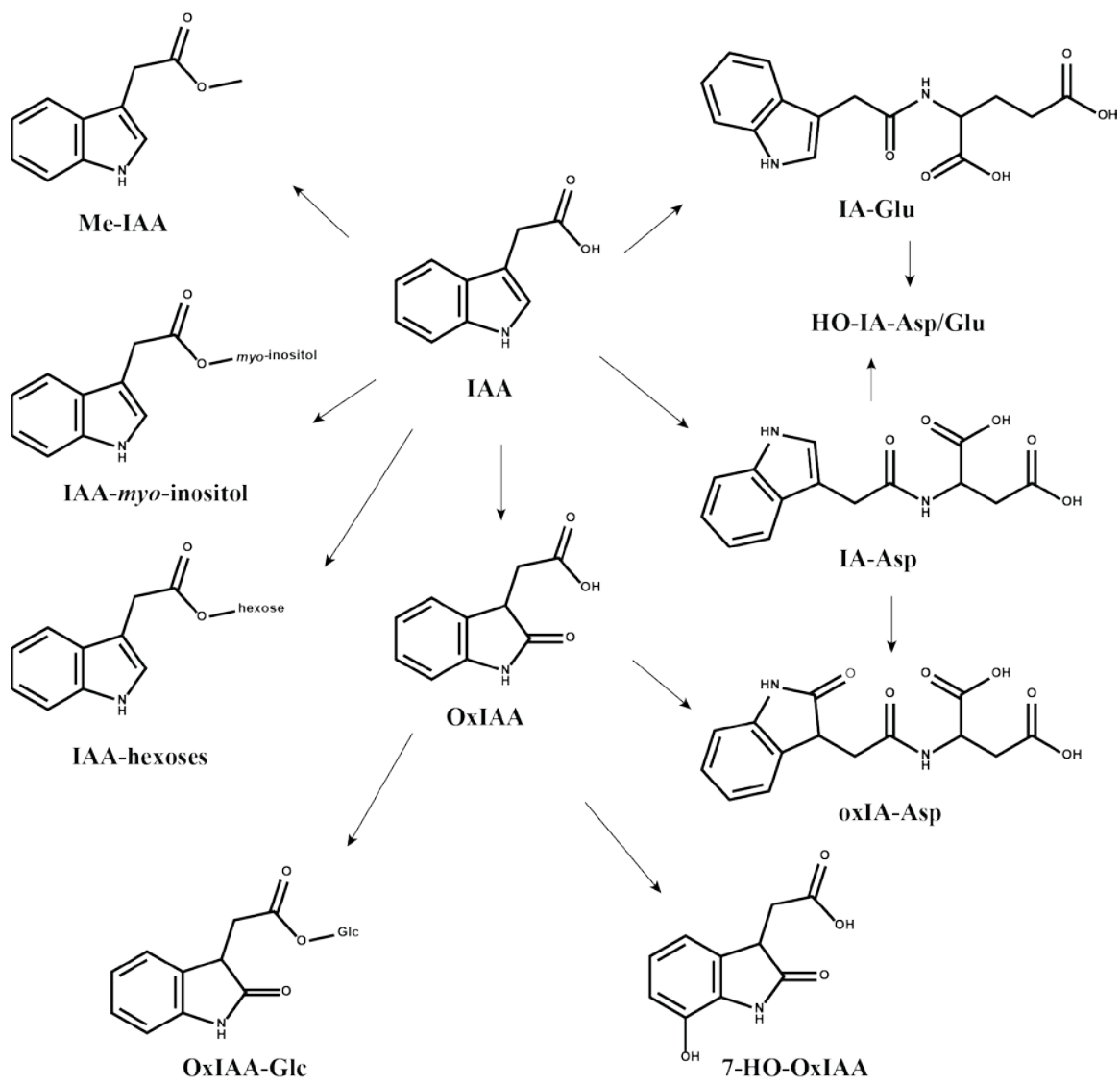


**Figure 1-2 Potential deactivation products of IAA.**

## **Chapter 2 A stable isotope labeling study of the IAA biosynthetic pathways in *Arabidopsis thaliana***

### **Abstract**

Auxin biosynthesis has been an active area of research since indole-3-acetic acid (IAA) was found to be the active hormone in plants. A number of precursors and pathways were proposed, notably tryptophan (Trp) dependent pathway and tryptophan independent pathways. Recently, the first complete pathway involving Trp, indole-3-pyruvic acid (IPyA) and IAA was established by means of genetic analysis and biochemical measurements. However, the literature was devoid of flux information in these proposed pathways, partially due to the analytical difficulties associated with the low abundances of such compounds. We propose an isotopic labeling strategy and a sensitive analytical method to obtain flux measurements through the various auxin precursors. Our analyses using such methods showed that IPyA and indole-3-acetaldehyde (IAAld) were quickly labeled after anthranilic acid (ANT) application. Given the relative pool size of IPyA, IAAld and IAA, the results suggest that IPyA likely plays a major role in IAA biosynthesis in *Arabidopsis* seedlings. Another finding was that the plants were able to accumulate Trp, IPyA and IAAld to a high level in a short period of time while maintaining the level of free IAA, suggesting an important feedback regulation at the IPyA to IAA conversion step. Lastly, minute-scale kinetic studies of Trp and IPyA synthesis from ANT showed the labeling patterns closely resembled each other, leaving open the possibility that IPyA was also synthesized from a precursor upstream of Trp.

### **Introduction**

Auxin is an important plant growth hormone that regulates many aspects of plant growth and development. The quest for its biosynthetic sources began around the same time as indole-3-acetic acid (IAA) was shown to be the active growth hormone in plants (Kögl, *et al.*, 1934; Thimann, 1935). In the subsequent decades of research, numerous

perspective auxin precursors have been proposed (Tivendale *et al.*, 2014), with most attention currently focused on tryptophan (Trp) dependent pathway while a tryptophan independent pathway has also been demonstrated (Baldi *et al.*, 1991; Wright *et al.*, 1991; Normanly *et al.*, 1993; Östin *et al.*, 1999; Ouyang *et al.*, 2000). Only recently has a well-defined pathway stemming from tryptophan, with indole-3-pyruvic acid (IPyA) being the intermediate, and then to the final product IAA, been genetically established and partially biochemically characterized (Won *et al.*, 2011). The qualitative studies have been important first steps in identifying this pathway, while a quantitative analysis would appear also to be critical in order to answer questions regarding other proposed auxin precursors. An analysis of the entire labeling kinetics of the intermediates and products involved in auxin biosynthesis would not only help to delineate the relative contributions of each proposed pathway, but also allow quantitative comparisons under different physiological conditions, and may lead to discovery of novel intermediates or new pathways (see Epstein *et al.*, 1980).

In *Arabidopsis thaliana*, in addition to the above mentioned IPyA pathway, indole-3-acetaldehyde (IAAld), indole-3-acetamide (IAM), indole-3-acetonitrile (IAN), indole-3-acetaldoxime (IAOx) have all been implicated in the Trp dependent pathway and indole and indole-3-glycerol phosphate (IGP) have been proposed to be precursors in the Trp independent pathway (Figure 1-1). However, despite continued long-term interest in their roles, the literature is largely devoid of flux information through these precursors, partially due to the analytical difficulties in analyzing these chemically diverse compounds present at concentrations as low as, or sometimes even lower, than IAA, and partially due to the incomplete biochemical pathways. With the recent advancements in HR/AM MS technologies, we aim to illustrate the potential of this technology in pathway analysis by conducting a primary study using stable isotope labeled indolic precursors to analyze the rates of labeling and thus turnover rates of different potential precursors of IAA. Although metabolic steady-state assumptions allows less complex modeling, non-steady state is likely more biologically relevant. One challenge with non-steady state studies is that the pool size of the metabolites may not stay the same during the course of the experiment, necessitating the continuous measurement of the pool sizes. In other

words, the amount of the endogenous compound and that of the newly synthesized must be separately measured, preferably with an isotope labeled internal standard (Rittenberg and Foster, 1940). We have devised a generic stable isotope labeling strategy for such analyses. *Arabidopsis* seedlings can be grown on stable isotope labeled media and the endogenous compounds would then be isotopically labeled at the beginning of an experiment. A different isotopic form of a labeled precursor is then fed to the plants to differentiate the newly synthesized compounds from endogenous ones through the use of mass spectrometry. “Unlabeled” compounds can then be used as internal standards to quantify both forms. The convenience of using unlabeled compounds as internal standard (“reverse isotope dilution”; Bloch and Anker, 1948) is obvious: the availability of isotope labeled compounds is much more limited than their non-labeled counterparts.

## **Results**

### **Turnover of IAA precursors**

Following the reasoning in the Introduction, we created [ $^{13}\text{C}$ ]-labeled plants by growing *Arabidopsis* on agar plates with [ $^{13}\text{C}_6$ ]glucose as carbon source. To further increase the label incorporation into the auxin pathway, the growth media was supplemented with low levels of [ $^{13}\text{C}_6$ ]anthranilic acid. At 17 days, most precursors were close to fully labeled except tryptophan where high amounts of tryptophan reserves diluted the label substantially, as shown in Figure 2-2 at the zero time point. To mitigate problems associated with overlapping isotopic envelopes (e.g. [ $^{15}\text{N}$ ,  $^{13}\text{C}_5$ ]Trp and [ $^{13}\text{C}_6$ ]Trp have the same nominal mass) using unit resolution quadrupole based mass analyzers, we developed a method to quantitate auxin precursors based on HR/AM mass spectrometry, where different isotopic forms of a compound with the same nominal masses can be resolved. This high resolution is key to the success of this approach in another aspect: improved resolution brings improved signal to noise ratio and better sensitivity which is crucial to detect the auxin metabolites present at extremely low levels.

To quantitatively assess the auxin precursors, we developed a one-step solid phase extraction protocol (Figure 2-1) modified from prior work from our laboratory and from

others (Liu, *et al.*, 2012; Novák, *et al.*, 2012). Harvested plant material were split into two halves: one half to measure anthranilic acid (ANT), tryptophan (Trp), indole-3-acetamide (IAM), indole-3-acetonitrile (IAN), indole-3-acetaldoxime (IAOx) and indole-3-acetic acid (IAA); the other half to measure indole-3-pyruvic acid (IPyA) and indole-3-acetaldehyde (IAAld) after sodium borodeuteride ( $\text{NaB}^2\text{H}_4$ ) derivatization (Liu *et al.*, 2012) to produce indole-3-lactic acid (ILA) and indole-3-ethanol (IEt). The interference of low level ILA and IEt naturally present was resolved by the presence of the extra deuteride label in the IPyA and IAAld derived compounds, thus avoiding the need to correct for them. This sample splitting was necessary because  $\text{NaB}^2\text{H}_4$  was only stable under basic conditions, which will likely hydrolyze IAA ester conjugates (Baldi *et al.*, 1989).

Since the turnover in the IAA biosynthesis pathway is relatively fast, a precursor that can quickly label the intermediates would be most desirable. In an initial experiment, we fed  $[\text{}^{15}\text{N}]\text{ANT}$ ,  $[\text{}^{15}\text{N}]\text{indole}$ , and  $[\text{}^{13}\text{C}_{11}, \text{}^{15}\text{N}_2]\text{Trp}$  to *Arabidopsis* seedlings grown on “isotopically natural” media and followed label incorporation into each individual IAA precursor over time (Figure 2-2). IAOx was not recovered by this method, presumably because of base lability of oximes. As can be seen, both ANT and indole were capable of quickly labeling the precursor pools at moderate concentrations, while Trp was not so effective. Since it is likely that the Trp independent pathway stems from precursors upstream of indole (Ouyang *et al.*, 2000), we used ANT as a labeling precursor for subsequent studies. It was also obvious from our initial studies that Trp, IPyA, IAAld and IAA had fast turnover rates from ANT and indole labeling, while IAN and IAM were very slowly turned over. In subsequently studies, IAOx was found to have labeling kinetics similar to that of IAN (Table 2-1).

### **Studies using $[\text{}^{13}\text{C}]$ -labeled plants**

In the next experiments we fed  $[\text{}^{15}\text{N}]\text{ANT}$  to  $[\text{}^{13}\text{C}]$ -labeled plants and quantified the metabolites in the IAA pathway using unlabeled compounds. Since IPyA showed the most significant labeling, we only present the results from Trp, IPyA, and IAA in Figure 2-3. A few important conclusions could be drawn from this experiment. First, the level of

IAA was an order of magnitude lower than that of IPyA, which was in turn one to two orders of magnitude lower than that of Trp. This was relevant when considering the labeling dynamics of the IAA precursors. A slow labeling compound with a large pool size could still be biochemically upstream of a fast labeling compound with a small pool size by actively channeling part of the upstream compound for downstream synthesis. Second, there was a significant accumulation of Trp and IPyA, necessitating a more complex approach to model this metabolically non-steady state flux information. Interestingly, the unlabeled form of most IAA precursors did not decrease with time. Third, the level of total IAA was relatively stable, even when the level of precursors increased substantially, suggesting an important feedback regulation between IPyA and IAA, possibly through modulating the YUCCA enzyme activities. Fourth, although the metabolites had many of the carbon atoms labeled, the number of [ $^{13}\text{C}$ ]-atoms present in a particular molecule varied significantly. The less labeled forms were still pervasive and this labeling inhomogeneity inevitably spread out the already weak signals from auxin metabolites and also complicated interpretation efforts.

Nevertheless, we showed quantitatively that IPyA and IAAlc were among the fastest auxin precursors to be labeled. Given that the pool size of IPyA is one to two orders of magnitude larger than that IAA, and the pool size of IAAlc is smaller than IAA, then the flux through IPyA was probably two to three orders of magnitude larger than that of IAAlc. This result suggests that the YUCCA pathway was likely the major IAA biosynthesis pathway in *Arabidopsis* under these physiological conditions, as had been suggested earlier without the required flux information for confirmation (Mashiguchi *et al.*, 2011).

### **Studies using [ $^{15}\text{N}$ ]-labeled plants**

To circumvent the limitations associated with inhomogeneity in labeling via  $^{13}\text{C}$ , we tested the system by labeling the plants with [ $^{15}\text{N}$ ]-salts. This approach provided the following advantages: 1) the only new nitrogen source came from the  $^{15}\text{N}$ -salts in the growth media and thus a high level of labeling could be achieved where photosynthetic carbon fixation can potentially lower the [ $^{13}\text{C}$ ]-label percentage; 2) all IAA metabolites

have only one or two nitrogen atoms, making the number of isotopomers much less than the [ $^{13}\text{C}$ ]-counterparts and in turn leading to increased signal for the individual isotopomers. To further reduce the amount of tissues needed for auxin measurement and allow earlier stages of *Arabidopsis* seedlings to be used, we needed a method to measure all the auxin precursors at once without splitting the samples. This was achieved by using methoxylamine as a derivatization reagent for IPyA and IAAlD to generate their respective oximes (IPyA-MeOx and IAAlD-MeOx), under a slightly acidic condition which avoided the hydrolysis of IAA esters and also rendered IAOx more stable, as illustrated in Figure 2-4. Using this simplified approach, we were able to measure most of the proposed auxin precursors (Figure 2-5). Two forms of IAAlD-MeOx (can also be viewed as O-methyl indole-3-acetaldoxime) were produced, presumably a pair of *-trans* and *-cis* isomers, and one form of IPyA was produced (Figure 2-5).

Using this method, we repeated our earlier experiment with much finer time resolution. Again, to simplify the results we only showed the predominant IPyA pathway metabolites (Figure 2-6) while the complete information for all the compounds measured is available in Table 2-1. Only one isotopic trace each, representing the endogenous (M+N or M+2N) and the newly synthesized (M+6C or M+N6C) compounds, were displayed because they were capable of representing the majority of the respective pools (Table 2-1). It appeared to be that the [ $^{13}\text{C}_6$ ]-label first appeared in IPyA and then Trp, which corroborated an early finding that indole-3-glycerol phosphate (IGP) might be the branch point of Trp independent IAA biosynthesis (Ouyang *et al.*, 2000). Given the structural similarities of IGP and IPyA, it was possible that such a novel reaction could occur *in vivo*.

### **On the possibility of IPyA being an intermediate in Trp independent IAA biosynthesis**

To test the possibility that IPyA was labeled by upstream precursors ahead of Trp, we conducted the same labeling experiment with a time scale of minutes (Figure 2-7). From Figure 2-6, it was safe to assume that the levels of endogenous Trp and IPyA remained stable, at least for the few minutes this experiment was carried out. The ratio of

labeled over unlabeled compound could then be used as a proxy for how much new material was synthesized from [ $^{13}\text{C}_6$ ]ANT. Since the pool size of Trp is one order of magnitude larger than that of IPyA, much more labeled Trp was synthesized than labeled ANT. The close resemblance of the labeling patterns suggested that IPyA being solely synthesized from Trp or alternatively also from an upstream common precursor were both possible.

## Discussion

We have evaluated two different labeling schemes for the study of the turnover rates of different proposed IAA precursors in the IAA biosynthesis pathway in *Arabidopsis*, namely feeding [ $^{15}\text{N}$ ]ANT to [ $^{13}\text{C}$ ]-labeled plants, or feeding [ $^{13}\text{C}_6$ ]ANT to [ $^{15}\text{N}$ ]-labeled plants. As proof of concept, we only did a single replicate measurement in this initial study. Nevertheless, useful results were obtained. We found that IPyA and IAAlD were among the fastest proposed IAA precursors to be labeled. This raised the question as to the role of IAAlD in IAA biosynthesis, especially given that IPyA was recently concluded to be the main pathway. Further investigation of the relationship between IPyA and IAAlD in terms of labeling kinetics will hopefully shed additional light on this topic. For instance, a pulse-chase experiment using an isotope labeled upstream precursor might define the metabolic relationship between IPyA and IAAlD, and potentially other IAA precursors that have been proposed (Tatsis *et al.*, 2014). There were also significant accumulations of Trp, IPyA and IAAlD when ANT or indole was fed to wild type plants, but the level of free IAA remained relatively stable, indicating a significant regulation in the oxidative decarboxylation of IPyA to produce a specific level of IAA.

The large accumulation of precursors in the wild type plants likely disturbed the normal biochemical state of the plants to some extent. Thus, our next approach to the problem will be to exchange the labeling of the endogenous upstream precursor (ANT, for example) with a different labeled counterpart in a relatively short period of time, rather than longer term feeding of the exogenous compound that created the observed

buildup of intermediates. The other benefit of this approach lies in that one could use a pseudo steady state assumption to model the fluxes through the network when the experimental process is relatively short on a plant development scale and this will greatly simplify the modeling (Leighty and Antoniewicz, 2011; Yuan *et al.*, 2008). One way to do such an experiment would be to grow *Arabidopsis* auxotrophs of a particular precursor (ANT, for example) supplemented with it and then do a quick media exchange to the labeled form of that precursor, achieving fast swap-over of the precursor while minimally perturbing the system. Indeed, such work is now under way and will be the topic of a subsequent study in our laboratory.

While both [<sup>13</sup>C]- and [<sup>15</sup>N]-labeled plants were used successfully to illustrate the fluxes through different IAA precursors, the second scheme was much easier to implement since [<sup>15</sup>N]-salts provided the only nitrogen source, where [<sup>13</sup>C]-labeling had to face the dilution obtained from photosynthetic carbon fixation, and [<sup>13</sup>C<sub>6</sub>]ANT supplementation in the media was necessary to create adequately labeled plants before the experiment began. Subsequent quantitation of each metabolite was also easier in the [<sup>15</sup>N]-plants because much fewer isotopic traces had to be measured (5-7 versus ~20). The natural abundance of <sup>15</sup>N is only less than 0.4%, making it suitable to use unlabeled compounds as internal standards as long as the amount added was similar to that of its endogenous [<sup>15</sup>N]-labeled counterpart. One thing worth pointing out was that the labeling approach only worked well with *Arabidopsis*, whose small seeds allowed nearly complete labeling of most IAA related metabolites within two weeks. Tryptophan was an exception and a significant amount was still unlabeled even after two and a half weeks (Table 2-1 - Trp). In this instance, some other forms of labeled tryptophan could be used as an internal standard, for example [<sup>13</sup>C<sub>11</sub>, <sup>15</sup>N<sub>2</sub>]Trp. The use of deuterium labeling should be carefully characterized, because of possibilities of hydrogen/deuterium exchange *in vivo* and under certain MS conditions (Davies *et al.*, 2010). The other advantage of using <sup>13</sup>C or <sup>15</sup>N over <sup>2</sup>H labeled precursors lies in the much smaller isotope effects on enzymatic reactions, while this small effect may still warrant further investigation with regards to isotope sorting (Cleland, 2005; Werner and Schmidt, 2002).

The derivatization procedure we used for IPyA and IAAld was based on the well-known hydroxylamine derivatization chemistry of carbonyls. To avoid converting IAAld to IAOx, we had to use some derivatives of hydroxylamine and we chose methoxylamine. Even larger derivatization groups will push the analyte ions into the less noisy high mass region of a mass spectrum, however the resolution of the Orbitrap MS also decreases as the mass increases and maintaining high resolution was critical to separate analyte signal from interference. Methoxylamine was a good balance in terms of achieving both enough mass resolution and signal to noise. Another concern in this chemistry was the reversible base catalyzed inter-conversion of IAAld and IAOx. This would be a more serious problem in the original  $\text{NaB}^2\text{H}_4$  chemistry where basic conditions were necessary. Methoxylamine derivation, as we have demonstrated, could be easily implemented under slightly acid conditions.

The general labeling strategies employed here for studying the fluxes through the auxin biosynthesis pathway could also be easily adapted to study other biochemical pathways under metabolically non-steady state conditions, provided a suitable isotope labeled precursor can be found. The ability to use naturally occurring, unlabeled compounds as internal standards greatly expands the metabolic pathways that can be easily studied. This general principle could also be used for the quantitation of chemically complex molecules, whose isotopically labeled forms were difficult to obtain, via reverse isotope dilution.

## **Experimental Procedures**

### *Plant materials and growth conditions*

*Arabidopsis thaliana* ecotype Columbia 0 seeds were from Dr. Wen-Ping Chen and bulked up for use in the experiments described. Seeds were surface sterilized with 30% commercial bleach (5.25% hypochlorite) with 1% Triton X-100 for 20 min and sown onto appropriate agar plates (see below). The plates were kept at 4 °C in the dark for three days before moving to the growth chamber. Growth conditions were 22 °C, 10 h day length, 60% relative humidity, and  $80 \mu\text{mol} \cdot \text{m}^{-2} \cdot \text{s}^{-1}$  photosynthetically active radiation. On the day of the experiment, the agar plates were flooded with desired

amounts of [ $^{15}\text{N}$ ] or [ $^{13}\text{C}_6$ ]ANT (described in the text) in the liquid media containing the same salts as the plates. Plant material were harvested at desired time interval, quickly blotted dry, weighed and frozen in liquid nitrogen. The material were then kept at  $-80\text{ }^\circ\text{C}$  to be processed within one week.

[ $^{13}\text{C}$ ]-labeled *Arabidopsis* seedlings were grown on half strength Murashige and Skoog (Murashige and Skoog, 1962) salts, 1% [ $^{13}\text{C}_6$ ]glucose (Cambridge Isotope Laboratories, Tewksbury, MA), and 0.68% agar plates supplemented with  $1\text{ }\mu\text{M}$  [ $^{13}\text{C}_6$ ]ANT at pH 5.8.

[ $^{15}\text{N}$ ]-labeled *Arabidopsis* seedlings were grown on ATS media (Lincoln *et al.*, 1990), with potassium nitrate and calcium nitrated substituted with [ $^{15}\text{N}$ ]-salts (Cambridge Isotope Laboratories, Tewksbury, MA), and 0.68% agar at pH 5.8.

### *Chemicals*

[ $^{15}\text{N}$ ]ANT, [ $^{15}\text{N}$ ]indole, [ $^{13}\text{C}_{11}$ ,  $^{15}\text{N}_2$ ]Trp were from Cambridge Isotope Laboratories (Tewksbury, MA). IAOx was synthesized by reacting IAAlD with hydroxylamine (Ahmad *et al.*, 1960). Water was distilled in house in a glass still from reverse osmosis treated deionized feed water. Formic acid used in LC-MS was from Fisher Scientific (Hampton, New Hampshire). All other chemicals including [ $^{13}\text{C}_6$ ]ANT, sodium borodeuteride and methoxylamine hydrochloride were purchased from Sigma-Aldrich (Saint Louis, MO).

### *LC-MS analysis of auxin precursors*

$\text{NaB}^2\text{H}_4$  based extraction. Plant materials (~50 mg) were extracted in  $200\text{ }\mu\text{L}$  65% 2-propanol, 35% 0.2 M imidazole (pH 7.0) containing 10 pmol ANT, 1 nmol Trp, 200 fmol IAM, 500 pmol IAN, , 2 pmol *-trans* and *-cis* IAOx each, 20 pmol IPyA, 2 pmol IAAlD, 2 pmol IAA. Tissues were homogenated with an MM 300 model ball mill (Restch, Hann, Germany) at 25 Hz for 5 min and kept on ice for one hour for isotope equilibration. The homogenate were then centrifuged and the liquid was taken out and split into two equal halves. The first half was diluted 10 fold with water and adjusted to pH 2.5 with 0.5 M hydrochloric acid, 0.5 M phosphoric acid. The second half was diluted 10 fold with water and treated with  $100\text{ }\mu\text{L}$  0.5 M  $\text{NaB}^2\text{H}_4$  in 0.1 M NaOH for 0.5 h in the

dark before adjusted to pH 2.5. The two halves were separately extracted with SUPEL-SELECT HLB SPE tubes (SUPELCO, Bellefonte, PA) containing 30 mg resin. Columns were first equilibrated with 1 mL acetonitrile and 1 mL 5% acetonitrile and the diluted plant extracts were loaded. The columns were next washed with 2 mL 5% acetonitrile and 20  $\mu$ L 80% acetonitrile and eluted with 500  $\mu$ L 80% acetonitrile. The eluents were reduced to  $\sim$ 25  $\mu$ L in a SpeedVac (Savant Instruments Inc., Farmingdale, NY), clarified by centrifugation and injected onto the LC-MS.

$\text{CH}_3\text{ONH}_2$  based extraction. Plant materials ( $\sim$ 25 mg) were extracted in 200  $\mu$ L 65% 2-propanol, 35% 0.2 M imidazole (pH 7.0) containing 10 pmol ANT, 1 nmol Trp, 200 fmol IAM, 500 pmol IAN, , 2 pmol *-trans* and *-cis* IAOx each, 20 pmol IPyA, 2 pmol IAAld, 2 pmol IAA, and 100 mM methoxylamine hydrochloride ( $\text{CH}_3\text{ONH}_2 \cdot \text{HCl}$ ). Tissues were homogenated with an MM 300 model beadmill (Restch, Hann, Germany) at 25 Hz for 5 min and kept on ice for one hour for isotope equilibration and  $\text{CH}_3\text{ONH}_2$  reaction. The extracts were then centrifuged and the supernatants were recovered and diluted 5 times with water before HLB extraction. The pH of the extract was 3.5 at this point. The same SPE columns were used. Columns were first equilibrated with 1 mL acetonitrile and 1 mL 5% acetonitrile and the diluted plant extracts were loaded. The columns were next washed with 1 mL 20% acetonitrile and 100  $\mu$ L 80% acetonitrile and eluted with 400  $\mu$ L 80% acetonitrile. The eluents were reduced to  $\sim$ 25  $\mu$ L in a SpeedVac (Savant Instruments Inc., Farmingdale, NY), clarified by centrifugation and injected onto the LC-MS.

The eluents were analyzed on a Dionex Ultimate 3000 RSLC HPLC coupled to a hybrid quadrupole Orbitrap Q Exactive mass spectrometer (Thermo Scientific, San Jose, California). 20  $\mu$ L extract was injected onto a 2.1x100 mm, 1.7  $\mu$ m particle size Kinetex XB-C18 column (Phenomenex, Torrance, CA) and eluted with a solvent gradient. Solvents were A: 0.1% formic acid in water, B: 0.1% formic acid in acetonitrile. Flow rate was 0.3 mL  $\cdot$  min<sup>-1</sup>. For the  $\text{NaB}^2\text{H}_4$  treated samples, gradient was; 0-2 min: 5% B, 2-10 min: 5-50% B, 10-11 min: 50-80% B; 11-13 min: 80% B. For  $\text{CH}_3\text{ONH}_2$  treated samples, gradient was; 0-2 min: 5% B, 2-8 min: 5-38.8% B, 8-12 min: 38.8-50% B; 12-13 min: 50-80% B, 13-15 min: 80% B. A HESI (heated electrospray ionization) II probe was used to interface the LC and MS. Ion source conditions were: spray voltage: 3.6 kV,

capillary temperature: 350 °C, probe heater temperature: 300 °C, sheath gas: 35 arbitrary units, aux gas: 8 arbitrary units, S-lens RF level: 47. Orbitrap resolution was 70,000 full width at half maximum (FWHM) with maximum ionization time of 200 milliseconds and automatic gain control (AGC) of  $5 \times 10^5$ . MS was set to acquire several segments of full scans each targeting one or two compounds. For the  $\text{NaB}^2\text{H}_4$  treated samples, the segments were; 0-4 min: 200-224  $m/z$ , 4-5.77 min: 133-150  $m/z$ , 5.77-6.4 min: 170-190  $m/z$ , 6.4-7.2 min: 202-223  $m/z$ , 7.2-7.7 min: 159-191  $m/z$ , 7.7-8.6 min: 170-190  $m/z$ , 8.6-9.5 min: 152-172  $m/z$ . For  $\text{CH}_3\text{ONH}_2$  treated samples, 2-4 min: 200-213.5  $m/z$ , 4-5.73 min: 133-148  $m/z$ , 5.73-8.59 min: 170-186  $m/z$ , 8.59-9.2 min: 152-170  $m/z$ , 9.2-10.05 min: 227-245  $m/z$ , 10.05-12.1 min: 170-190  $m/z$ .

#### *Data analysis*

Raw files from the Orbitrap Q Exactive instrument were converted to mzXML files using the msconvert tool from the ProteoWizzard software suite (Chambers *et al.*, 2012). Quantitative information was extracted using a R code employing the XCMS package (Smith *et al.*, 2006) for raw data processing. Isotopic traces were extracted using a mass accuracy of  $\pm 0.0015$   $m/z$  and quantified by using a simple linear regression against the monoisotopmer (the primary trace in the internal standard) (MacCoss *et al.*, 2003; Huttlin *et al.*, 2007). The slope of each linear regression line was taken as the ratio of respective isotopic trace to that of the monoisotopmer. This approach was preferred over integrating the area under the curve when processing data with moderate instrument noise and high background due to low analyte abundance.

**Table 2-1 Isotopic traces measured in the [<sup>15</sup>N]ANT labeling experiment.**

| ANT (fmol · mg <sup>-1</sup> ) |                    |                   |       |       |       |       |       |       |       |
|--------------------------------|--------------------|-------------------|-------|-------|-------|-------|-------|-------|-------|
| Isotopic trace                 | before experiment* | Sampling time (h) |       |       |       |       |       |       |       |
|                                |                    | 0                 | 0.25  | 0.5   | 0.75  | 1     | 1.5   | 2     | 4     |
| M                              | 256                | 357               | 313   | 333   | 323   | 370   | 294   | 294   | 385   |
| M+N                            | 553                | 92                | 60    | 66    | 50    | 66    | 47    | 52    | 40    |
| M+C                            | 21                 | 28                | 22    | 27    | 25    | 29    | 21    | 21    | 30    |
| M+NC                           | 48                 | 7.59              | 3.51  | 2.82  | 3.97  | 5.40  | 3.22  | 3.32  | 1.80  |
| M+5C                           | 0                  | 0.00              | 423   | 267   | 217   | 272   | 279   | 305   | 269   |
| M+6C                           | 57.76              | 8.29              | 19866 | 14246 | 10513 | 14999 | 13706 | 15252 | 12769 |
| M+N6C                          | 0                  | 0                 | 49    | 47    | 29    | 44    | 37    | 40    | 32    |
| M+7C                           | 0                  | 0                 | 223   | 149   | 116   | 164   | 151   | 166   | 141   |

| Trp (pmol · mg <sup>-1</sup> ) |                    |                   |      |      |      |      |      |      |      |
|--------------------------------|--------------------|-------------------|------|------|------|------|------|------|------|
| Isotopic trace                 | before experiment* | Sampling time (h) |      |      |      |      |      |      |      |
|                                |                    | 0                 | 0.25 | 0.5  | 0.75 | 1    | 1.5  | 2    | 4    |
| M                              | 25.6               | 35.7              | 31.3 | 33.3 | 32.3 | 37.0 | 29.4 | 29.4 | 38.5 |
| M+N                            | 3.86               | 1.54              | 2.04 | 0.31 | 3.28 | 3.66 | 2.74 | 5.39 | 3.83 |
| M+C                            | 2.19               | 4.06              | 4.30 | 4.25 | 4.28 | 5.55 | 3.67 | 4.35 | 4.59 |
| M+2N                           | 52.9               | 19.6              | 21.5 | 1.26 | 27.4 | 24.5 | 34.2 | 44.5 | 29.8 |
| M+6C                           | 0.01               | 0.09              | 2.59 | 0.00 | 4.21 | 4.67 | 13.4 | 22.3 | 24.7 |
| M+N6C                          | 0                  | 0                 | 23.9 | 2.00 | 58.7 | 51.1 | 134  | 192  | 167  |
| M+N7C                          | 0                  | 0                 | 1.34 | 0.04 | 2.31 | 2.86 | 5.91 | 8.23 | 6.64 |

IPyA (fmol · mg<sup>-1</sup>)

| Isotopic trace | before experiment* | Sampling time (h) |      |      |      |      |      |      |      |
|----------------|--------------------|-------------------|------|------|------|------|------|------|------|
|                |                    | 0                 | 0.25 | 0.5  | 0.75 | 1    | 1.5  | 2    | 4    |
| M              | 513                | 714               | 625  | 667  | 645  | 741  | 588  | 588  | 769  |
| M+N            | 12776              | 4925              | 1787 | 2854 | 3381 | 3636 | 3680 | 3280 | 2462 |
| M+C            | 124                | 70                | 51   | 30   | 22   | 30   | 59   | 55   | 49   |
| M+NC           | 1765               | 880               | 274  | 421  | 446  | 637  | 659  | 419  | 363  |
| M+6C           | 0                  | 1.30              | 984  | 2376 | 3593 | 4012 | 6901 | 5691 | 3623 |
| M+7C           | 0                  | 0                 | 76   | 178  | 303  | 335  | 624  | 445  | 331  |

IAAId (fmol · mg<sup>-1</sup>)

| Isotopic trace | before experiment* | Sampling time (h) |       |       |       |       |       |       |       |
|----------------|--------------------|-------------------|-------|-------|-------|-------|-------|-------|-------|
|                |                    | 0                 | 0.25  | 0.5   | 0.75  | 1     | 1.5   | 2     | 4     |
| M              | 51.28              | 71.43             | 62.50 | 66.67 | 64.52 | 74.07 | 58.82 | 58.82 | 76.92 |
| M+N            | 520.02             | 24.67             | 16.62 | 19.33 | 20.45 | 1.32  | 15.53 | 11.48 | 22.40 |
| M+C            | 0.00               | 8.55              | 8.87  | 9.12  | 10.14 | 9.07  | 8.33  | 7.44  | 10.98 |
| M+NC           | 62.12              | 2.61              | 1.76  | 1.74  | 2.83  | 0.13  | 1.78  | 1.78  | 2.26  |
| M+6C           | 0.00               | 0.00              | 3.90  | 7.20  | 6.28  | 0.34  | 10.22 | 16.24 | 46.46 |
| M+7C           | 0.60               | 0.44              | 0.83  | 0.06  | 1.19  | 0.04  | 0.64  | 1.19  | 2.67  |

IAN (pmol · mg<sup>-1</sup>)

| Isotopic trace | before experiment* | Sampling time (h) |       |       |       |       |       |       |       |
|----------------|--------------------|-------------------|-------|-------|-------|-------|-------|-------|-------|
|                |                    | 0                 | 0.25  | 0.5   | 0.75  | 1     | 1.5   | 2     | 4     |
| M              | 12.82              | 17.86             | 15.63 | 16.67 | 16.13 | 18.52 | 14.71 | 14.71 | 19.23 |
| M+N            | 60.57              | 4.21              | 6.62  | 4.41  | 3.04  | 1.96  | 2.36  | 2.46  | 4.79  |
| M+C            | 0.00               | 1.57              | 1.40  | 1.12  | 1.58  | 1.82  | 1.44  | 1.24  | 1.81  |
| M+NN           | 1218               | 52.65             | 63.39 | 50.18 | 30.53 | 20.74 | 26.70 | 22.55 | 41.16 |
| M+NNC          | 18.95              | 0.93              | 1.39  | 1.07  | 0.68  | 0.46  | 0.51  | 0.60  | 1.18  |
| M+N6C          | 0.00               | 0.00              | 0.00  | 0.09  | 0.06  | 0.13  | 0.43  | 1.05  | 2.84  |
| M+N7C          | 0.00               | 0.00              | 0.00  | 0.00  | 0.00  | 0.00  | 0.00  | 0.00  | 0.07  |

*trans*-IAOx \*\* (fmol · mg<sup>-1</sup>)

| Isotopic trace | before experiment* | Sampling time (h) |       |       |       |       |       |       |       |
|----------------|--------------------|-------------------|-------|-------|-------|-------|-------|-------|-------|
|                |                    | 0                 | 0.25  | 0.5   | 0.75  | 1     | 1.5   | 2     | 4     |
| M              | 51.28              | 71.43             | 62.50 | 66.67 | 64.52 | 74.07 | 58.82 | 58.82 | 76.92 |
| M+N            | 0.00               | 6.77              | 1.74  | 13.01 | 2.39  | 4.06  | 4.11  | 5.43  | 6.10  |
| M+C            | 0.03               | 11.20             | 7.73  | 5.28  | 8.10  | 8.87  | 7.48  | 3.24  | 8.15  |
| M+NN           | 0.00               | 63.91             | 29.88 | 51.67 | 42.44 | 23.90 | 28.37 | 28.52 | 24.71 |
| M+NC           | 7.43               | 3.21              | 0.00  | 3.28  | 0.00  | 3.22  | 0.00  | 7.48  | 7.59  |
| M+2NC          | 0.00               | 0.00              | 0.00  | 0.00  | 0.00  | 0.00  | 0.00  | 0.00  | 0.00  |
| M+N6C          | 0.00               | 9.96              | 585   | 343   | 348   | 6.37  | 7.40  | 10.20 | 541   |
| M+N7C          | 0.00               | 0.00              | 0.00  | 0.00  | 0.00  | 0.00  | 0.00  | 0.00  | 0.00  |

*cis*-IAOx (fmol · mg<sup>-1</sup>)

| Isotopic trace | before experiment* | Sampling time (h) |       |       |       |       |       |       |       |
|----------------|--------------------|-------------------|-------|-------|-------|-------|-------|-------|-------|
|                |                    | 0                 | 0.25  | 0.5   | 0.75  | 1     | 1.5   | 2     | 4     |
| M              | 51.28              | 71.43             | 62.50 | 66.67 | 64.52 | 74.07 | 58.82 | 58.82 | 76.92 |
| M+N            | 9.15               | 3.97              | 0.00  | 0.00  | 3.32  | 7.45  | 4.32  | 0.00  | 0.71  |
| M+C            | 0.00               | 11.75             | 7.81  | 8.41  | 4.70  | 10.91 | 7.57  | 8.93  | 3.81  |
| M+NN           | 0.00               | 69.18             | 40.91 | 36.65 | 40.84 | 28.98 | 36.72 | 45.98 | 29.18 |
| M+NC           | 21.46              | 0.90              | 0.00  | 0.00  | 0.00  | 0.80  | 0.23  | 3.56  | 2.84  |
| M+2NC          | 36.96              | 0.00              | 2.91  | 3.34  | 0.00  | 0.00  | 0.00  | 0.00  | 2.79  |
| M+N6C          | 0.00               | 0.00              | 4.77  | 0.00  | 0.40  | 1.71  | 4.59  | 4.93  | 0.00  |
| M+N7C          | 0.00               | 0.00              | 0.00  | 0.00  | 0.45  | 0.00  | 0.00  | 0.90  | 0.00  |

IAA (fmol · mg<sup>-1</sup>)

| Isotopic trace | before experiment* | Sampling time (h) |      |      |      |      |      |      |      |
|----------------|--------------------|-------------------|------|------|------|------|------|------|------|
|                |                    | 0                 | 0.25 | 0.5  | 0.75 | 1    | 1.5  | 2    | 4    |
| M              | 51.28              | 71.4              | 62.5 | 66.7 | 64.5 | 74.1 | 58.8 | 58.8 | 76.9 |
| M+N            | 1830.25            | 27.3              | 17.3 | 17.7 | 17.2 | 18.3 | 13.1 | 13.8 | 13.4 |
| M+C            | 0                  | 7.13              | 6.51 | 7.22 | 7.22 | 7.64 | 6.16 | 6.36 | 8.29 |
| M+NC           | 222.42             | 2.96              | 1.93 | 2.02 | 1.95 | 1.96 | 1.44 | 1.59 | 1.40 |
| M+6C           | 2.77               | 0                 | 0.64 | 0.96 | 2.10 | 3.48 | 7.59 | 6.75 | 8.84 |
| M+7C           | 0                  | 0                 | 0    | 0    | 0.02 | 0.18 | 0.31 | 0.36 | 0.43 |

In the table, M is the monoisotoper for each compound. M+N means the single [<sup>15</sup>N] isotopmer, M+N6C means the [<sup>15</sup>N, <sup>13</sup>C<sub>6</sub>] isotopmer, etc. The monoisotopic trace was calculated as the amount of internal standard divided by fresh weight of tissue. All other traces were normalized to the monoisotopomer by means of linear regression of the chromatographic peaks. \* Isotopic state data collected prior to labeling precursor application (no internal standard added) and processed mathematically in an identical manner, allowing the evaluation of isotopic labeling state of the plants after a certain period of time growing on [<sup>15</sup>N]-media. \*\*The M+N6C

trace for *trans*-IOAx was artificially high due to background noise fluctuations and low signal. *cis*-IAOx gave a more accurate reflection of the labeling kinetics.

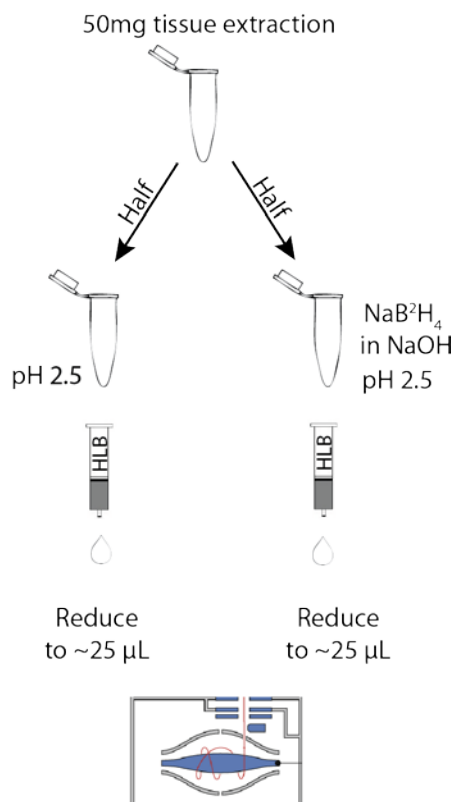
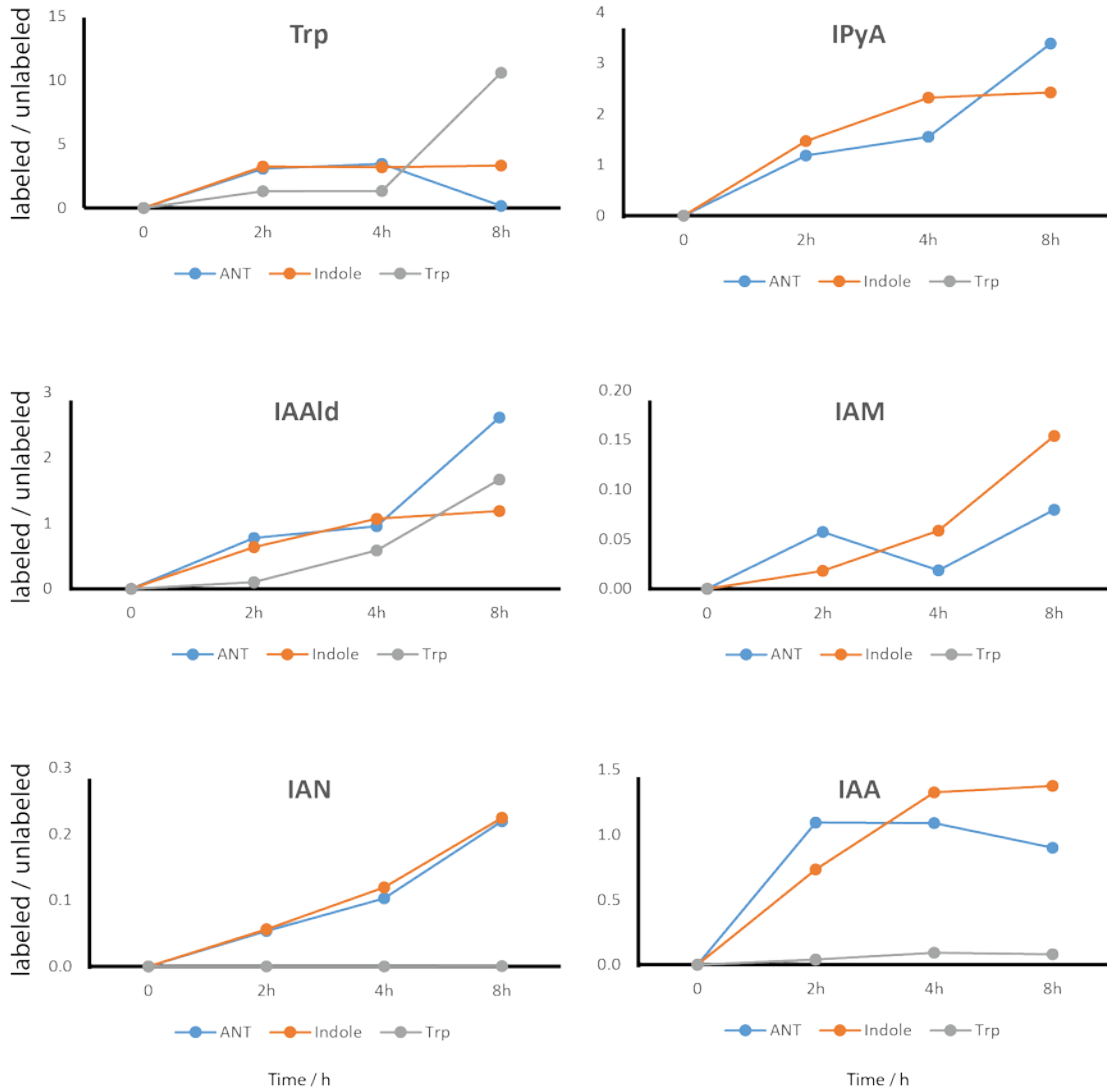


**Figure 2-1 NaB<sub>2</sub>H<sub>4</sub> derivatization based workflow for measuring auxin precursors.** Plant tissues were extracted in buffer and split into two batches. One was used to analyze IPyA and IAAld after derivatization, and the other one was used to quantify the rest of the compounds. A one step HLB solid phase extraction was performed prior to LC-MS analysis. Absolute quantification was achieved by isotope dilution.



Fed precursor

Fed precursor

**Figure 2-2 Labeling patterns of auxin precursors via ANT, Indole or Trp feeding.** 75  $\mu\text{M}$  [ $^{15}\text{N}$ ]-ANT, 50  $\mu\text{M}$  [ $^{15}\text{N}$ ]-Indole, 25  $\mu\text{M}$  [ $^{13}\text{C}_{11}$ ,  $^{15}\text{N}_2$ ]-Trp used to label 18d *Arabidopsis* for 8 h. Plants were harvested at specific time intervals and were then extracted for LC-MS analysis. Each isotopic trace of different auxin precursors was individual measured using the method described in Figure 2-1. Labeled / unlabeled refers to the amount of a certain compound synthesized from the fed precursor to that of the endogenous. Note the difference in the y-scale. Clearly, IPyA and IAAld were labeled much faster than the other precursors.

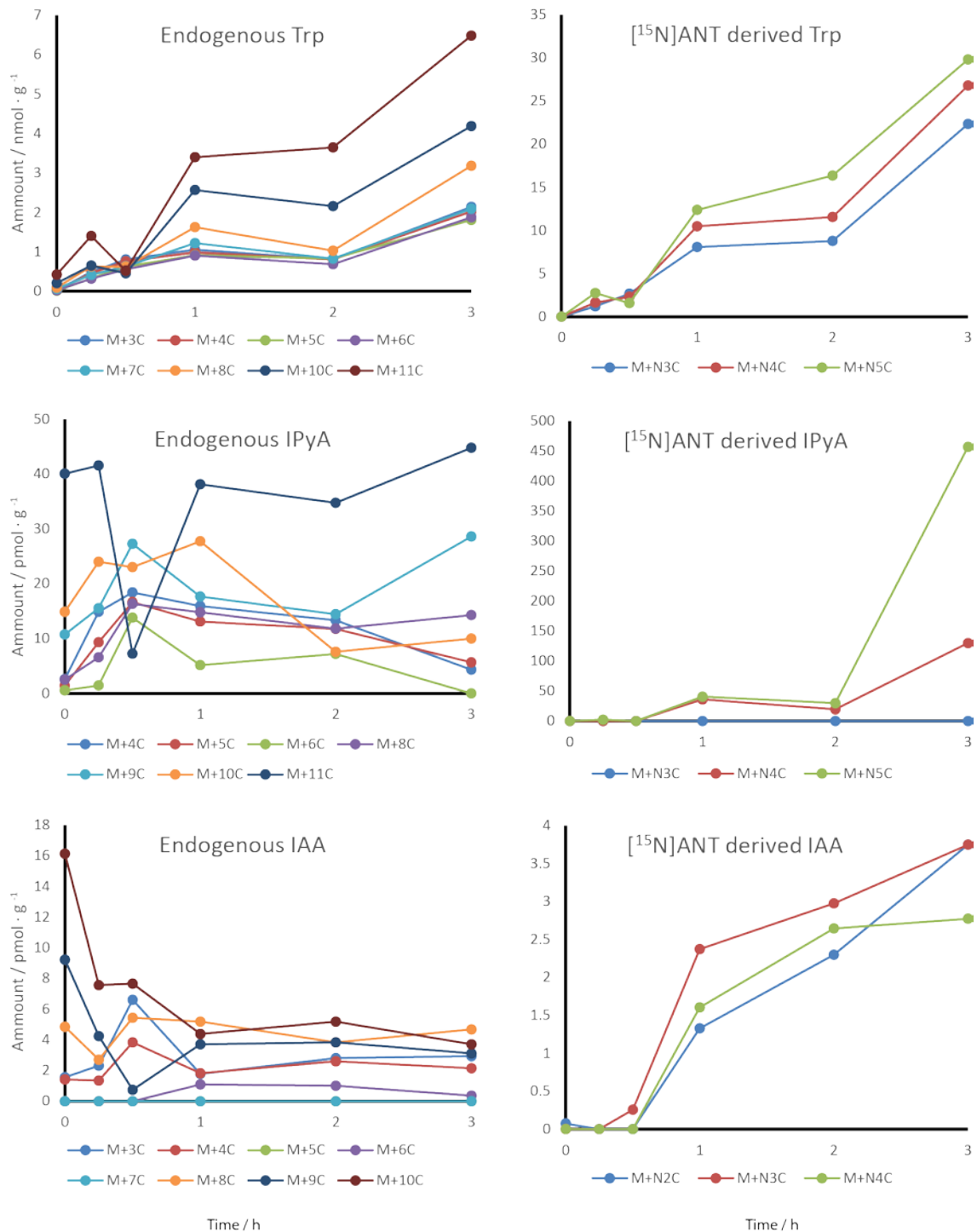


**Figure 2-3 Quantitative analysis of auxin precursor labeling patterns.** 50  $\mu\text{M}$  [<sup>15</sup>N]ANT was used to label 17d *Arabidopsis* seedlings grown on [<sup>13</sup>C]glucose supplemented with 1  $\mu\text{M}$  ANT. Auxin precursors were quantified using the method described in Figure 2-1. It was obvious that there was a high degree of labeling inhomogeneity after 17d of [<sup>13</sup>C] labeling. Also notice the fast accumulation of Trp and IPyA, but IAA level was relatively stable.

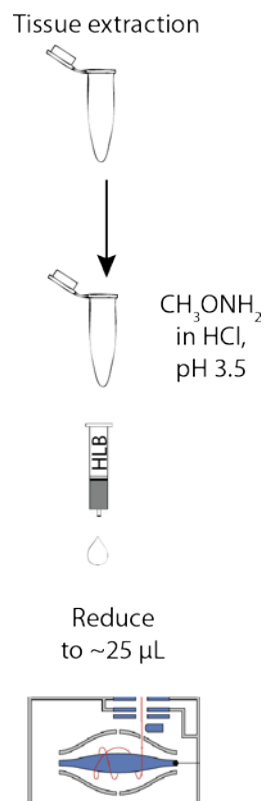


**Figure 2-4 CH<sub>3</sub>ONH<sub>2</sub> derivatization-based workflow of auxin precursor measurement.** Using the CH<sub>3</sub>ONH<sub>2</sub> derivatization chemistry, IPyA and IAAld can be derivatized *in situ*, and all auxin precursors can be quantified at once. One HLB solid phase extraction step was necessary to prepare the sample for LC-MS analysis. Each isotopic trace for all compounds were individual measured via high resolution / accurate mass MS and normalized to that of the internal standard where applicable.

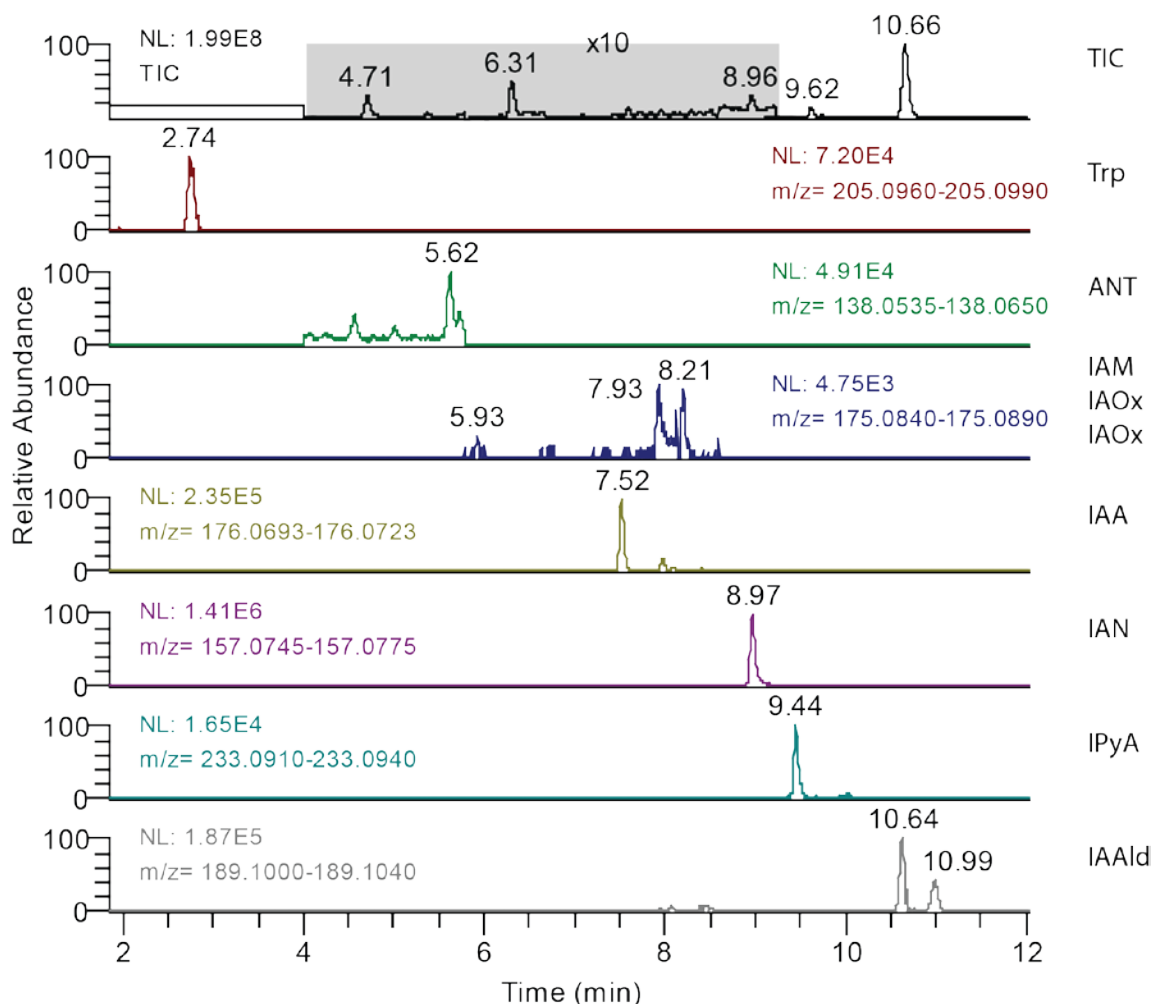


**Figure 2-5 Quantitative measurement of auxin precursors by LC-MS.** Top panel is the total ion chromatogram (TIC). Subsequent panels are the extracted ion chromatograms (EIC) for the individual compounds. MS was operated in full scan mode and the specificity and signal-to-noise ratio were afforded by high resolution / accurate mass (HR/MS), which also ensured the required sensitivity for the low level auxin precursors amid high background noise.

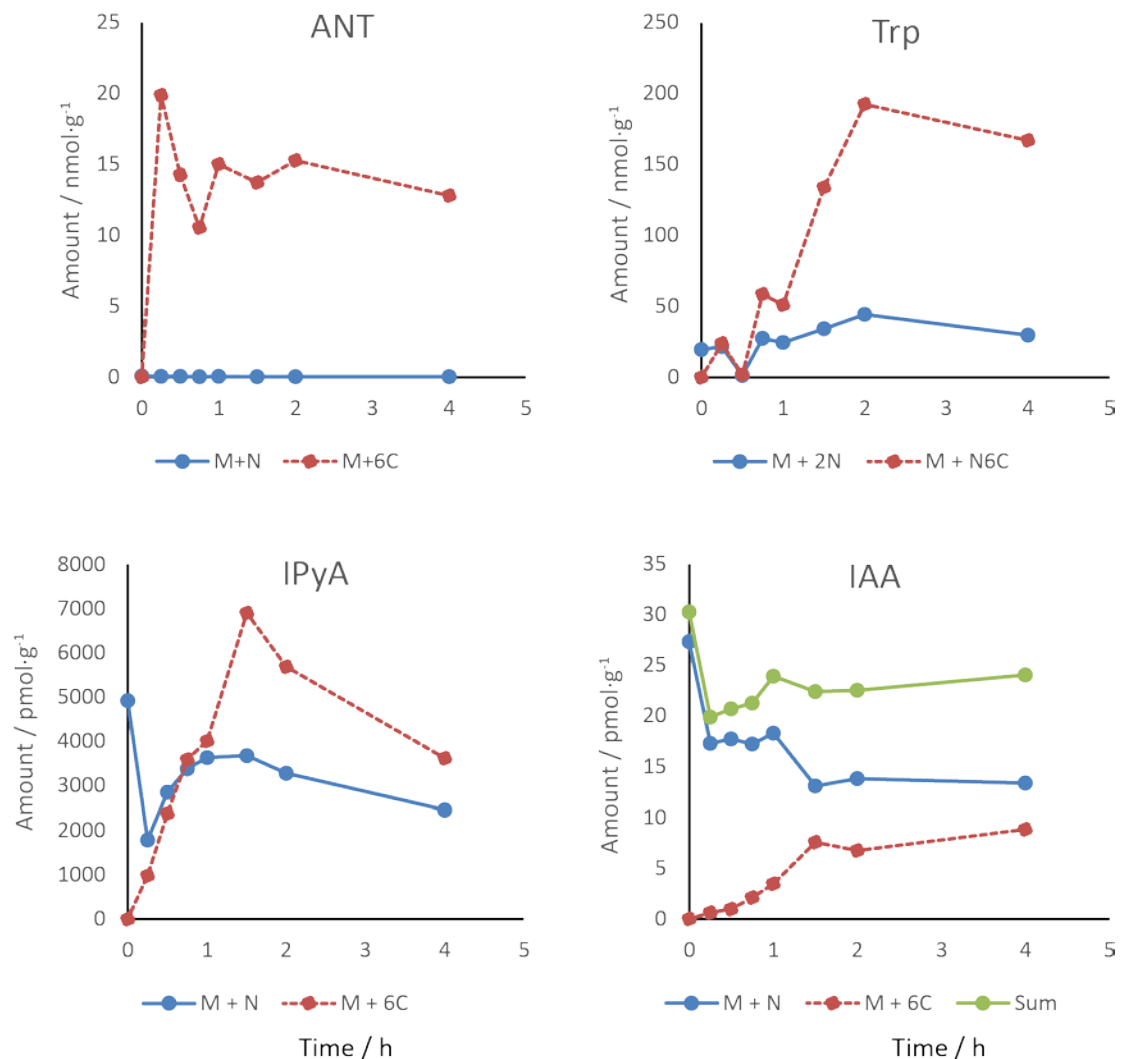


**Figure 2-6** [<sup>13</sup>C<sub>6</sub>]ANT labeling of auxin precursors. *Arabidopsis* seedlings were grown for 16d on [<sup>15</sup>N]-media followed by a flooding application of [<sup>13</sup>C<sub>6</sub>]ANT. “M+N” is the [<sup>15</sup>N]-labeled version of each compound and also the endogenous form. “M+6C” or “M+N6C” is the [<sup>13</sup>C<sub>6</sub>] or [<sup>13</sup>C<sub>6</sub>, <sup>15</sup>N]-labeled form of the compound, derived from [<sup>13</sup>C<sub>6</sub>]ANT. The isotopic forms were much simpler, and fast Trp and IPyA accumulation, steady IAA level were also observed.

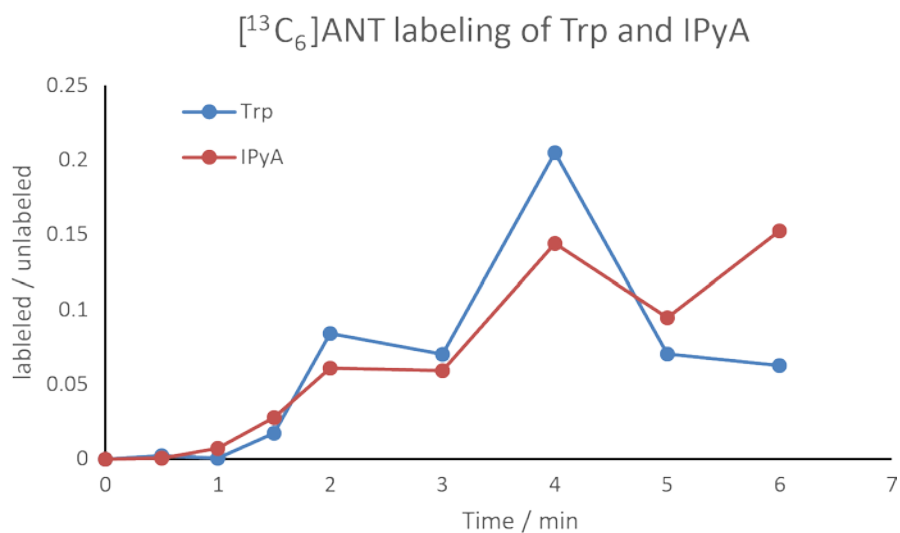


**Figure 2-7 Minute-scale labeling patterns of IPyA and Trp following ANT application.** 25  $\mu$ M [<sup>13</sup>C<sub>6</sub>]ANT was used to label 11d *Arabidopsis* seedlings. The similar labeling kinetics indicated either the conversion from Trp to IPyA was very fast or they were parallelly synthesized from common upstream precursors.

## Chapter 3 Quantitative evaluation of IAA conjugate pools in *Arabidopsis thaliana*

### Abstract

The concept of 'bound auxin' traces its origin to more than eighty years ago and has driven research on the sources and forms of these plant hormones in plant materials since. Indeed, analytical studies have demonstrated that the majority of cellular auxin is conjugated to simple sugars, cyclitols, glycans, amino acids, and other biomolecules. A number of studies have confirmed the enzymatic systems and genes responsible for the synthesis and hydrolysis of a number of such conjugated forms of the auxin IAA in *Arabidopsis thaliana* and a number of these compounds have been identified *in situ*. However, the amount of IAA released upon treating *Arabidopsis* tissue extracts with base, a commonly employed technique for estimating the conjugated forms, greatly exceeded the summation of all the IAA conjugates known individually to be present in *Arabidopsis*. This discrepancy has remained as an unsolved question. In this study, however, we found that a significant portion of the IAA found after base treatment could be attributed to chemical conversions other than conjugate hydrolysis. Specifically, we showed that glucobrassicin conversion, previously thought to occur at insignificant levels, actually accounted for the majority of solvent soluble IAA released and that proteinaceous tryptophan degradation accounted for a large portion of solvent insoluble IAA. These studies clearly demonstrated the limits associated with using a harsh technique such as base hydrolysis in determining IAA conjugates and support using more direct approaches such as mass spectrometry and nuclear magnetic resonance spectroscopy based strategies for unambiguous characterizations of the total complement of IAA conjugates in new plant materials under study.

### Introduction

Within most plant tissues the conjugation of indole-3-acetic acid (IAA) to other biomolecules accounts for a significant amount of the total IAA pool and this biochemical process has been known for well over half a century (Andreae and Good, 1955). Indeed, the concepts of “bound auxin” and “seed auxin precursor” were proposed around the same time as when IAA itself was discovered to be the active growth substance in plants (Cholodny, 1935; Kögl *et al.*, 1934; Thimann, 1935). Since then, researchers have used a variety of analytical approaches to show that the majority of IAA in many parts of the plants, especially in seeds and endosperm, is actually conjugated to various biomolecules and these conjugates serve many functions involved in the regulation of the levels of the active hormone in target tissues. These functions include: 1) protection against enzymatic degradation (Cohen and Bandurski, 1978); 2) facilitation of auxin transport (Chisnell and Bandurski, 1988; Komoszynski and Bandurski, 1986; Nowacki and Bandurski, 1980); 3) storage forms of IAA during seed development and seedling growth (Ljung *et al.*, 2001); 4) entry route in auxin catabolism (Tsurumi and Wada, 1986; Östin *et al.*, 1998); 5) Involvement in stress responses and pathogen interactions (Ding *et al.*, 2008; González-Lamothe *et al.*, 2012).

The endosperm of *Zea mays*, beginning with an initial report (Labarca *et al.*, 1965), was the focus of a comprehensive analysis covering the identity, amounts as well as both the biochemistry and physiology of endogenous IAA conjugates and their role in seedling growth (Cohen and Bandurski, 1982). In these classic studies both base hydrolysis and ammonolysis were used to confirm the ester linkage of the sugar conjugates (Bandurski and Ehmann, 1986; Hall, 1980). At the time, isotopically labeled internal standards were not available for the known conjugates and many conjugated forms were unknown. Thus, selective base hydrolysis of the solvent extractable fractions of the plant materials was very useful in the early characterization of IAA conjugates. These investigative efforts included the exploration of extraction conditions (Bandurski *et al.*, 1970), the prevalence of IAA conjugates among various plant species (Bandurski and Schulze, 1977; Bandurski and Schulze, 1974), the identification of unknown forms (Bandurski and Piskornik, 1973), and chemical classification of IAA conjugates (Bandurski and Schulze, 1977). Along with other analytical approaches, using such

methods established that IAA was present in plant tissues as: ester conjugates characterized by the “-O” linkage between the IAA and a sugar or alcohol moiety, such as IAA myo-inositol, IAA glucans, IAA glycoproteins, IAA glucose esters and the 1-O-acyl alkyl acetal; and amide conjugates characterized by the “-N” linkage between IAA and amino acids, such as IAA amino acids and IAA-peptide conjugates (Slovin *et al.*, 1999). In a study of seeds from a diverse number of both dicotyledonous and monocotyledonous species, this method of selective hydrolysis was based on the widely different conditions required for hydrolysis of ester and amide bonds. Typically, 1 M sodium hydroxide (NaOH) treatment of the sample for 1 h at room temperature was found to be adequate to hydrolyze IAA ester conjugates completely to release free IAA without affecting IAA amide conjugates (Bandurski and Schulze, 1977). In contrast, 7 M NaOH treatment at 100 °C for 3 h was found to completely hydrolyze all conjugated forms of IAA and this total hydrolysable IAA was termed “total IAA”. By subtraction, the amount of free IAA, ester conjugates, and amide conjugates were then derived. By such techniques it was found that the majority of IAA in seeds as well as many other tissues existed in conjugated forms, and endosperm tissues were typically enriched in ester conjugates while amide conjugates were more prevalent in dicotyledonous seeds (Bajguz and Piotrowska, 2009; Bandurski and Schulze, 1977; Ljung *et al.*, 2002; Tam *et al.*, 2000).

In relation to hydrolysis, several aspects of the procedure were examined. First, the issue of inadvertent hydrolysis, especially of esters, was discussed and studied (Bandurski and Schulze, 1974; Ueda and Bandurski, 1969) such that conditions where IAA-esters were stable during free IAA extraction were determined. In addition, issues of incomplete extraction as well as incomplete hydrolysis were considered regarding their potential for errors (Bandurski and Schulze, 1977). Early on, several authors raised the issue of auxin biogenesis during protein hydrolysis (Gordon, 1946; Schocken, 1949; Vlitos and Meudt, 1953), although in these early studies low concentrations of base (0.1 M NaOH) yielded IAA from a variety of different proteins while higher concentrations of base (4.5 M NaOH) at 100 °C did not (Schocken, 1949). This issue of protein yielding IAA upon hydrolysis was also studied in maize, where 1 M NaOH liberated IAA only

from the ethanol-soluble protein fraction and not from the ethanol insoluble fraction (Hamilton, 1961). Treatment of either zein protein (which has a low relative level of protein tryptophan) or free tryptophan itself also did not yield IAA, and this was interpreted as suggesting that tryptophan conversion was not accounting for the IAA released under these conditions (Hamilton, 1961). Later studies, however, indicated that a small fraction (molar ratio of 1:175) of zein protein contained esterified IAA (Leverone *et al.*, 1991) but no additional IAA was formed by hydrolysis of the zein protein in 7 M NaOH, at 100 °C for 3 h. Although it has been commonly recognized that an oxidative deamination and decarboxylation of tryptophan could yield IAA under basic conditions, the exact conditions for this to happen were not well defined by these earlier studies.

Conversion of proteinaceous tryptophan to IAA became a more complex issue when unextracted plant materials were subjected to 7 M NaOH hydrolysis conditions (Bialek and Cohen, 1989). Such studies were required to further characterize the auxin conjugates in *Phaseolus vulgaris* seeds, where the conjugate pools consisted of a small solvent extractable peptide (Bialek and Cohen, 1986) and a larger water soluble protein that did not contain tryptophan (Walz *et al.*, 2002). Hydrolysis conditions that rigorously excluded oxygen resulted in a stable yield of IAA from bean seed powder up to 6 h in 7 M NaOH at 100 °C. However, the time course for hydrolysis from plant materials was significantly slower (3 h to completion) than with an IAA-glycine standard (1 h) and simply using nitrogen sparging without an oxygen trap yielded significant ‘excess’ IAA production after four or more hours of exposure to hydrolysis conditions (Bialek and Cohen, 1989). These studies defined a workable solution to approach the characterization of the novel conjugates in *Phaseolus*, but the authors noted caution about its application more broadly: “Within the plant kingdom a vast array of indolic compounds are present, some of which can be converted to IAA under extreme conditions such as are required for amide hydrolysis. Therefore, application of such techniques to new diverse plant species should always be undertaken with due caution and with appropriate control experimental studies.”

Based on labeled IAA feeding experiments, indole-3-acetyl aspartic acid (IA-Asp), indole-3-acetyl glutamic acid (IA-Glu) were shown to be formed by *Arabidopsis*

*thaliana* tissue (Östin, *et al.*, 1998), a metabolic pathway well established for auxins applied to plant tissues of diverse species (Cohen and Bandurski, 1982). These two conjugates, as well as IAA-glucose and IAA-glutamine, were also shown to be present at low levels in *Arabidopsis* without IAA addition by subsequent investigators (Barratt *et al.*, 1999; Tam *et al.*, 2000); and, in addition, indole-3-acetyl alanine (IA-Ala; (Kowalczyk and Sandberg, 2001)), indole-3-acetyl leucine (IA-Leu; (Kowalczyk and Sandberg, 2001)), and indole-3-acetyl tryptophan (IA-Trp; (Staswick, 2009)) were later identified in untreated *Arabidopsis* tissues. Because of the diverse array of indolic natural products, intermediates in their formation and degradation, and the potential for accumulation of large excesses of compounds such as the indole glucosinolates and camalexin, aspects of auxin analysis in *Arabidopsis* remain an important but difficult analytical challenge. Thus, a large discrepancy exists between the concentrations measured for known forms of IAA conjugates and the amount of IAA measured following base hydrolysis (Ljung *et al.*, 2002; Tam *et al.*, 2000) even after correction for endogenous indole-3-acetonitrile (IAN) conversion to IAA during hydrolysis (Ilić *et al.*, 1996). The identities of these “unknown IAA conjugates” remained elusive and were the topic of some speculation in subsequent review articles (Woodward and Bartel, 2005; Ludwig-Müller, 2011; Korasick, *et al.*, 2013). In this study we have investigated the origins of total IAA profile, with special attention to analytical artifacts, for *Arabidopsis*, guided by the results of the classical base hydrolysis method while now complemented with sensitive modern analytical methodologies. We separately targeted solvent soluble small molecule conjugates and solvent insoluble IAA protein conjugates. We found chemical species other than IAA conjugates were capable of converting to IAA under alkaline conditions at very small yet significant rates. These findings and their implications, as well as recommendations for future approaches, are discussed.

## **Results and discussion**

### **Low molecular weight IAA conjugates**

In *Arabidopsis*, consistent with what has been reported in other dicotyledonous plants, most of the as yet unidentified IAA conjugates were proposed to be alcohol

extractable amide conjugates (Tam *et al.*, 2000). The amount of ‘free IAA’, ‘ester conjugates’, and ‘amide conjugates’ in the material we analyzed were about  $0.25 \text{ nmol} \cdot \text{g}^{-1}$ ,  $9.5 \text{ nmol} \cdot \text{g}^{-1}$ , and  $34.4 \text{ nmol} \cdot \text{g}^{-1}$  respectively, as determined by the differential hydrolysis method. In our initial studies for the previously uncharacterized IAA conjugates we attempted to establish their approximate molecular weight range by analysis of the 65% 2-propanol extracts of the seeds. Extracted compounds were filter fractionated using a 3 KDa molecular weight cut-off filter. The filtrate obtained after passage through a 3 kDa sizing membrane contained the majority of the IAA conjugates (data not shown), suggesting their size was below the filter’s cutoff. Further fractionation of the extract, with strong anion exchange chromatography, and analysis of the IAA conjugate profile in each of the fractions showed that the vast majority of the IAA recovered after hydrolysis was in a single fraction (Figure 3-1). Surprisingly, we identified the major indolic compound in this fraction to be glucobrassicin (also known as indol-3-ylmethylglucosinolate) which was unexpected, given a previous report showed glucobrassicin was unlikely to yield IAA under these conditions (Ilić *et al.*, 1996).

However, further investigation revealed that there was actually a very minor conversion from glucobrassicin to IAA (Table 3-1) during a 7 M NaOH hydrolysis. The rate of conversion was a mere 1.5%, but somewhat higher than that in a previous study where it was reported to be below the level of detection (Ilić *et al.*, 1996). However, given the relative abundance of glucobrassicin to IAA in the Brassicaceae plant *Arabidopsis thaliana*, the amount of IAA yielded from glucobrassicin was a substantial interference to the analytical need to determine the native auxin conjugates in this plant material. To calculate how much solvent soluble IAA amide conjugates can be attributed to glucobrassicin, we used the literature value of glucobrassicin abundance of  $1.5 \text{ } \mu\text{mol} \cdot \text{g}^{-1}$  in mature seeds (Brown *et al.*, 2003). Based on our observed conversion rate, we estimated that over  $20 \text{ } \mu\text{mol} \cdot \text{g}^{-1}$  or more than 2/3 of the solvent soluble putative ‘IAA amide conjugates’ potentially can be attributable to glucobrassicin.

The observation that glucobrassicin can be chemically converted to IAA, even at relatively minor rates, is not entirely surprising given the structural similarities and this

prospect had been of concern previously, in part because of the known catabolic and chemical degradation route through IAN which itself is hydrolysable to IAA (Ilić *et al.*, 1996; Slominski and Campbell, 1989). Thermo degradation of pure glucobrassicin has also been reported before (Chevolleau *et al.*, 1997; Chevolleau *et al.*, 2002), but neither IAN nor IAA was a stable product. Enzymatic degradation of glucobrassicin is known to produce indole-3-acetonitrile under specific circumstances (Burow *et al.*, 2008), which has at various times been proposed as a potential IAA precursor. If not extracted properly, myrosinase catalyzed IAN production could give rise to significant amounts of IAA upon hydrolysis. Whether indole-3-acetonitrile is also a minor intermediate in the base hydrolysis experiment has yet to be determined and it must be pointed out that most prior work on thermal conversions of glucobrassicin did not exclude oxygen during the temperature treatment, so that additional studies are clearly needed to clarify the chemical degradation noted in our studies. These quantitative estimates for conversion to IAA still leave the potential for a portion (about one third) of low MW IAA-yielding compounds with potentially unknown identities. However, the finding that under these conditions some tryptophan species can also convert to IAA adds to the question of how much of the remaining IAA yield can be accounted for by IAA amine-linked compounds (see the following section). Nevertheless, we cannot exclude the presence of a low level of IAA-peptide(s), as previously suggested (Ljung *et al.*, 2002). Also note for example, that in addition to the known IAA-amino acids, there has also been a 3.6 kDa IAA peptide conjugate described in common bean (*Phaseolus vulgaris*) (Bialek and Cohen, 1986), a plant devoid of glucosinolates, where the peptide moiety did not contain tryptophan.

### **High molecular weight IAA conjugates**

Organic solvent insoluble conjugates include mostly IAA polysaccharides and IAA proteins (Cohen and Bandurski, 1982), and the latter is the form suggested based primarily on immunological data as occurring in *Arabidopsis* (Park *et al.*, 2006; Park *et al.*, 2010; Seidel *et al.*, 2006). While there has been a long history of research on the possibility for IAA being attached to proteins in plants, only two IAA protein conjugates have been explicitly identified to date; a heterogeneous IAA-glycoprotein fraction, with IAA esterified to the carbohydrate portion, was isolated from oat (Percival and

Bandurski, 1976), and a protein with IAA attached was reported in *Phaseolus vulgaris* seeds (Walz *et al.*, 2002). Both of these appear to be species-specific and the sites of IAA modification on the protein remain to be identified. When the bean protein was overexpressed in *Arabidopsis* or *Medicago*, it was not modified by IAA (Walz *et al.*, 2008) and a protein with a closely related amino acid sequence was isolated from soybean and it was not modified by IAA either (Walz *et al.*, 2002). However, there have been reports supporting the presence of IAA protein conjugates in *Arabidopsis*, strawberries and pea (Park *et al.*, 2006; Park *et al.*, 2010; Seidel *et al.*, 2006), and the sequence identities of these proteins and further characterizations remain to be determined.

We began the investigation of IAA protein conjugates in *Arabidopsis* by fractionating the seed protein extract and enriching for proteins with IAA modifications. We used both ion exchange chromatography and reversed phase chromatography for the fractionation, but could not achieve substantial enrichment on a protein basis. In other words, the amount of IAA released after base treatment always correlated with the amount of protein in the fractions (data not shown). We then digested the protein with trypsin into shorter peptides and repeated the fractionation and enrichment processes. Interestingly, the IAA content in each fraction loosely correlated with the UV absorption at 280 nm (Figure 3-2), which is indicative of the presence of IAA, tryptophan, or tyrosine residues.

Next, we tested the possibility whether IAA came from tryptophan residues in the peptide during base treatment. For this purpose, we treated tryptophan, two non-plant proteins, BSA and ovalbumin, and an *Arabidopsis* seed protein extract under conditions for IAA amide conjugate hydrolysis. Results are shown in Table 3-2. Again, there is a small but noticeable conversion from proteins to IAA, amounting to 0.05% tryptophan converted to IAA. We hypothesized that tryptophan, rather than some other amino acid residue, was potentially responsible for producing IAA, because tryptophan is the only amino acid that has the indole ring structure and thus it was capable of conversion by simple oxidative steps (Table 3-2). It is important to note that while different proteins

exhibit quite different reaction stoichiometry on a weight basis, they nevertheless were much closer together when normalized on a tryptophan basis (Table 3-2). While there were older reports of IAA genesis from protein and tryptophan under alkaline conditions (Gordon and Wildman, 1943; Schocken, 1949), these studies had not excluded oxygen from the reaction. Only a very low conversion of free [<sup>15</sup>N]tryptophan to IAA was noted during 7 M NaOH hydrolysis (Bialek and Cohen, 1989), but they noted that Felker (1976) had reported a greater instability of tryptophan in proteins during acid hydrolysis as compared to the free amino acid and suggested a similar differential stability during basic hydrolysis could explain their findings. Because *Arabidopsis* contains relatively low amounts of conjugated IAA, even low levels of tryptophan conversion that did not cause significant problems with analysis of bean protein conjugates (Bialek and Cohen, 1989) have a significant impact on the specificity of the procedures when applied to *Arabidopsis* seeds.

Although tryptophan is one of the rarest amino acids contained in cellular proteins; the level of free tryptophan in most tissues is still three orders of magnitude higher than the level of free IAA (Tam *et al.*, 1995), and tryptophan residues in proteinaceous species would be substantially (10<sup>2</sup>-10<sup>3</sup> times as much) more (USDA, 2013). To calculate how much total insoluble IAA conjugates can be attributed to protein degradation, we separately treated *Arabidopsis* seed tissues and seed protein extracts under identical condition for measuring total IAA (Table 3-2). *Arabidopsis* seed was estimated to have 50% of its dry weight as proteins (Baud *et al.*, 2002; Mansfield and Briarty, 1992). If we consider the protein in the seed extract to represent the average seed protein, the amount of IAA produced from proteinaceous tryptophan is approximately calculated as: IAA yield per unit amount of protein on weight basis (Table 3-2) x percentage of protein weight over entire seed weight x seed weight per weight unit, or 86 ± 22 nmol · g<sup>-1</sup> x 50% x 1 g · g<sup>-1</sup> = 43 ± 11 nmol · g<sup>-1</sup>. The amount of solvent insoluble IAA conjugates is calculated as: ‘Total IAA after tissue hydrolysis (Table 3-2)’ - ‘Solvent soluble IAA (Free IAA + IAA ester conjugates + IAA amide conjugates, found under **Low molecular weight IAA conjugates**)’, or (181 - 0.25 - 9.5 - 34.4) nmol · g<sup>-1</sup> = 137 nmol · g<sup>-1</sup>. In other words, approximately 30% of the ‘insoluble IAA conjugate’ fraction

potentially resulted from the degradation of tryptophan in the base treatment process. Again, the calculation should be viewed as only an approximation. The conversion of tryptophan to IAA clearly would best be viewed as a stochastic process and it is only safe to assume it varies with the different proteins. This point is also illustrated by the large variations seen in the replicated experiments (Table 3-2). Because of these considerations, it is difficult to tell the full contribution of seed protein tryptophan to this “IAA protein conjugate” fraction without pure preparation of all the tryptophan containing species to study individually. Hence, the proportion of 7 M sodium hydroxide hydrolysable IAA that can be attributed to protein tryptophan is difficult to precisely gauge.

It is worth pointing out; however, that the only IAA protein conjugate clearly identified so far does not have tryptophan residues in its sequence (Walz *et al.*, 2002). There is also evidence for 4-Cl-IAA protein conjugates (not likely to be a protein degradation product) (Park *et al.*, 2010), which suggest conjugation of IAA to proteins is likely to be not a single unique biological event, and should not be fully ascribed as only a possible hydrolysis artifact.

The finding that tryptophan can convert to IAA in low amounts also has implication on the low molecular weight IAA conjugates. Apart from glucobrassicin, small tryptophan containing species may also be solvent soluble and hydrolyzed into IAA, further obfuscating the quest for IAA conjugates. It is possible that there are many such species that individually are present at very low levels, making the efforts to eliminate these false positives even more difficult.

### **Total IAA conjugate profiles**

Combining our results from investigation of IAA released by strong base hydrolysis in both low and high molecular weight ‘IAA conjugate’ fractions, we can now re-estimate the total IAA constituents in *Arabidopsis* seeds. From these results, the base hydrolysis method greatly over-estimates the amount of unknown IAA conjugates in *Arabidopsis* seeds (Figure 3-3), and this is possibly true for other tissues and other

species where IAA-conjugates are present in relatively low amounts. The semi-quantitative nature of these chemical artifacts makes it difficult to accurately assess the size of the total IAA pool and thus it is not certain what portions remain unidentified. However, our results show that the amount of IAA conjugates is much less than previously anticipated and it will be more challenging therefore to identify these potentially important remaining signaling-related molecules. The fact that glucobrassicin and tryptophan related compounds can convert to IAA under alkaline conditions makes it conceivable that other indolic species may also yield IAA under such treatments, further exacerbating the problem and necessitating additional controls.

The complexities associated with base hydrolysis, however, suggest a more targeted approach based on direct identification. For example, we have recently described an approach based on the use of the quinolinium ion at high resolution ( $m/z = 130.0651$ ) that specifically targets indolic compounds within defined molecular weight ranges and is applicable to early stages of purification and less subject to false positives (Yu *et al.*, 2014). This high resolution LC-MS approach also addresses the ever increasing sensitivity demands in such work, where femtomol amounts of IAA conjugates can be detected and milligrams of tissues is needed.

## **Materials and methods**

**Plants and chemicals.** *Arabidopsis thaliana* ecotype Columbia 0 seeds were purchased from Lehle Seeds (Round Rock, Texas). Glucobrassicin was from Cerrilant Corp (Round Rock, Texas). [ $^{13}\text{C}_6$ ]IAA was from Cambridge Isotope Laboratories (Tewksbury, MA). All other chemicals were from Sigma-Aldrich (Saint Louis, MO).

**Plant tissue extraction.** For the low molecular weight (also termed solvent soluble) IAA conjugate fraction, 100 mg of seeds were ground in liquid nitrogen and washed with 2 mL cold acetone and hexane sequentially. The defatted tissue was then extracted with 1 mL 65% 2-propanol, 35% 0.2 M imidazole (pH 7.0) for 1 h with constant vortex mixing. The extract was centrifuged at  $10,000 \times g$  for 5 min, and the supernatant was removed and centrifuged again at  $25,000 \times g$  for 10 min. Supernatant was stored at  $-20\text{ }^\circ\text{C}$  until

analysis. For the high molecular weight (also termed solvent insoluble) IAA conjugate fraction, 500 mg of seeds were ground and extracted in 5 mL urea buffer (6M urea, 50 mM HEPES, 5 mM DTT, pH 7.4) for 1 h with constant vortex mixing. The extract was centrifuged at  $25,000 \times g$  for 10 min and supernatant removed. Protein was precipitated by adding trichloroacetic acid (TCA) to 20% and the pellet was washed once with 20% TCA and three more times with cold 80% acetone. The pellet was dried and resuspended in the urea buffer. The protein preparation was kept at 4 °C until use.

**Quantification of IAA and its conjugates.** Free IAA was quantified by isotope dilution either by GC-SIM-MS as described (Barkawi *et al.*, 2008) or by GC-SRM-MS as described (Liu *et al.*, 2012). IAA ester conjugates were hydrolyzed by 1 M sodium hydroxide (NaOH) at room temperature for 1 hour. The amount of presumptive ‘ester conjugate’ was derived by subtracting free IAA from the amount of IAA determined following the 1 M NaOH hydrolysis. Presumptive ‘total IAA’ levels were determined by treating the sample with 7 M NaOH at 100 °C for 3 h under a water saturated nitrogen gas stream with an inline Oxisorb oxygen scrubber cartridge (Supelco, Bellefonte, PA, USA) installed between the nitrogen gas tank and water bubbler (Bialek and Cohen, 1989). Vials containing the samples were placed in a rack in a sealed aluminum block heated by a Fisher Scientific (Hampton, NH) Isotemp 145D block heater. The samples were taken out after the 3 h heating period and acidified to pH 2.5 immediately for IAA analysis. The amount of presumptive ‘amide conjugates’ was taken as the difference between the measured IAA levels following 1 M and 7 M NaOH hydrolysis treatments. To calculate the yield of IAA from glucobrassicin, tryptophan, and proteins, these samples were treated with 7 M NaOH at 100 °C for 3 h and the resulting IAA measured, as described above and the amounts used are listed in Table 3-1 and Table 3-2.

**Fractionation of plant extracts.** The 65% 2-propanol extracts were diluted 4 times with water and filtered using an Amicon 3 KDa molecular weight cut-off membrane filter (Millipore Ireland, Tullagreen Carrigtwohill, County Cork Ireland). 1 mL of the extract was loaded on the filter and centrifuged at  $2,800 \times g$  for approximately 1 hr. 100  $\mu$ L filtrate was injected onto a  $4.6 \times 200$  mm Spherisorb strong cation exchange (SAX) column (Waters Corp., Milford, MA, USA) and eluted with an ammonium formate

gradient. Solvent A: 10 mM ammonium bicarbonate, pH 6.7; Solvent B: 10 mM ammonium bicarbonate, pH 3.9; Solvent C: 1 M ammonium bicarbonate, pH 3.9. Gradient was; 0 – 5 min: 100% A, 5 – 10 min: 90% B, 10% C, 10 – 17.5 min: 10% – 100% C, 17.5 – 22.5 min: 100% C. Flow rate was  $0.5 \text{ mL} \cdot \text{min}^{-1}$  for the first five minutes and  $1 \text{ mL} \cdot \text{min}^{-1}$  for the rest of the run. 1 min fractions were collected.

**Fractionation of proteins and peptides.** The protein extract was fractionated on a  $5 \times 50$  mm Mono S column (GE Healthcare Life Sciences, Chalfont, Buckinghamshire, UK) with a sodium chloride gradient over 20 column volumes (1 CV = 1 mL), on a GE ÄKTAFPLC system. Solvent A was 20 mM 2-(N-morpholino)ethanesulfonic acid (MES) with 6 M urea at pH 6.0. Solvent B was Solvent A plus 1 M sodium chloride. Flow rate was  $1 \text{ mL} \cdot \text{min}^{-1}$  and 1 mL fractions were collected. A gradient delay of 3 CV was used. The first 4 fractions were pooled based on UV chromatogram and trypsin digested using a filter-aided sample preparation protocol (Wiśniewski, *et al.*, 2009). The resulting peptide mixture was then fractionated on a  $4.6 \times 150$  mm Ultra Aqueous C18 column (Restek, Bellefonte, PA) with gradient elution. Solvent A: 0.1 % trifluoroacetic acid (TFA) in water; solvent B: 0.1 % TFA in acetonitrile. Gradient was; 0 – 3 min: 2% B, 3 – 63 min: 2% – 50% B, 63 – 70 min: 50% – 90% B. Flow rate was  $0.8 \text{ mL} \cdot \text{min}^{-1}$  and 1.6 mL fractions were collected.

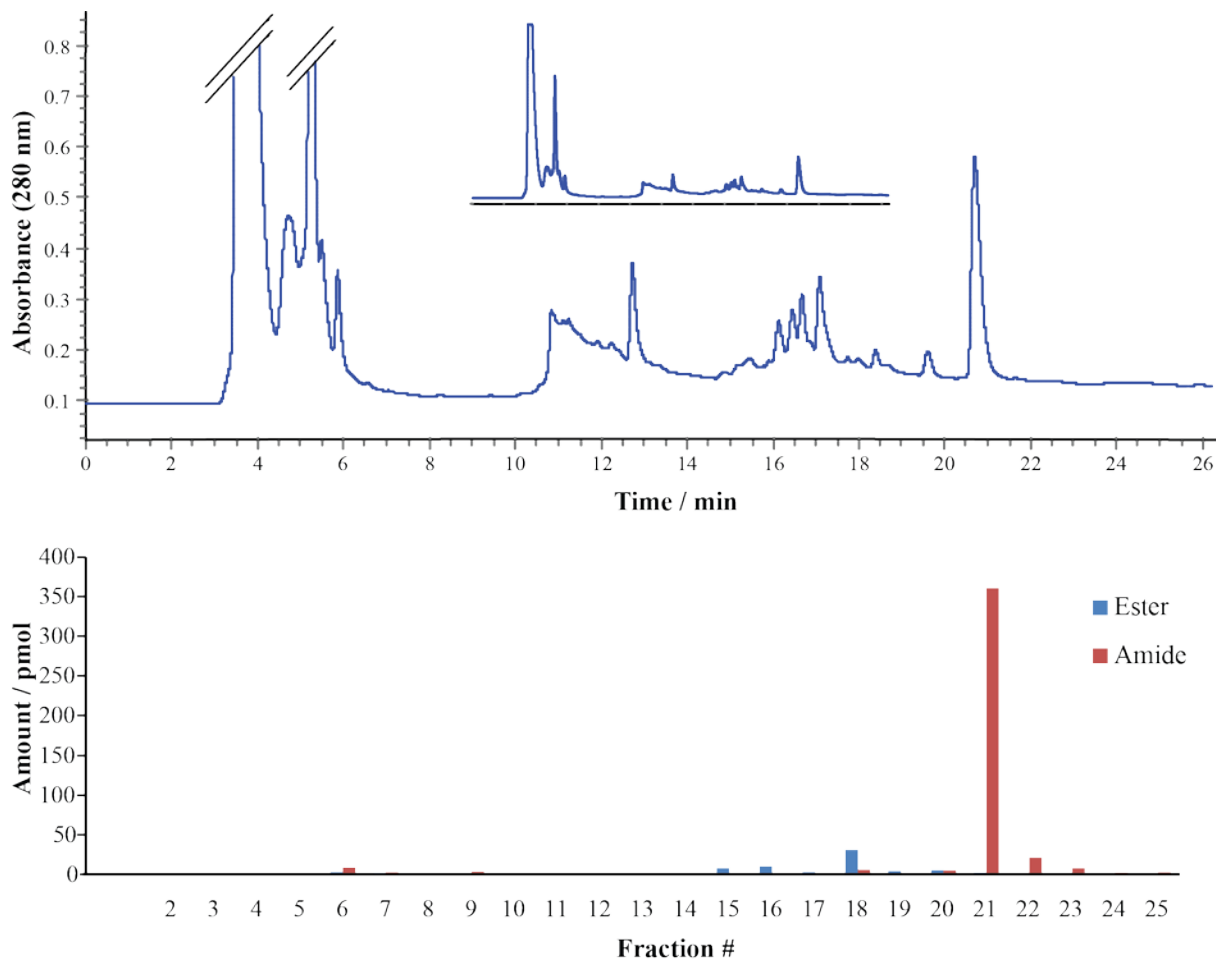


**Figure 3-1 Strong anion exchange fractionation of 65% 2-propanol extracts of about 20 mg *Arabidopsis* seeds.** Upper panel is the UV chromatogram at 280 nm. Lower panel is the IAA released by 1 N and 7 N NaOH hydrolysis from each fraction. In the main view the early peaks were cropped in the LC chromatogram to allow for better viewing of the later details. The entire chromatogram is shown in the inset. Clearly, the majority of the IAA is released by stronger base hydrolysis and the bulk of this was found in fraction 21. The column was tested using standards of IA-Lys (6.05 min), IA-Ala (17.80 min) and IA-Asp (19.90).

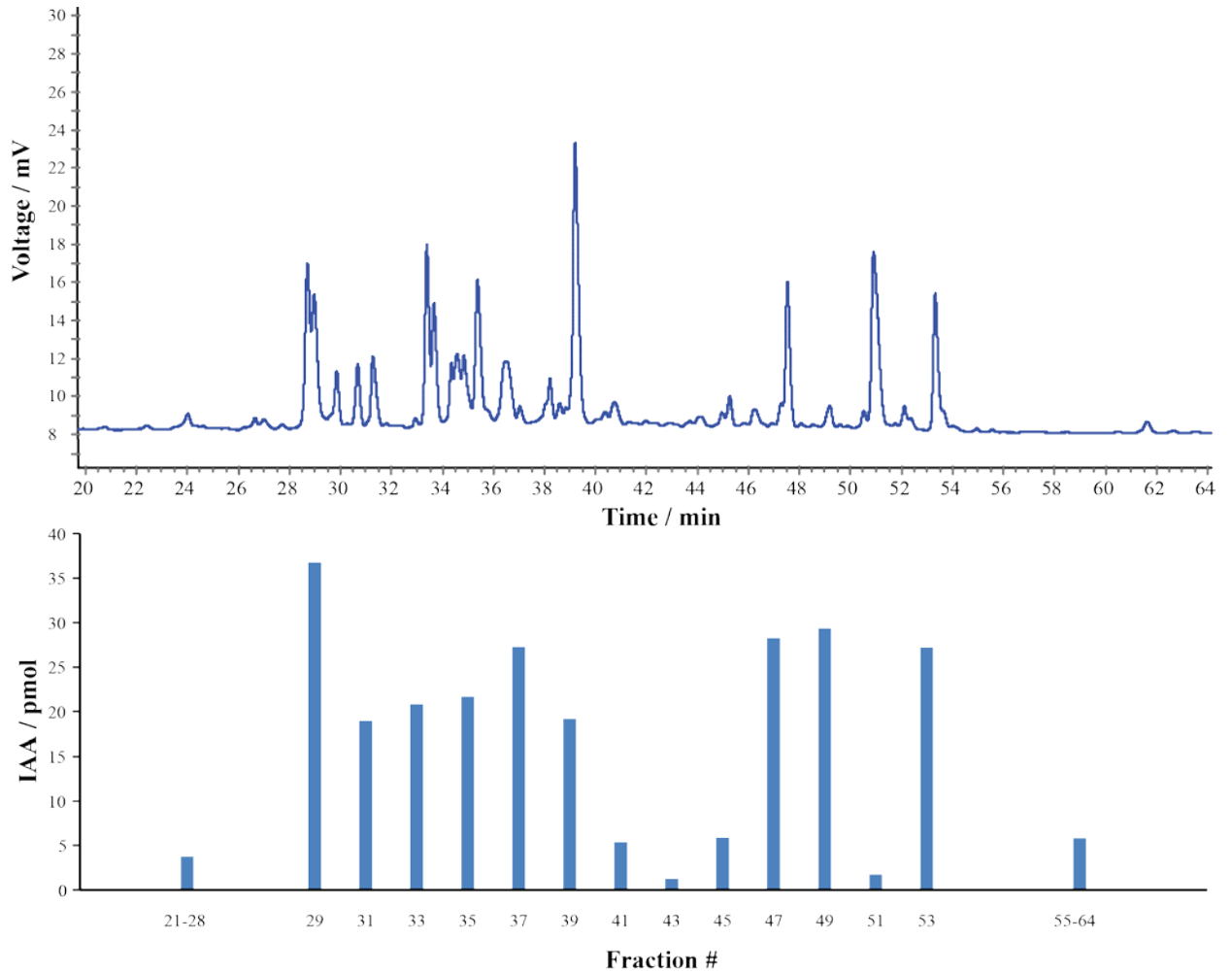


**Figure 3-2 C18 fractionation of a protein digest and total IAA released following hydrolysis in each fraction.** Upper panel is the UV chromatogram at 280 nm, and lower panel is the amount of IAA released after 7M sodium hydroxide treatment. Fraction 29 contains LC eluent 29-31 min, and such is the case through fraction 53. The amount of IAA conjugates clearly correlates with UV 280 nm absorption, indicative of IAA, tryptophan or tyrosine.

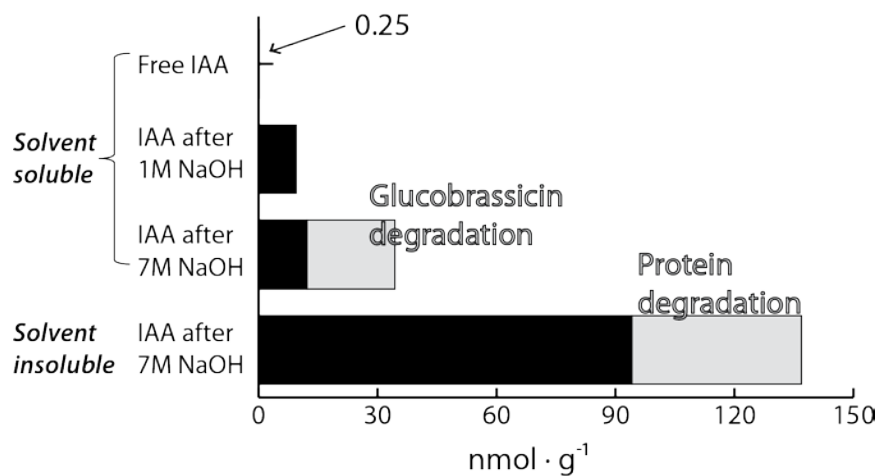


**Figure 3-3 Total IAA profile measured by the differential base hydrolysis method.** The lighter area indicates the proportions of IAA attributable to glucobrassicin and protein degradation based on the estimates described.

**Table 3-1 Chemical conversion of glucobrassicin into IAA.**

|                    | GB   | [ <sup>13</sup> C <sub>6</sub> ]IAA | AUC            | AUC            |          | Conversion |
|--------------------|------|-------------------------------------|----------------|----------------|----------|------------|
|                    | pmol | pmol                                | 130 <i>m/z</i> | 136 <i>m/z</i> | 130/136  | rate / %   |
|                    |      |                                     | 11231          | 68783          | 0.163282 | 1.44       |
| GB+IAA             | 100  | 10                                  | 6818           | 40617          | 0.167861 | 1.49       |
|                    |      |                                     | 10763          | 61757          | 0.17428  | 1.54       |
| GB                 | 100  | 0                                   | 7758           | ND             | NA       | NA         |
| IAA                | 0    | 10                                  | ND             | 40730          | NA       | NA         |
| ddH <sub>2</sub> O | 0    | 0                                   | ND             | ND             | NA       | NA         |

Glucobrassicin with [<sup>13</sup>C<sub>6</sub>]IAA were treated with 7M sodium hydroxide for 3 hr at 100 °C and the resulting IAA were quantified by GC-SIM-MS. 130 *m/z* and 136 *m/z* are signals from glucobrassicin derived IAA and the [<sup>13</sup>C<sub>6</sub>]IAA respectively. GB: glucobrassicin; AUC: area under curve in arbitrary units. Conversion rate is calculated on a molar basis.

**Table 3-2 IAA genesis during protein degradation and tissue hydrolysis**

|             | weight | IAA<br>produced | IAA yield               | Trp<br>Amount | IAA yield based on Trp |
|-------------|--------|-----------------|-------------------------|---------------|------------------------|
|             | mg     | pmol            | pmol · mg <sup>-1</sup> | nmol          | %                      |
| BSA         | 0.25   | 7.7±1.7         | 30.6±6.9                | 7.52          | 0.1±0.02               |
| Ovalbumin   | 0.25   | 13.4±2.5        | 53.7±9.8                | 16.7          | 0.08±0.01              |
| At protein  | 0.032  | 2.8±0.7         | 85.7±22.5               | N/A           | N/A                    |
| Tryptophan  | N/A    | 2.5±0.4         | N/A                     | 5.00          | 0.05±0.01              |
| Seed tissue | 5.3*   | 0.96*           | 181±7                   | N/A           | N/A                    |

\* Average numbers given here. IAA yield was calculated individually for each replicated experiment and then averaged. N/A: not applicable. Four replicates performed.

## Chapter 4 Indole metabolomics: a facile means for the identification of indolic compounds

### Summary

The bulk of the indole-3-acetic acid in plants is found in the form of conjugated molecules, yet past research on identifying these compounds has largely relied on methods that were both laborious and inefficient. Utilizing recent advances in analytical instrumentation, we have developed a simple yet powerful liquid chromatography-mass spectrometry (LC-MS) based method for the facile characterization of the small IAA conjugate profile of plants. The method uses the well-known quinolinium ion (130.0651  $m/z$ ) generated in MS processes as a signature with high mass accuracy that can be used to screen plant extracts for indolic compounds including IAA conjugates. We reinvestigated soybean for its indoles and found indole-3-acetyl-tryptophan (IA-Trp) in addition to the already known indole-3-acetyl-aspartic acid (IA-Asp) and indole-3-acetyl-glutamic acid (IA-Glu) conjugates. Surprisingly, several organic acid conjugates of tryptophan were also discovered, many of which have not been reported *in planta* before. These compounds may have important physiological roles in tryptophan metabolism, which in turn can affect human nutrition. We also demonstrated the general applicability of this method by identifying indolic compounds in different plant tissues of diverse phylogenetic origins. It involves minimal sample preparation but can work in conjunction with sample enrichment techniques. This method enables quick screening of IAA conjugates in both previously characterized as well as uncharacterized species and facilitates identification of indolic compounds in general.

### Introduction

Most plants and plant tissues so far examined contain the bulk of their IAA in conjugated forms, with typically only minute amounts as the free acid (Slovin *et al.*, 1999). Despite this fact, relatively few IAA conjugates have been identified. These include IAA conjugated by amide linkage to amino acids as well as esters or acyl alkyl acetal with simple sugars or cyclitols (reviewed in Cohen and Bandurski, 1982; Slovin *et al.*, 1999). A comparatively large amount of information is now available on the

biosynthesis and hydrolysis of these conjugates in higher plants (Ludwig-Müller, 2011). Auxin conjugates are thought to be involved in a variety of hormonally related processes: a) the transport of IAA within the plant (Chisnell and Bandurski, 1988; Komoszynski and Bandurski, 1986; Nowacki and Bandurski, 1980); b) protection of IAA from enzymatic destruction (Cohen and Bandurski, 1978); c) as components of a homeostatic mechanism for control of IAA levels (Cohen, 1983); d) as an entry route into the subsequent catabolism of IAA (Tsurumi and Wada, 1986; Östin *et al.*, 1998); and e) as part of the stress responses of plants cells (González-Lamothe *et al.*, 2012; Oetiker and Aeschbacher, 1997). Identification efforts for endogenous conjugates began with the isolation of IAA-inositol in the 1960's (reviewed in Slovin *et al.*, 1999) and since those reports isolation of the chemical entities involved in auxin metabolism has traditionally been approached on a compound by compound basis. More recent approaches have utilized immunoaffinity extraction (Pencík *et al.*, 2009), used isolated enzyme reactions studied with LC-tandem MS (Chen *et al.*, 2009), or required solid phase extraction steps prior to LC-tandem MS (Matsuda *et al.*, 2005). An important advance to improve such studies would be a technique to comprehensively measure and identify the full range of indolic compounds present in plants, especially those involved in auxin metabolism, rapidly, in small tissue samples, and with little or no prior purification.

Here we present a liquid chromatography-mass spectrometry (LC-MS) based method that dramatically improves the identification of indolic compounds present in plant tissues. The procedure is based on the observation that 2- and 3- substituted indoles yield a characteristic fragment that after rearrangement results in a relatively stable quinolinium ion at  $m/z$  130 (Marx and Djerassi, 1968). This ion has been previously used as an MS/MS signature for indolic compounds on quadrupole based instruments and has been particularly useful for quantification by selected ion and selected reaction monitoring techniques and also as part of the identification protocol for some IAA conjugates (Kowalczyk and Sandberg, 2001; Liu *et al.*, 2012; Pencík *et al.*, 2009; Östin *et al.*, 1998). While monitoring this ion can provide a moderate level of specificity, the unit mass resolution utilized in these previous studies can also result in fairly high false discovery rates. This ambiguity has unfortunately degraded the effectiveness of previous

implementations of the approach, especially since signaling molecules, such as IAA and their metabolically related compounds, are typically present in low levels relative to other potential interfering compounds.

We have significantly improved on this basic concept by use of the quinolinium ion signature at high sensitivity, resolution and mass accuracy, by employing a hybrid quadrupole Orbitrap instrument. This improvement, along with a greatly simplified sample preparation procedure that it enables, eliminates most of the false positives that confounded previous attempts to use 130 *m/z* nominal mass as a signature for discovery of unknown indolic compounds. The higher specificity of the technique also leads to a higher sensitivity, because background noise is reduced. It also allows for simplified procedures for sample preparation and analysis, which in turn reduces sampling bias. To illustrate the utility of the procedure, we reinvestigated soybean (*Glycine max*), which is an important crop species that we had previously studied in relation to its auxin conjugates. Our prior work, using classical approaches more than 25 years ago (Cohen, 1982; Epstein *et al.*, 1986), reported that essentially all the IAA conjugates in soybean seeds were accounted for by the two forms: IA-Asp and IA-Glu. These previous results were obtained after almost five years of active study by multiple investigators. Now we confirmed the findings and discovered additional indolic compounds, while using much less time and effort. To demonstrate the versatility and adaptability of the method, we also analyzed tissues as diverse as tomato (*Solanum lycopersicum*) leaf, coconut (*Cocos nucifera*) milk, and ginkgo (*Ginkgo biloba*) flower with only minimum modification to the sample preparation methods.

## **Results**

### **Design of workflow**

To identify as many indolic compounds as possible and to decrease bias against unexpected chemical forms, we developed a protocol with the goal of minimizing the number of sample preparation steps. Our reasoning was that each additional step would inevitably result in some degree of sample loss as well as potentially exclude or select against specific classes of compounds. Since it is certainly possible that quite unusual

chemical forms might be present as additional plant species are investigated, this was considered a particularly important aspect of this approach. Thus, our basic procedure used only 50 mg or less of plant tissue and involved only sample extraction, liquid clarification, and dilution prior to LC-MS analysis (Figure 4-1). Additional sample preparation methods can also be performed to suit particular types of samples. For example, solvent precipitation can be employed for the processing of liquid sample, as was demonstrated here with the analysis of coconut milk.

To minimize enzymatic reactions, acid or base catalyzed hydrolysis, acid catalyzed esterifications, and transesterifications we extracted the soybean tissue with cold 50% 2-propanol (Chen *et al.*, 1988; Fukui *et al.*, 1957; Maltese *et al.*, 2009). The extract was then diluted to 5% 2-propanol with water prior to C18 reversed phase HPLC separation coupled to MS analysis, as detailed below.

### **Mass spectrometric detection**

A highly sensitive and selective mass spectrometric method was required to identify minor indolic compounds from a crude extract. For this purpose we monitored the quinolinium signature ion ( $m/z = 130.0651$ ) from indolic compounds with high mass accuracy using a hybrid quadrupole Orbitrap Q Exactive mass spectrometer (Thermo Scientific, San Jose, CA). Crude extracts were separated using C18 reversed phase liquid chromatography directly coupled to the electrospray ionization source of the mass spectrometer. The routine delivery of sub 2 ppm mass accuracy on the Orbitrap ensured the high selectivity required for the successful application of this approach.

The mass spectrometer was set to acquire a limited full scan (216-370  $m/z$ ) followed by a series of data independent MS/MS (a process to study the fragmentation patterns of precursor ions) scans. We were interested in both tryptophan metabolites and IAA amino acid conjugates, so we only covered a mass range of  $m/z$  216-370. We did 8 data independent scans with a 20  $m/z$  isolation window (segment) each. Mass spectra were then extracted for 130.0651  $m/z$  signatures. Segments containing the signatures were then divided into smaller segments and analyzed for the signature ion in subsequent

reinjections. This process was continued until unambiguous precursor ions were identified. We then obtained the exact mass and fragmentation patterns of these precursors to aid compound identification. The mass spectrometric method setup is illustrated in Figure 4-1.

To further improve the sensitivity and speed of the analysis of potential indolic compounds, a targeted MS/MS approach was used. We examined  $m/z$  values corresponding to those predicted for each of the IAA amino acid conjugates and many of the common tryptophan derivatives to see if they were present *in vivo*.

Using a combination of the two approaches, we identified several indolic compounds from soybean seeds, as summarized in Table 1. A facile survey approach to demonstrate the potential of the method across a variety of plant tissues was also applied to samples from tomato leaf, ginkgo flower and coconut milk and showed the presence of a number of indolic compounds, some of which have been tentatively identified (Table 4-2 and Table 4- 1-3). Note that we only looked for ions between 216  $m/z$  and 370  $m/z$ . IAA precursors are generally below that range and polypeptides are generally higher, so such compounds are not covered by this method as applied here. This method can also be used to investigate such compounds, which will be the topic of a separate study. All compound identifications were based on LC retention time and MS spectra as compared with their respective standards. The mass spectral comparisons are detailed in the following sections. Authentic standards are displayed in the lower half of each graph and endogenous compounds are on the upper half in Figs.4- 2, 3, 4, 6.

### **IAA amino acid conjugates**

Indole-3-acetyl-aspartic acid (IA-Asp) and Indole-3-acetyl-glutamic acid (IA-Glu)

IA-Asp and IA-Glu (Figure 4-2a, b) were reported to account for “essentially all the IAA conjugates” in soybean (Epstein *et al.*, 1986), at a concentration of  $10 \text{ pmol} \cdot \text{mg}^{-1}$  and  $7.4 \text{ pmol} \cdot \text{mg}^{-1}$ , respectively. The fact that we could easily identify them in a fraction of a milligram of tissue showed the sensitivity of this method, verified the approach and confirmed the previous isolations of these compounds.

#### Indole-3-acetyl-tryptophan (IA-Trp)

IA-Trp (Figure 4-2c) was recently reported as an endogenous compound in *Arabidopsis thaliana* (Staswick, 2009) but had not been identified as a native plant IAA amino acid conjugate previously. The same study reported this compound possessed antagonistic properties to bioactive auxins and showed it was present at the  $\text{fmol} \cdot \text{mg}^{-1}$  level. Comparing the signal of IA-Trp to that of IA-Asp and IA-Glu, it would appear to be also a minor IAA conjugate in soybean (Figure 4-8).

### **Organic acid conjugates of tryptophan**

#### N( $\alpha$ )-Acetyl tryptophan (Ac-Trp)

N( $\alpha$ )-acetyl tryptophan (Figure 4-3a) has been reported previously in *Rhizobium* bacteria (Badenoch-Jones *et al.*, 1982). As far as we are aware, no reports of its presence in plants can be found in the literature, even though it may be quite common *in planta*, as all material we have examined contained this compound (Table 4- 1,2,3,4). The peak intensity of N( $\alpha$ )-acetyl tryptophan was on the same order of magnitude on the total ion chromatogram (TIC) as that of IA-Asp, without corrections for compounds' response factors.

#### N( $\alpha$ )-Malonyl -tryptophan (Malonyl-Trp)

This compound (Figure 4-3b) was first reported by Andreae and Good (1957) as a metabolic product of tryptophan in spinach leaves and drew a lot of attention in the following decades for the possibility of it being an auxin precursor (Ludwig-Müller and Hilgenberg, 1989; Rekoslavskaya, 1986). There was also an intensive debate regarding the chirality of tryptophan in the molecule (Markova and Gamburg, 1997; Sakagami *et al.*, 1993; Sakagami *et al.*, 1995). Based on those previous studies it is likely that the compound found in soybean is N( $\alpha$ )-malonyl-(S)-tryptophan. Further, N( $\alpha$ )-(S)-malonyl-(S)-tryptophan was shown to be the more likely endogenous compound than its counterparts (see following section).

#### N( $\alpha$ )-Succinyl-tryptophan (SA-Trp)

N-succinyl amino acids were recently shown to be important intermediates in the production of enantiomerically pure amino acids by a pathway involving the enolase enzyme superfamily that serves for the irreversible conversion of D- to L-amino acids (Sakai *et al.*, 2006; SUMIDA *et al.*, 2012). However, the pathway and the enzymes involved in their biosynthesis have so far only been described from microorganisms. The presence of this compound (Figure 4-3c) in higher plants is thus potentially intriguing, especially since D-amino acids are often reported in plants (Brückner and Westhauser, 2003) and in retrospect to the debate on the chirality of N( $\alpha$ )-malonyl-tryptophan (see above) and an interest in the 1980s in D-tryptophan as a possible auxin precursor (Baldi *et al.*, 1991; Law, 1987).

#### N( $\alpha$ )-(S)-Malyl-(S)-tryptophans (Malyl-Trp)

Although malyl-amino acids have been reported as products of a reverse peptidase reaction from an enzyme isolated from gram-positive bacteria (Auriol *et al.*, 1990), the biochemical literature seems mostly devoid of references to malyl-tryptophan (Figure 4-4). However, these tryptophan derivatives would appear likely to be related metabolically to malonyl-Trp and the other N( $\alpha$ )-modified tryptophans. We synthesized both N( $\alpha$ )-(S)-malyl-(S)-tryptophan and N( $\alpha$ )-(R)-malyl-(S)-tryptophan and from those syntheses were able to conclude that the former was more likely to be the endogenous form based on chromatographic retention studies (Figure 4-9). Chemical synthesis also resulted in two structural isomers of the former chiral isomer, where the hydroxyl group on the malic acid can be either on the  $-\alpha$  (Figure 4-4a) or  $-\beta$  (Figure 4-4b) position relative to the free carboxyl group. The structural assignment for the isolated compound was then based on NMR experiments (See Experimental Procedures and Figure 4-5). Interestingly, the two structural isomers,  $-\alpha$  or  $-\beta$ , both existed *in vivo* and their relative proportions were similar to those derived from the chemical synthesis (Figure 4- 4, 9).

To assign the absolute structures, we synthesized the tryptophan methyl esters of the malyl-Trps because they had better solubility in solvents and more retention on preparative LC. We first acquired <sup>1</sup>H NMR spectrum on the  $\alpha$  isomer of the N( $\alpha$ )-(S)-malyl-(S)-tryptophan methyl ester (Malyl-Trp-Me) and the peaks were consistent with

the structure (Figure 4-5a).  $^1\text{H}$ ,  $^{13}\text{C}$  HSQC and  $^1\text{H}$ ,  $^{13}\text{C}$  HMBC experiments further helped assign the carbon backbone. Initially, we tried to use  $^1\text{H}$ ,  $^{13}\text{C}$  HMBC and  $^1\text{H}$ ,  $^{15}\text{N}$  HMBC data to assign the position of the hydroxyl group on the carbon backbone. The information was not conclusive, as was the case with one of the previous similar studies (Serrano *et al.*, 2007). However, we did observe some differences in the chemical shifts of the carbonyl carbon atoms between the two isomers (Figure 4-5b and 4-5c). The isomers otherwise looked very similar. Specifically, the difference in chemical shift between the two malyl carbonyl carbon peaks is larger in one isomer than the other, likely caused by the influence of the hydroxyl group on the adjacent carboxylic acid versus amide carbons. This pattern was observed before when similar malic acid derivatives were studied (Lorenz *et al.*, 1998). We assigned the isomer with the larger carbonyl chemical shift difference to be the  $\alpha$  isomer based on our comparison with the published data (Lorenz *et al.*, 1998).

### **Other tryptophan derivatives**

#### **Tryptophan alcohols (Trp-OH)**

Tryptophan alcohols (Figure 4-6) were previously discovered in the studies of the photo-degradation of tryptophan *in vitro* (Nakagawa *et al.*, 1985). These compounds are also apparently present *in vivo* in soybean. We found at least four of these compounds, all of which showed very similar fragmentation patterns (Figure 4-10). We identified two diastereomers that were more abundant and well separated on reversed phase chromatography. To test the possibility of spontaneous oxidation of tryptophan during extraction, we spiked in fully labeled [ $^{13}\text{C}_{11}$ ,  $^{15}\text{N}_2$ ]-tryptophan into our extraction buffers and did not recover any labeled Trp-OH (Figure 4-11), confirming the plant origins of these compounds. The biochemical literature lacks information regarding the physiological or biochemical roles of these compounds since they were not previously known to be endogenous.

### **Indolic compounds from tomato, coconut, and ginkgo**

To demonstrate the general utility of this method for different plant tissues, we analyzed tomato leaf, coconut milk, and ginkgo flower for their indolic compounds. It

was only necessary to added one solvent removal/concentration step in the sample preparation processes (see Experimental Procedures for details); thus still maintaining the overall simplicity of the procedure. Some representative compounds found in this survey analysis are listed in Table 4-2. A full list of putative indolic compounds found in these materials is shown in Table 4-2, 3, 4. Some compounds, such as IA-Asp, Ac-Trp and Trp-OH, were common among the different plants while others were more limited or possibly unique.

## **Discussion**

We have developed a sensitive and selective LC-MS based method for the identification of indolic compounds. Several different classes of these compounds spanning an array of abundances and chemical properties were recovered in an extract containing less than one milligram of desiccated soybean seed or a few milligrams of fresh plant tissue. The aim of the present study was to demonstrate both the simplicity and effectiveness of the entire procedure on a material that had already been well characterized using classic approaches and its applicability to less studied materials. In addition, we have described new compounds in the indolic profile of soybean and a few other species that lead us to a number of interesting questions regarding the role for such compounds and their metabolic origins for subsequent studies. For example, a re-evaluation of the biological significance of conjugating tryptophan to various organic acids would now be possible with facile identification and spatial resolution. Also, questions about the role of IA-Trp, and the current model for its biological activity, can now be addressed in various plants, in specific tissues and throughout development. Furthermore, tryptophan alcohols were found in all four different species including a monocot, two dicots, and a gymnosperm and from four different tissue types, suggesting it could be commonly present as more plant materials are examined. Given their associations with photo reactions and free radicals, these compounds could have important roles in plant stress responses, especially those involving free radicals. Tryptophan in humans cannot be synthesized *de novo* and is instead derived from dietary sources. Because of the low representation of tryptophan in proteins and its relatively high levels in some plant tissues, free tryptophan is a significant dietary constituent and

proposals to increase plant free tryptophan levels have appeared periodically (Klarskov *et al.*, 1999; Wenefrida *et al.*, 2013). Thus, the importance of understanding tryptophan metabolism in plants, especially if the content in tryptophan is going to be modified in nutritionally important ways, has important human health considerations. Clearly, the analytical method described, as well as the facile discovery of previously unreported plant tryptophan metabolites in a major crop species, highlights the importance of such specific and relatively unbiased methods for analysis of the tryptophan metabolites in edible crops.

The quinolinium ion employed in this method is highly, but not completely, specific. As a result it is important to exercise caution when using it as a selective marker in novel materials. We discovered, for example, that N-terminal phenylalanine in a peptide sequence will produce such an interfering ion (Figure 4-7). Other than that instance, we have not identified any other chemical moieties that result in false positives. On the other hand, this method is comprehensive and relatively unbiased, but not meant to be completely exhaustive. For example, it is always possible that not all indoles will go into solution and some may be very unstable and thus require specific handling techniques. Also, the huge dynamic range of different compounds necessitates sample purification and enrichment to detect trace level compounds. Hence, the coverage of the method can be expanded by using a plethora of sample preparation methods, while a quick survey of indolic compounds requires only relatively modest effort.

Recently, a computational algorithm was described that can assign fragments to a common precursor based on the properties of the chromatographic peak (Broeckling *et al.*, 2013). The same basic approach could potentially be employed for this type of analysis as well, where such an algorithm would help identify the precursor ion from which the signature was derived in addition to other associated product ions. Currently, the standard practice is that this process relies on gradually narrowing down the isolation window in the MS/MS experiment and manual signature picking. Data dependent MS/MS acquisition would not have this issue, but it would also not be effective in

targeting low abundance compounds, such as hormones, without significant improvements in the selectivity of sample preparation procedures.

By the identification of a range of indolic compounds, we have demonstrated the utility and sensitivity of this method. Soybean was selected because it was the first dicotyledonous plant to be characterized for its full IAA conjugate content by classical methods (Cohen, 1982; Epstein *et al.*, 1986). To confirm the wider utility of the approach, we investigated tomato, an important species for studies of fruit development for which an early report on natural occurring IA-Asp had been questioned and more recent reports had not looked for additional conjugates (Catalá *et al.*, 1992; Mounet *et al.*, 2012; Rekoslavskaya and Gamborg, 1983; Row *et al.*, 1961); coconut milk, which has a long history as an addition to plant tissue culture media (Caplin and Steward, 1948) and *Ginkgo biloba* because of the importance of IAA conjugates in a phylogenetic context (Ludwig-Müller, 2011; Sztein *et al.*, 2000). The analytical procedure described in this report has the distinct potential to enable researchers to identify more indolic compounds with less tissue and in a vastly shorter time. It works well with minimal sample preparation, but can also function in conjunction with sample purification/enrichment techniques to provide spectral data for compounds at even lower concentrations. The elegance of minimal sample preparation lies not only in the simplicity of the procedure, but more importantly, the universal applicability and adaptability. Different sample preparation techniques can be added to selectively enrich certain classes of indolic compounds, as experimental needs demand.

## **Experimental procedures**

### **Plant materials**

Soybean (Variety: Pioneer 90M80) seeds were provided by Dr. Seth Naeve, and were harvested from a farm near Rothsay, Minnesota in 2011. A greenhouse-grown tomato plant was provided by a University of Minnesota recombinant cherry tomato breeding program lead by Dr. Changbin Chen. One young compound leaf was taken from a six-week old plant, frozen in liquid nitrogen and kept at -80 °C until use. A flower (sperm cone, roughly 0.5 cm in diameter and 1 cm in length) of a male ginkgo tree was

harvested from a mature tree on the University of Minnesota Saint Paul campus in late May, frozen in liquid nitrogen and kept at -80 °C until use. Coconut milk was harvested from a mature intact coconut purchased at a local grocery store.

### **Chemicals and standards**

Acetonitrile (ChromaSolv), 2-propanol (ChromaSolv) and methanol (ChromaSolv) were from Sigma-Aldrich Corp (Saint Louis, Missouri). Formic acid was from Fisher Scientific (Hampton, New Hampshire). Water was distilled in house in a glass still from reverse osmosis treated deionized feed water.

Indole-3-acetyl-DL-aspartic acid was from Aldrich Chemical Co (Milwaukee, Wisconsin). Indole-3-acetyl-DL-tryptophan was from Biosynth Inc (Itasca, Illinois). N( $\alpha$ )-malonyl-D,L-tryptophan was from Cerrilant Corp (Round Rock, Texas). N( $\alpha$ )-acetyl-tryptophan was hydrolyzed from N( $\alpha$ )-acetyl-tryptophan methyl ester (Schweizerhall Inc, South Plainfield, New Jersey). All chemical reagents used in syntheses were from Sigma-Aldrich, unless otherwise noted.

Indole-3-acetyl-L-glutamic acid was synthesized essentially as described (Cohen, 1981). L-Glutamic acid di-*tert*-butyl ester was linked to IAA via dicyclohexylcarbodiimide (DCC) mediated acylation in acetonitrile at 4°C overnight. The solvent was evaporated and the product was then hydrolyzed in 2N KOH in 50% methanol/water at 60°C for 2 hr to yield indole-3-acetyl-L-glutamic acid.

The methyl esters of N( $\alpha$ )-(S)-malyl-(S)-tryptophan and N( $\alpha$ )-(S)-malyl-(R)-tryptophan were synthesized using a similar procedure to that used above for indole-3-acetyl-L-glutamic acid, as previously described (Cohen, 1981). Briefly, 255 mg L-tryptophan methyl ester hydrochloride was dissolved in 2.5 mL 80% acetonitrile, to which 1 mL acetonitrile containing 134 mg L- or D-malic acid was added. 206 mg DCC in 0.5 mL acetonitrile was then added to the respective reactions. The reaction mixtures were kept at 4°C overnight. The liquid was pipetted off and used for a larger scale preparation later, and the pellet was washed with 200  $\mu$ L of acetonitrile and retained.

The wash was lyophilized and dissolved in 500  $\mu$ L 10% acetonitrile. 50  $\mu$ L of the solution was injected onto an Ultra Aqueous C18 4.6 $\times$ 150 mm column (Restek, Bellefonte, Pennsylvania) with a gradient elution. Solvent A: 0.1% formic acid in water;

Solvent B: 0.1% formic acid in acetonitrile. Flow rate was 1 mL · min<sup>-1</sup>. Gradient was: 0-2 min: 20% B, 2-11 min: 20-50% B, 11-14 min: 50-90% B. Retention time for the two isomeric (S)-malyl-(S)-tryptophan methyl esters was 11.1 min ( $\beta$  isomer, Figure 4-4B) and 11.9 min ( $\alpha$  isomer, Figure 4-4A) respectively. The fraction (#12, 1 mL) containing both isomers was treated with 100  $\mu$ L 10.5 M sodium hydroxide for 1 hour at room temperature. The solution was adjusted to pH 2.0 with 5 M hydrochloric acid, 1 M phosphoric acid, diluted to 4 mL with water and concentrated to  $\sim$ 600  $\mu$ L with a SpeedVac (Savant Instruments Inc., Farmingdale, NY). A PrepSep C18 solid phase extraction column (500 mg, 6 mL, Fisher Scientific, Hampton, New Hampshire) was used to recover malyl-Trp. The column was conditioned with 1 column volume (CV) acetonitrile, 1 CV water and 1 CV 2% acetonitrile with 0.1% trifluoroacetic acid (TFA). The sample was then loaded and the column was washed with 1 CV 2% acetonitrile with 0.1% TFA and eluted with 2X0.75 mL 60% acetonitrile containing 0.1% formic acid. The eluent was diluted and used directly as reference standards described in the text. The liquid from the original synthesis was lyophilized and dissolved in 3 mL 10% acetonitrile and fractionated on an Agilent Eclipse XDB-C18 21.2 $\times$ 250mm column with a water and methanol gradient. Fractions from 4 repeated injections of 500  $\mu$ L each were pooled. Fractions containing the two different isomers were separately lyophilized and dissolved in 700  $\mu$ L [<sup>2</sup>H<sub>4</sub>]methanol. NMR analysis was performed directly on the methyl esters of malyl-Trp.

Tryptophan alcohols are synthesized according to procedures in the literature (Gracanin *et al.*, 2009; Ronsein *et al.*, 2009) with adaptations. A 2.5 mL solution of 20 mM L-tryptophan containing 10  $\mu$ M of Rose Bengal (dye sensitizer to generate reactive oxygen species) in deuterium oxide (<sup>2</sup>H<sub>2</sub>O) in a test tube was irradiated by a Kodak CAROUSEL 860H slide projector (Rochester, New York) for 3 hours with continuous aeration. A glass cylinder (10 cm diameter) filled with water was used to focus the light onto the test tube and filter out IR and UV light. The crude product was diluted 100 $\times$  and directly injected onto the LC-MS for reference purposes.

All synthetic compounds can be made available upon request.

## **NMR analysis**

NMR analysis of chemically synthesized Maly1-Trp-Me isomers was performed on a Varian Inova 600MHz spectrometer with a 5 mm HCN low temperature probe. 1D  $^1\text{H}$ ,  $^1\text{H}$ ,  $^1\text{H}$ -COSY,  $^1\text{H}$ ,  $^{13}\text{C}$ -HSQC,  $^1\text{H}$ ,  $^{13}\text{C}$ -HMBC data were collected.  $^1\text{H}$ ,  $^{15}\text{N}$  HMBC experiments were performed on a Bruker Avance 900MHz spectrometer with a 5 mm TCI CryoProbe. Data were processed by ACD/NMR processor Academic Edition.

### **Sample preparation and LC-MS analysis**

A 1 g sample of soybean (5-7 beans) was ground into a fine powder. 50 mg of soybean powder was then extracted in 200  $\mu\text{L}$  50% 2-propanol (initially equilibrated to  $-20^\circ\text{C}$ ) in a 1.5 mL microcentrifuge tube by constant vortexing for 30 min at room temperature. The sample was then centrifuged at  $25,000 \times g$ ,  $20^\circ\text{C}$  for 20 min. 100  $\mu\text{L}$  of the extract was taken out and diluted 10 times with water. Adequate sample was prepared via this method for 50-100 analytical determinations at the levels employed in this study. One tomato leaf ( $\sim 50$  mg) and one male ginkgo flower ( $\sim 80$  mg) were ground in 3 times (w:v) the volume of 80% 2-propanol and vortexed for 30 min. The liquid was decanted after centrifugation and diluted five times with water. The volume was reduced to approximately 150  $\mu\text{L}$  with a SpeedVac concentrator. The liquid was then clarified by centrifugation and used for LC-MS analysis.

Five mL of coconut milk was mixed with an equal volume of 2-propapnol and kept at  $-20^\circ\text{C}$  for three days to precipitate large biomolecules. The liquid was clarified by centrifugation and the volume reduced to  $\sim 500$   $\mu\text{L}$  using a SpeedVac. The liquid was then diluted twice with water before LC-MS analysis.

The extracts were analyzed on a Dionex Ultimate 3000 RSLC HPLC coupled to a hybrid quadrupole Orbitrap Q Exactive mass spectrometer (Thermo Scientific, San Jose, California). 20  $\mu\text{L}$  soybean extract (equivalent to 0.5 mg soybean extract) was injected onto a 2.1x100 mm Kinetex XB-C18, 1.7  $\mu\text{m}$ , column (Phenomenex, Torrance, CA) and eluted with a solvent gradient. Solvents were A: 0.1% formic acid in water, B: 0.1% formic acid in acetonitrile. Flow rate was  $0.2 \text{ mL} \cdot \text{min}^{-1}$ . Gradient was: -5 - 0 min: 3%B, 0 - 3.99 min: 3% B, 3.99 - 4.00 min: 3-16% B, 4 - 15 min: 16 - 46.3% B, 15 - 15.5 min: 46.3% - 80% B, 15.5 - 18 min: 80% B. 9  $\mu\text{L}$  tomato extract (equivalent to 3 mg leaf fresh weight), 9  $\mu\text{L}$  ginkgo extract (equivalent to 4 mg fresh flower tissue) and 5  $\mu\text{L}$  coconut

extract (equivalent to 25  $\mu$ L original coconut milk) were separately analyzed on the Kinetex XB-C18 column with same solvents and flow rate except using a slightly simplified gradient. The gradient was: -4 – 0 min: 5% B, 0 – 15 min: 5 – 46.3% B, 15 – 15.5 min: 46.3 – 80% B, and 15.5 – 18 min: 80% B. A HESI (heated electrospray ionization) II probe was used to interface the LC and MS. Ion source conditions were: spray voltage: 3.6 kV, capillary temperature: 350 °C, probe heater temperature: 300 °C, sheath gas: 35 arbitrary units, aux gas: 8 arbitrary units, S-lens RF level: 47. MS was set to acquire one full MS scan followed by 8 targeted-MS<sup>2</sup> in positive ionization mode. Full MS conditions were: 1 microscan at 70,000 resolution with AGC target of  $1 \times 10^6$ . Maximum accumulation time was 50 ms. Scan range was from 216 to 370  $m/z$ . MS<sup>2</sup> conditions were: 1 microscan at 17,500 resolution with AGC target of  $2 \times 10^5$ . Isolation width was 10  $m/z$  with multiplexing count of 2, effectively fragmenting a mass window of 20  $m/z$  while allowing independent ion accumulation time for each half to partially mitigate dynamic range issues see (Michalski *et al.*, 2011) for discussion of the multiplexing feature on the Orbitrap Q Exactive instrument). A normalized collision energy of 40% was used with fixed first mass at 60  $m/z$ . All data were saved in profile mode. Once an indolic precursor was found, the sample was then reinjected to acquire the fragmentation pattern at the optimal collision energy. Standard compounds were analyzed in an identical manner for reference purposes.

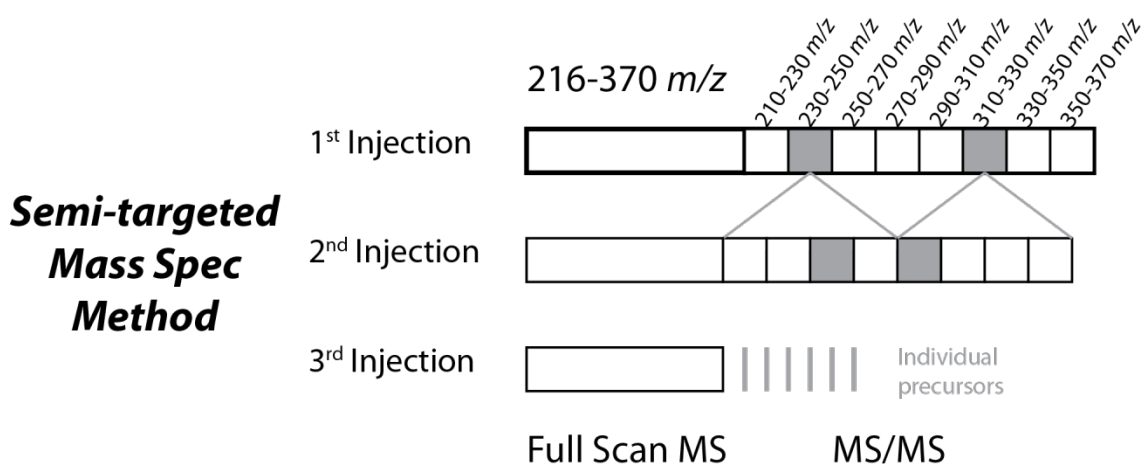
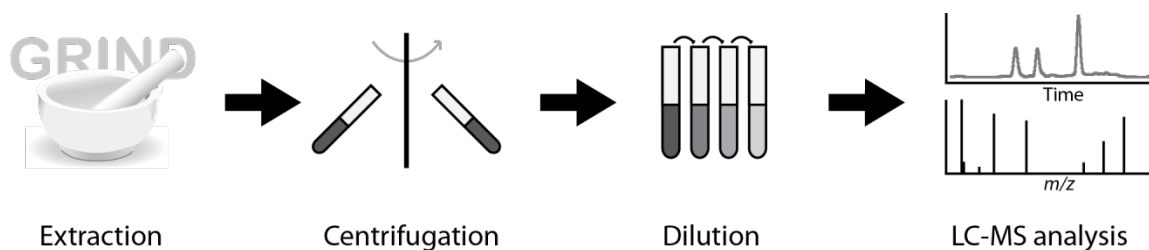


**Figure 4-1 Workflow of indolic compound identification from plant tissue.** Tissue was extracted with 50% 2-propanol. The extract was clarified by centrifugation, diluted to 5% 2-propanol and analyzed via LC-MS. An optional concentration step between dilution and analysis can be performed, if necessary. The LC-MS analysis typically involves three or more iterations. The first few iterations were to find out the exact precursors that produced the quinolinium signatures (shaded boxes and bars), and the last iteration was to acquire the fragmentation patterns for compound identification.

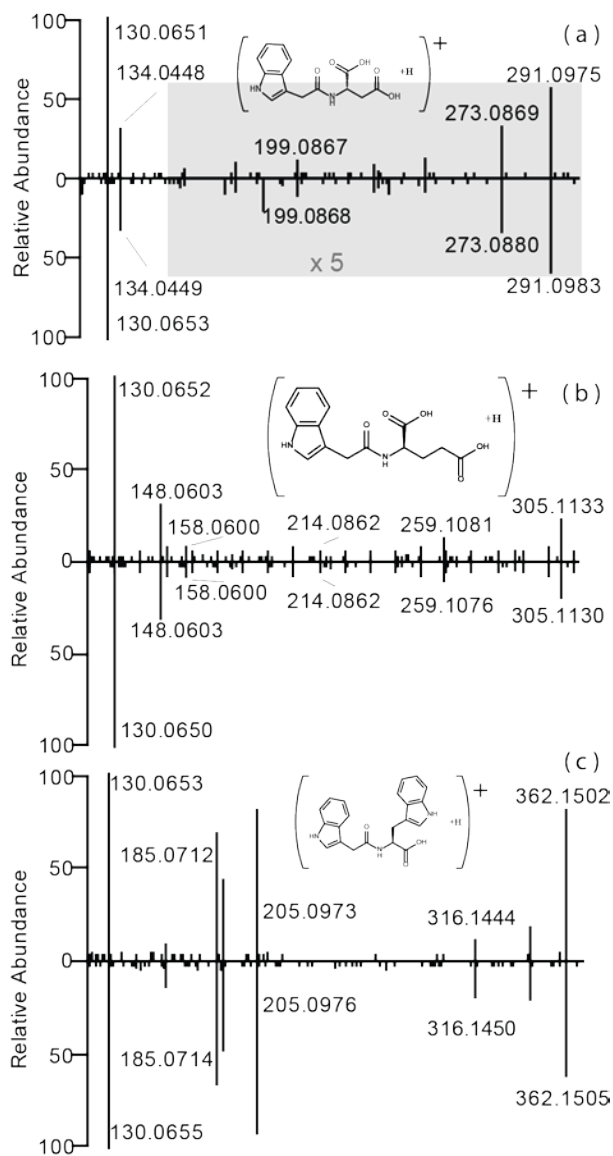


**Figure 4-2** Fragmentation patterns of endogenous indole-3-acetyl-aspartic acid (IA-Asp), indole-3-acetyl-glutamic acid (IA-Glu) and indole-3-acetyl-tryptophan (IA-Trp) compared with their respective standards. The endogenous compound is displayed on the upper half of each mass spectrum and the authentic standard is on the lower half. Molecular ions were fragmented in the HCD cell with a normalized collision energy of 10% for IA-Asp (A) and IA-Glu (B), and 15% for IA-Trp (C). The label  $\times 5$  indicates 5 times magnification in the shaded area. IA-Trp has previously only been reported in *Arabidopsis* and no reports of its presence in other species have appeared.

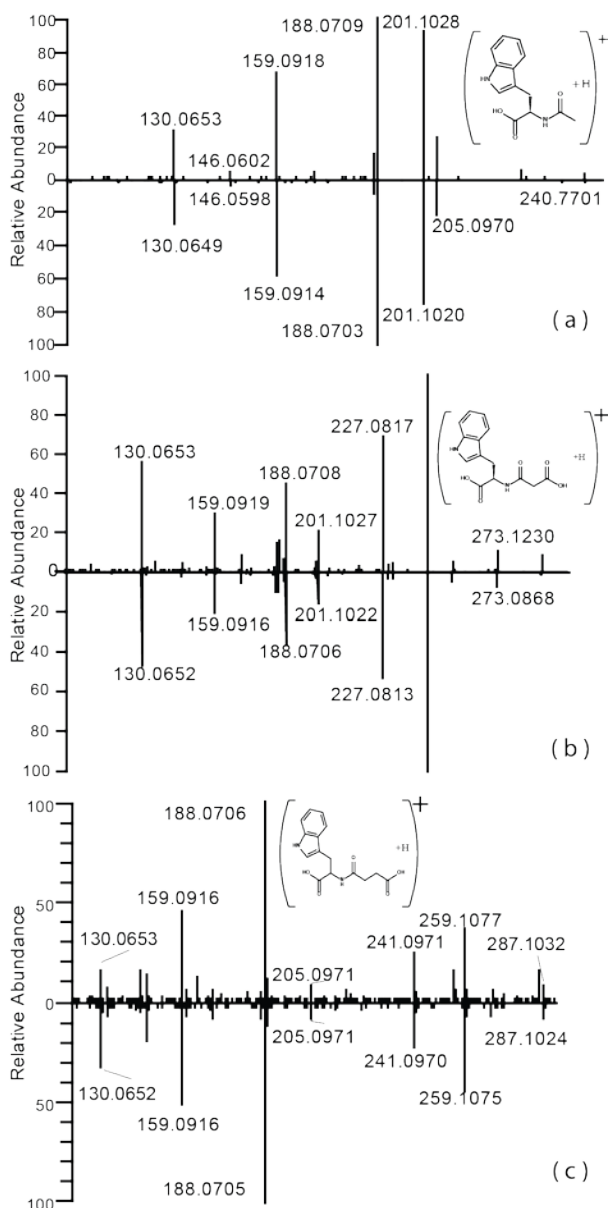


**Figure 4-3 Fragmentation pattern of endogenous N(α)-acetyl-tryptophan (Ac-Trp), N(α)-malonyl-tryptophan (Malonyl-Trp), and N(α)-succinyl-tryptophan (SA-Trp) compared with respective standards.** The endogenous compound is displayed on the upper half of each mass spectrum and the authentic standard is on the lower half. Molecular ions were fragmented in the HCD cell with a normalized collision energy of 25% for all three. Ac-Trp (A) was present in all four plants examined, but has not been reported from a plant source before. Malonyl-Trp (B) has been reported in various plant species. SA-Trp (C) also has not been reported in plants.

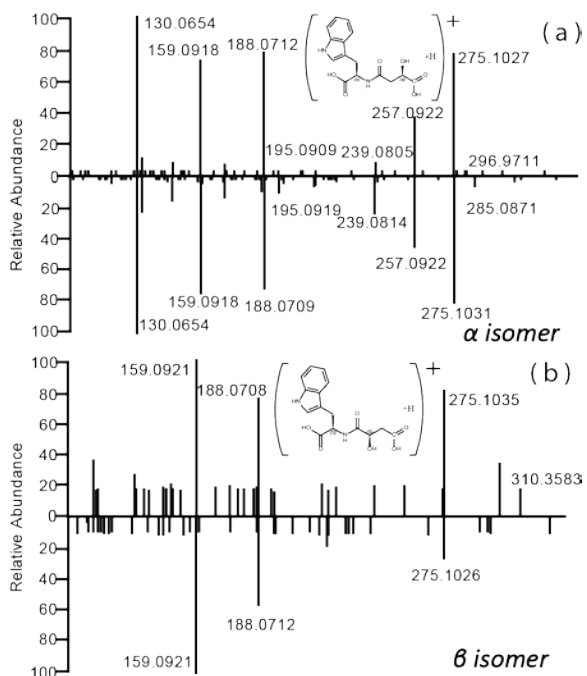


**Figure 4-4 Fragmentation patterns of endogenous  $N(\alpha)$ -methyl-tryptophan compared with the standard.** The endogenous compound is displayed on the upper half of each mass spectrum and the authentic standard is on the lower half. The two isomeric forms are listed separately, (a) and (b). Molecular ions were fragmented in the HCD cell with a normalized collision energy of 30%.

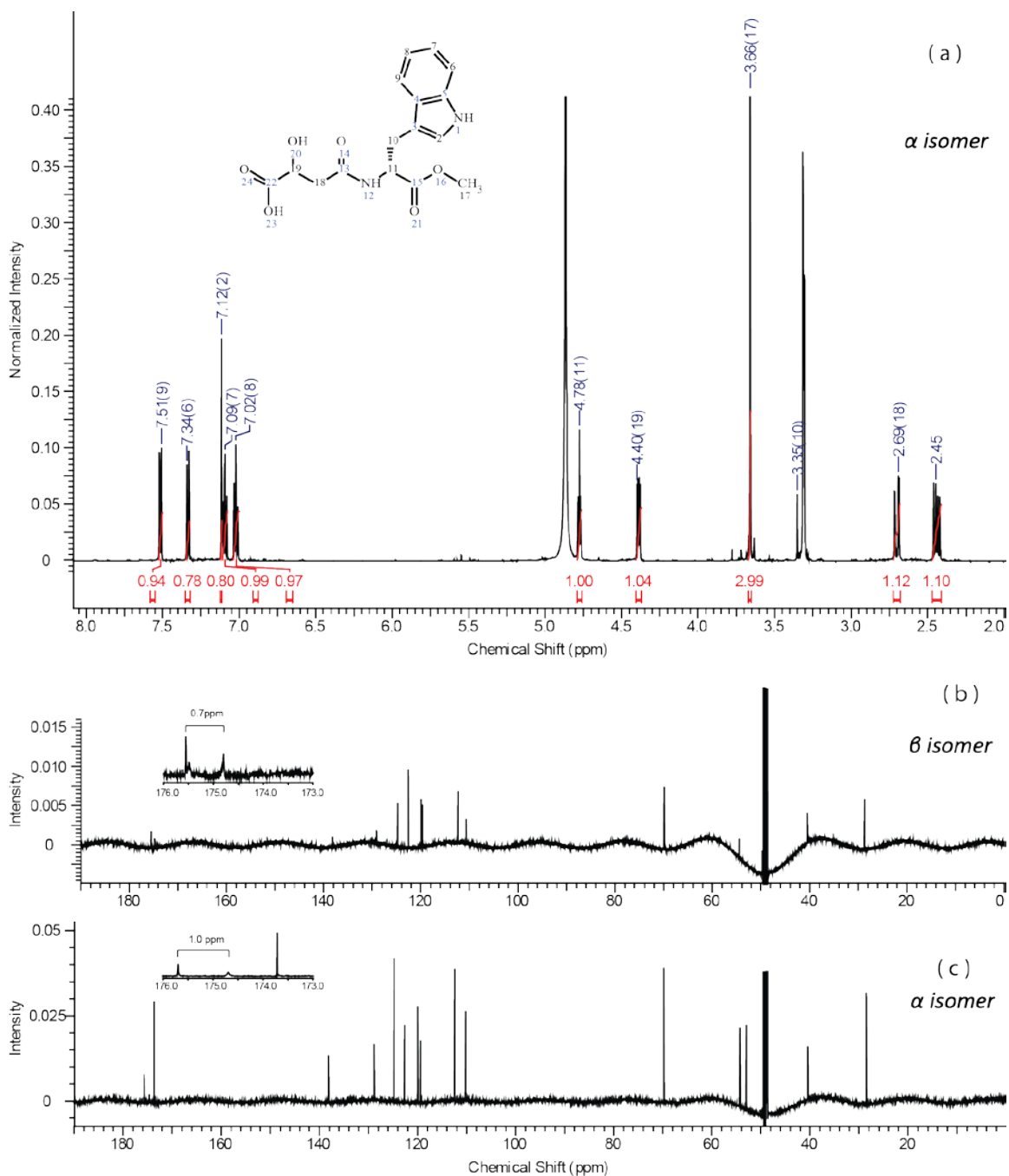


**Figure 4-5 (a) <sup>1</sup>H NMR spectrum of the α isomer of N(α)-(S)-malylyl-(S)-tryptophan methyl ester, (b) and (c) <sup>13</sup>C NMR spectra of α and β isomers of N(α)-(S)-malylyl-(S)-tryptophan methyl ester, respectively.** The difference in the chemical shifts of the carbonyl carbon atoms are highlighted in the insets. The change in chemical shifts agreed with literature and confirmed that the spectrum shown in (c) belongs to the α isomer (see text).

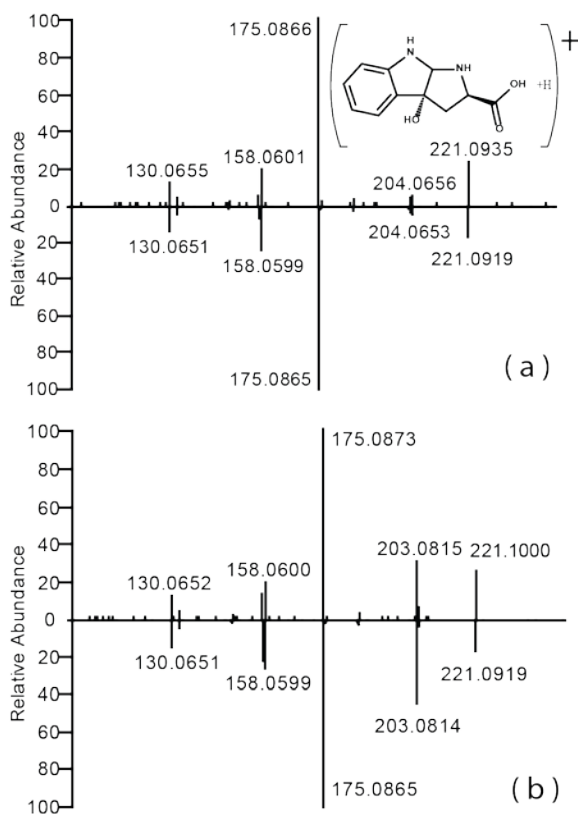


**Figure 4-6** Fragmentation patterns of endogenous *trans*-tryptophan alcohol and *cis*-tryptophan alcohol compared with their respective standard. The endogenous compound is displayed on the upper half of each mass spectrum and the authentic standard is on the lower half. Molecular ions were fragmented in the HCD cell with a normalized collision energy of 30%. Notice the relatively high abundance of 203 *m/z* in the *cis*-isomer. These compounds have previously only been described by *in vitro* chemical synthesis.

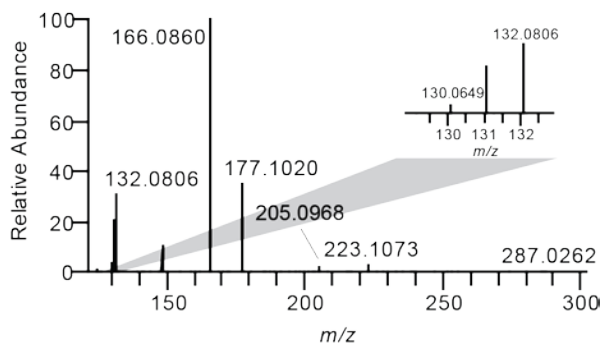


**Figure 4-7** Fragmentation pattern of a synthetic peptide **Phe-Gly-Gly-Phe**. The inset shows an expanded view around 130  $m/z$  region. Notice the absence of an indolic group in the compound's structure and the presence of the putative quinolinium ion (130.0651  $m/z$ ). Molecular ions were fragmented in the HCD cell with a normalized collision energy of 60%. A putative quinolinium ion can also be observed at 30% and 90% collision energy.

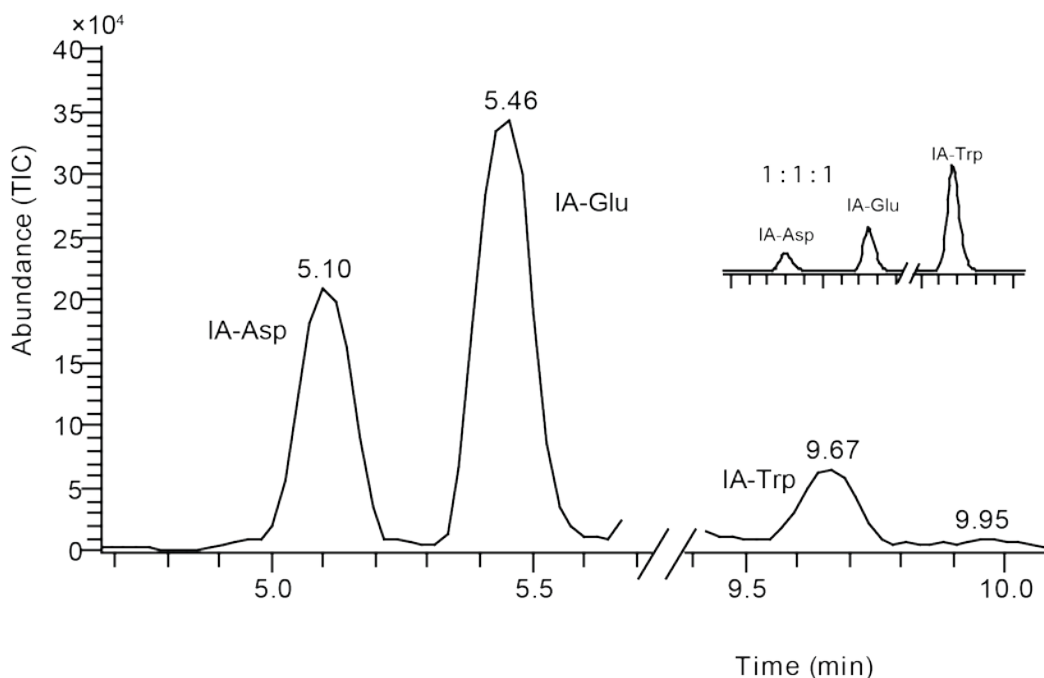


**Figure 4-8 LC-MS chromatogram showing the relative abundance of indole-3-acetyl-aspartic acid (IA-Asp), indole-3-acetyl-glutamic acid (IA-Glu), and indole-3-acetyl-tryptophan (IA-Trp).** TIC means total ion current, a measurement of ion intensity. The LC-MS chromatogram of a 1:1:1 molar mixture of these three compounds is shown in the inset to obtain the relative response factors. IA-Trp is estimated to be approximately 5% of the summation of the three conjugates based on the peak areas of each compound and adjusted for the relative response factors obtained from the insert.

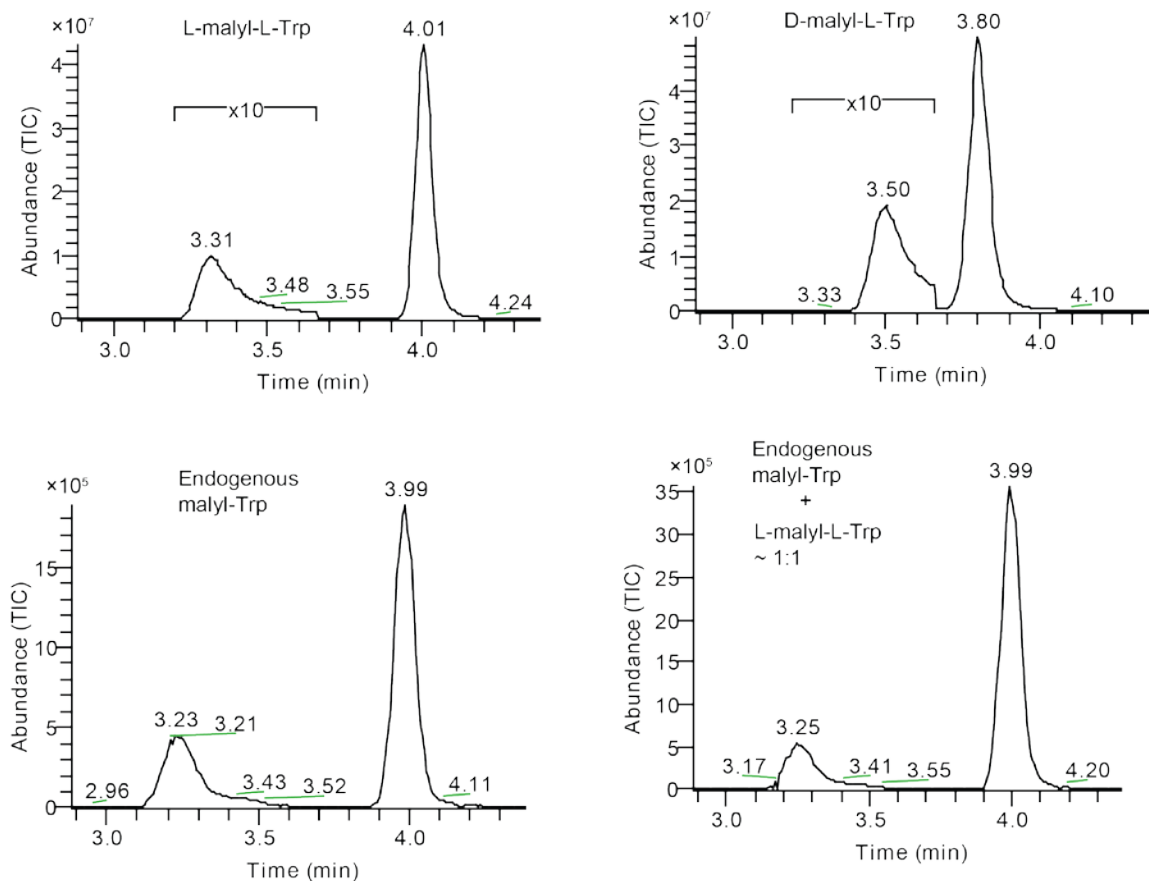


**Figure 4-9 LC-MS chromatogram of synthetic and endogenous N( $\alpha$ )-malylyl-L-(S)-tryptophans.** TIC means total ion current, a measurement of ion intensity. There is a pair of structural isomers ( $\alpha$  and  $\beta$ , see text) in each case, with the  $\beta$ -form eluting first. Upper panel shows the synthetic compounds, L-(2'S)-malylyl-L-(2S)-tryptophan and D-(2'R)-malylyl-L-(2S)-tryptophan, respectively. The  $\times 10$  indicates 10 times magnification on the y axis. Lower panel is a comparison between a plant sample and the same sample spiked with approximately the same amount of L-(2'S)-malylyl-L-(2S)-tryptophan. Notice the endogenous compound co-eluted with the spiked standard and intensity nearly doubled for both  $\alpha$  and  $\beta$  isomers.

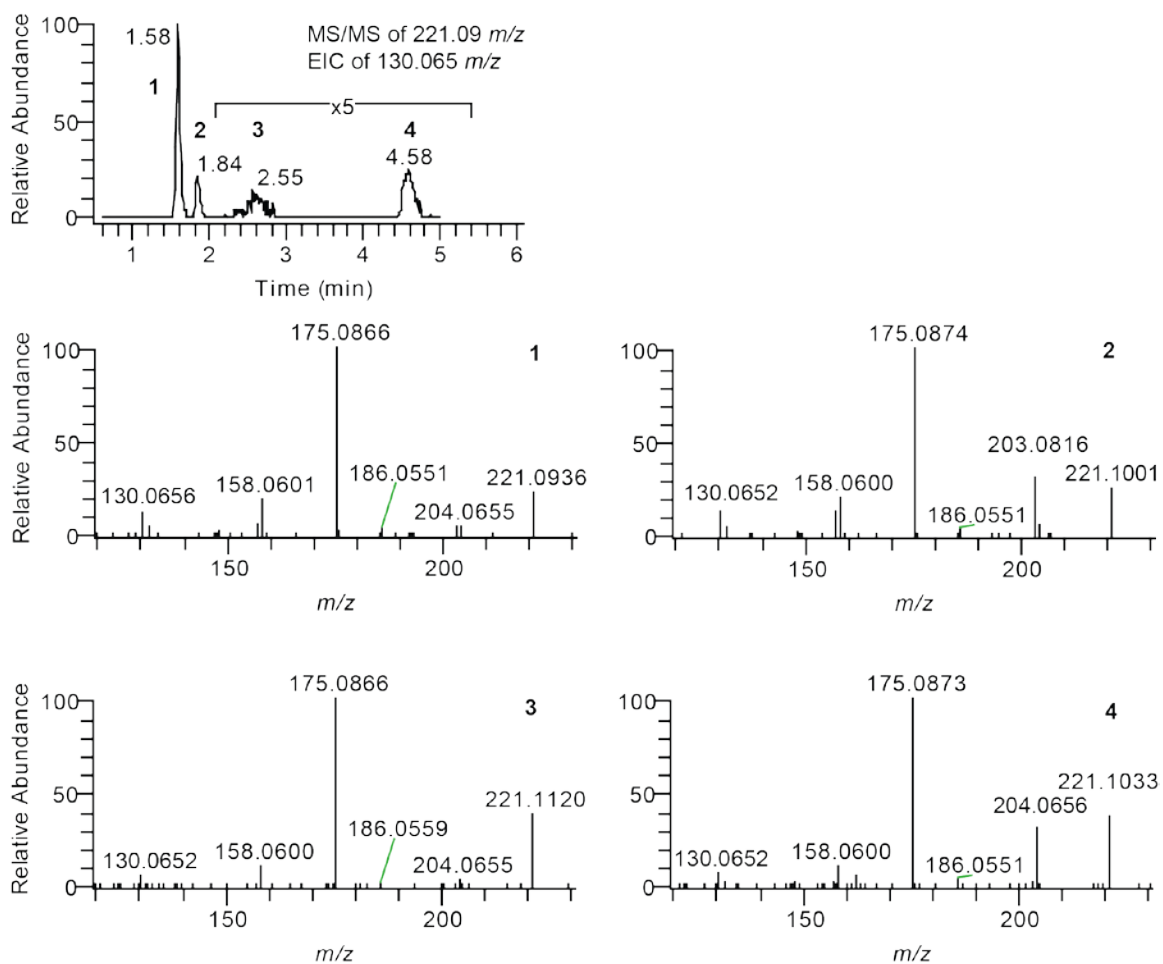


**Figure 4-10 LC chromatogram and MS/MS spectra of the four different tryptophan alcohols present in soybean.** Top panel is an extracted ion chromatogram (EIC) of the MS/MS channel at 221.09  $m/z$  (corresponds to Trp alcohols). The label  $\times 5$  indicates a 5 times magnification of the y axis to better visualize minor peaks. Middle and lower panels show the fragmentation pattern of these four compounds at a normalized collision energy of 25%.

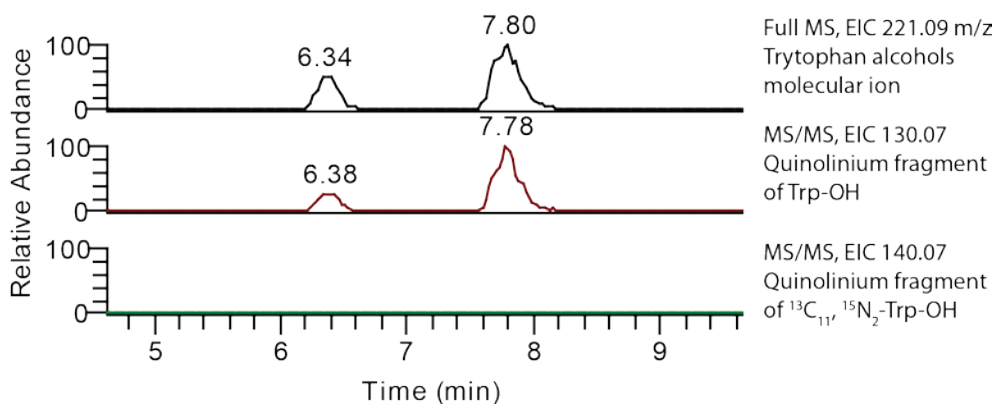


**Figure 4-11 Labeled tryptophan alcohols (Trp-OH) were not recovered after spiking in  $^{13}\text{C}_{11}$ ,  $^{15}\text{N}_2$ -labeled tryptophan.** Soybean was extracted with solvent (as described in the text) containing 10 pmol  $^{13}\text{C}_{11}$ ,  $^{15}\text{N}_2$  tryptophan per mg tissue. Top panel is the extracted ion chromatogram (EIC) corresponding to Trp-OH molecular ion at  $m/z$  221.09. Middle and lower panel is the EIC of the quinolinium ions expected from the fragmentation of Trp-OH and  $^{13}\text{C}_{11}$ ,  $^{15}\text{N}_2$ -labeled Trp-OH, respectively. Signal for the labeled quinolinium ion at  $m/z$  140.07 was not detected, indicating no labeled Trp-OH was generated from the added  $^{13}\text{C}_{11}$ ,  $^{15}\text{N}_2$ -labeled tryptophan during the extraction process.

**Table 4-1 List of indolic compounds identified**

| <b>Compound class:</b> | <b>IAA amino acid conjugates</b> | <b>Tryptophan acid conjugates</b>                                       | <b>Other tryptophan derivatives</b> |
|------------------------|----------------------------------|---|-------------------------------------|
|                        | Indole-3-acetyl-aspartic acid    | N( $\alpha$ )-acetyl-tryptophan*  |                                     |
|                        | Indole-3-acetyl-glutamic acid    | N( $\alpha$ )-malonyl - tryptophan                                      | Tryptophan alcohols*                |
|                        | Indole-3-acetyl-tryptophan*      | N( $\alpha$ )-succinyl - tryptophan*<br>N( $\alpha$ )-malyl-tryptophan* |                                     |

\* Indicates this compound had not been reported in this species before.

**Table 4-2 Partial list of indolic compounds obtained from one young tomato leaf**

| <i>m/z</i> (M+H) <sup>+</sup> | RT (min)  | Formula <sup>a</sup> (M+H)                                    | Compound ID <sup>b</sup> |
|-------------------------------|-----------|---|--------------------------|
| 221.0922                      | 1.6       | C <sub>11</sub> H <sub>13</sub> O <sub>3</sub> N <sub>2</sub> | trans-Trp-OH             |
| 221.0922                      | 1.77      | C <sub>11</sub> H <sub>13</sub> O <sub>3</sub> N <sub>2</sub> | cis-Trp-OH               |
| 291.098                       | 7.32      | C <sub>14</sub> H <sub>15</sub> O <sub>5</sub> N <sub>2</sub> | IA-Asp                   |
| 291.0975                      | 8.38      | C <sub>14</sub> H <sub>15</sub> O <sub>5</sub> N <sub>2</sub> | Malonyl-Trp              |
| 247.1077                      | 8.6       | C <sub>13</sub> H <sub>15</sub> O <sub>3</sub> N <sub>2</sub> | Ac-Trp                   |
| 346.1558                      | 3.74      | C <sub>21</sub> H <sub>20</sub> O <sub>2</sub> N <sub>3</sub> | Trp-deri                 |
| 352.1391                      | 4.25/4.53 | C <sub>17</sub> H <sub>22</sub> O <sub>7</sub> N              | Ind-deri                 |
| 366.1183                      | 5.21/6.21 | C <sub>17</sub> H <sub>20</sub> O <sub>8</sub> N              | Ind-deri                 |
| 307.0932                      | 6.04      | C <sub>14</sub> H <sub>15</sub> O <sub>6</sub> N <sub>2</sub> | Trp-deri                 |

<sup>a</sup>Formulae were calculated based on exact mass ( $\pm 2$  ppm) of the protonated molecular ion.

<sup>b</sup>Compound putative identification (ID) was based on mass spectrum similarities to authentic standards. Trp-deri indicates an unidentified tryptophan derivative based on the presence of the 188.0700 *m/z* secondary mass signature (deamination product of tryptophan). Ind-deri indicates an unidentified indole derivative with 130.0651 *m/z* signature ion only.

**Table 4-3 Partial list of indolic compounds from one male ginkgo flower**

| $m/z$ (M+H) <sup>+</sup> | RT (min) | Formula <sup>a</sup> (M+H)                                    | Compound ID <sup>b</sup> |
|--------------------------|----------|---|--------------------------|
| 221.0922                 | 1.56     | C <sub>11</sub> H <sub>13</sub> O <sub>3</sub> N <sub>2</sub> | trans-Trp-OH             |
| 221.0922                 | 1.72     | C <sub>11</sub> H <sub>13</sub> O <sub>3</sub> N <sub>2</sub> | cis-Trp-OH               |
| 291.0976                 | 7.37     | C <sub>14</sub> H <sub>15</sub> O <sub>5</sub> N <sub>2</sub> | IA-Asp                   |
| 305.1136                 | 7.83     | C <sub>15</sub> H <sub>17</sub> O <sub>5</sub> N <sub>2</sub> | IA-Glu                   |
| 247.1076                 | 8.58     | C <sub>13</sub> H <sub>15</sub> O <sub>3</sub> N <sub>2</sub> | Ac-Trp                   |
| 346.1547                 | 3.58     | C <sub>21</sub> H <sub>20</sub> O <sub>2</sub> N <sub>3</sub> | Trp-deri                 |
| 291.0974                 | 5.29     | C <sub>14</sub> H <sub>15</sub> O <sub>5</sub> N <sub>2</sub> | Ind-deri                 |
| 304.165                  | 5.41     | C <sub>16</sub> H <sub>22</sub> O <sub>3</sub> N <sub>3</sub> | Trp-deri                 |
| 305.1136                 | 5.68     | C <sub>15</sub> H <sub>17</sub> O <sub>5</sub> N <sub>2</sub> | Ind-deri                 |
| 338.1233                 | 6.42     | C <sub>16</sub> H <sub>20</sub> O <sub>7</sub> N              | Trp-deri                 |

<sup>a</sup>Formulae were calculated based on exact mass ( $\pm 2$  ppm) of the protonated molecular ion.

<sup>b</sup>Compound putative identification (ID) was based on mass spectrum similarities to authentic standards. Trp-deri indicates an unidentified tryptophan derivative based on the presence of the 188.0700  $m/z$  secondary mass signature (deamination product of tryptophan). Ind-deri indicates an unidentified indole derivative with 130.0651  $m/z$  signature ion only.

**Table 4-4 Partial list of indolic compounds obtained from coconut milk sample**

| <i>m/z</i> (M+H) <sup>+</sup> | RT (min)  | Formula <sup>a</sup> (M+H)                                    | Compound ID <sup>b</sup> |
|-------------------------------|-----------|---|--------------------------|
| 221.0922                      | 1.57      | C <sub>11</sub> H <sub>13</sub> O <sub>3</sub> N <sub>2</sub> | trans-Trp-OH             |
| 221.0921                      | 1.76      | C <sub>11</sub> H <sub>13</sub> O <sub>3</sub> N <sub>2</sub> | cis-Trp-OH               |
| 291.0979                      | 7.4       | C <sub>14</sub> H <sub>15</sub> O <sub>5</sub> N <sub>2</sub> | IA-Asp                   |
| 305.1138                      | 7.85      | C <sub>15</sub> H <sub>17</sub> O <sub>5</sub> N <sub>2</sub> | IA-Glu                   |
| 291.0976                      | 8.38      | C <sub>14</sub> H <sub>15</sub> O <sub>5</sub> N <sub>2</sub> | Malonyl-Trp              |
| 247.1077                      | 8.59      | C <sub>13</sub> H <sub>15</sub> O <sub>3</sub> N <sub>2</sub> | Ac-Trp                   |
| 346.155                       | 3.64      | C <sub>21</sub> H <sub>20</sub> O <sub>2</sub> N <sub>3</sub> | Trp-deri                 |
| 333.1556                      | 4.4       | C <sub>16</sub> H <sub>21</sub> O <sub>4</sub> N <sub>4</sub> | Trp-deri                 |
| 334.1397                      | 4.75      | C <sub>16</sub> H <sub>20</sub> O <sub>5</sub> N <sub>3</sub> | Trp-deri                 |
| 292.1181                      | 4.94      | C <sub>15</sub> H <sub>18</sub> O <sub>5</sub> N              | Ind-deri                 |
| 291.0976                      | 5.35/5.85 | C <sub>14</sub> H <sub>15</sub> O <sub>5</sub> N <sub>2</sub> | Ind-deri                 |
| 304.1654                      | 5.46      | C <sub>16</sub> H <sub>22</sub> O <sub>3</sub> N <sub>3</sub> | Trp-deri                 |
| 338.1233                      | 6.44/6.77 | C <sub>16</sub> H <sub>20</sub> O <sub>7</sub> N              | Trp-deri                 |
| 320.1128                      | 6.66      | C <sub>16</sub> H <sub>18</sub> O <sub>6</sub> N              | Ind-deri                 |
| 367.1261                      | 7         | C <sub>15</sub> H <sub>19</sub> O <sub>7</sub> N <sub>4</sub> | Trp-deri                 |

<sup>a</sup>Formulae are calculated based on exact mass ( $\pm 3$  ppm) of the protonated molecular ion.

<sup>b</sup>Compound putative identification (ID) is based on mass spectrum similarities to authentic standards. Trp-deri indicates an unidentified tryptophan derivative based on the presence of the 188.0700 *m/z* secondary mass signature (deamination product of tryptophan). Ind-deri indicates an unidentified indole derivative with 130.0651 *m/z* signature ion only.

## **Chapter 5 Conclusions: Towards understanding auxin networks**

Auxin metabolism is a set of biochemical processes that play central roles in regulating plant growth and development. Plants possess complicated yet elegant networks that include numerous players that regulate auxin metabolism and its interplay with other biochemical and physiological processes, altogether contributing to a robust, self-organizing, and hierarchal system capable of reproducing themselves and interact with the physical environment. Past studies have uncovered many metabolites, enzymes, and genes integral to such networks using a variety of molecular biology, genetic, chemical and biochemical techniques. Mechanisms behind many aspects of plant growth and development pertaining to the action of auxin have been gradually unveiled and that has led to improved horticultural and agricultural products that we enjoy today.

The study of auxin metabolism has been fruitful, yet challenging, partially due to the complex biochemical networks and extremely low levels of auxin metabolites. Fortunately, advances in analytical and information technologies have brought forward the capabilities to systemically study such complicated networks. In this dissertation, I first attempted to dissect the auxin biosynthesis network using analytical approaches (Chapter 2), in the hope of reconciling the mysteries still remaining regarding the biochemical origin of auxin. The feasibility and utilities of such approaches were demonstrated by confirming previous reports of the role of IPyA in auxin biosynthesis which was based largely on genetic and limited biochemical evidences, as well as by discovery of novel regulatory steps between IPyA and IAA. Another network of auxin metabolism, IAA conjugates, was also examined in this thesis (Chapter 3). Conjugation is one important means of modulating the active hormone, and I showed that harsh chemical treatment (the primary means of quantifying unknown conjugates) may inflict substantial artifacts in the quantification. Lastly, I also established an unbiased approach in characterizing the players in indole metabolism (Chapter 4), which IAA metabolism is an important subset. This technique allows a quick survey of the members of the indole

network and the identification of previously unknown ones, making network comprehension easier with more complete knowledge.

Altogether, the efforts of characterizing the network of auxin metabolism in this thesis have yielded significant insights and this systemic approach itself shall be a valuable tool in studying many of the auxin related processes.

In addition to the analytical methods and technical discoveries reported in this dissertation, a number of important biological questions have been revealed by these studies and these warrant further investigation. Firstly, the labelling kinetics of Trp, IPyA and IAAld closely resembled each other, indicating a very close metabolic relationship among them. A pulse chase study by feeding an upstream precursor may help to define the substrate-product relationships among these intermediates. Secondly, it appeared there was a key regulatory step between IPyA and IAA in the synthesis of the latter. It will be important in future work to determine if this regulation also functions *in vitro* in order to determine how the specific enzymatic activities are themselves regulated. Thirdly, many tryptophan metabolites were identified in the studies described in Chapter 4. It will be important to find out the metabolic routes leading to these compounds and their biochemical fate in plants and plant consuming organisms, given that tryptophan is an important animal and human dietary nutrient. Finally, with the LC-MS based facile technique for indolic compound identification, it is now possible to study the occurrence and prevalence of many of the IAA conjugates *in planta* by doing a quick survey of taxonomically diverse plant species. This should give us an opportunity to obtain an important evolutionary perspective regarding auxin metabolism.

## Bibliography

- Ahmad, A., Eelnurme, I. and Spenser, I. D.** (1960) Indolyl-3-acetaldoxime. *Canadian Journal of Chemistry*, **38**(12), 2523-2523.
- Andreae, W.A. and Good, N. E.** (1955) The formation of indoleacetylaspartic acid in pea seedlings. *Plant Physiol.*, **30**(4), 380-382.
- Auriol, D., Paul, F. and Monsan, P.** (1990) A new peptidase enzyme useful for peptide and amino acid derivative synthesis by reverse hydrolysis reactions. *Ann. N. Y. Acad. Sci.*, **613**(1), 201-206.
- Badenoch-Jones, J., Summons, R., Entsch, B., Rolfe, B., Parker, C. and Letham, D.** (1982) Mass spectrometric identification of indole compounds produced by rhizobium strains. *Biol. Mass Spectrom.*, **9**(10), 429-437.
- Bajguz, A. and Piotrowska, A.** (2009) Conjugates of auxin and cytokinin. *Phytochemistry*, **70**(8), 957-969.
- Baldi, B.G., Maher, B. R. and Cohen, J. D.** (1989) Hydrolysis of indole-3-acetic acid esters exposed to mild alkaline conditions. *Plant Physiol.*, **91**(1), 9-12.
- Baldi, B.G., Maher, B. R., Slovin, J. P. and Cohen, J. D.** (1991) Stable isotope labeling, in vivo, of D- and L-tryptophan pools in *Lemna gibba* and the low incorporation of label into indole-3-acetic acid. *Plant Physiol.*, **95**(4), 1203-1208.
- Bandurski, R.S. and Schulze, A.** (1977) Concentration of indole-3-acetic acid and its derivatives in plants. *Plant Physiol.*, **60**(2), 211-213.
- Bandurski, R.S. and Piskornik, Z.** (1973) An indole-3-acetic acid ester of a cellulosic glucan. In *Biogenesis of Plant Cell Wall Polysaccharides* (F. Loewus, ed.) New York: Academic Press, pp. 297-314.
- Bandurski, R. and Ehmann, A.** (1986) GC-MS methods for the quantitative determination and structural characterization of esters of indole-3-acetic acid and *myo*-inositol. In *Gas Chromatography/Mass Spectrometry: Modern Methods of Plant Analysis, New Series*. (H.F. Linskens, J.F. Jackson, eds) Springer-Verlag, Berlin Heidelberg, 3:189-213
- Bandurski, R.S. and Schulze, A.** (1974) Concentrations of indole-3-acetic acid and its esters in *Avena* and *Zea*. *Plant Physiol.*, **54**(3), 257-262.
- Bandurski, R.S., Ueda, M. and Nicholls, P. B.** (1970) Esters of indole-3-acetic acid and *myo*-inositol. *Ann. N. Y. Acad. Sci.*, **165**(2), 655-667.

- Barkawi, L.S., Tam, Y. Y., Tillman, J. A., Pederson, B., Calio, J., Al-Amier, H., Emerick, M., Normanly, J. and Cohen, J. D.** (2008) A high-throughput method for the quantitative analysis of indole-3-acetic acid and other auxins from plant tissue. *Anal. Biochem.*, **372**(2), 177-188.
- Barratt, N.M., Dong, W., Gage, D. A., Magnus, V. and Town, C. D.** (1999) Metabolism of exogenous auxin by *Arabidopsis thaliana*: Identification of the conjugate N-(indol-3-ylacetyl)-glutamine and initiation of a mutant screen. *Physiol. Plantarum*, **105**(2), 207-217.
- Baud, S., Boutin, J., Miquel, M., Lepiniec, L. and Rochat, C.** (2002) An integrated overview of seed development in *Arabidopsis thaliana* ecotype WS. *Plant Physiology and Biochemistry*, **40**(2), 151-160.
- Bialek, K. and Cohen, J. D.** (1989) Quantitation of indoleacetic acid conjugates in bean seeds by direct tissue hydrolysis. *Plant Physiol.*, **90**(2), 398-400.
- Bialek, K. and Cohen, J. D.** (1986) Isolation and partial characterization of the major amide-linked conjugate of indole-3-acetic acid from *Phaseolus vulgaris* L. *Plant Physiol.*, **80**(1), 99-104.
- Bloch, K. and Anker, H. S.** (1948) An extension of the isotope dilution method. *Science*, **107**(2774), 228.
- Broeckling, C.D., Heuberger, A. L., Prince, J. A., Ingelsson, E. and Prenni, J. E.** (2013) Assigning precursor-product ion relationships in indiscriminant MS/MS data from non-targeted metabolite profiling studies. *Metabolomics*, **9**(1), 33-43.
- Brown, P.D., Tokuhisa, J. G., Reichelt, M. and Gershenzon, J.** (2003) Variation of glucosinolate accumulation among different organs and developmental stages of *Arabidopsis thaliana*. *Phytochemistry*, **62**(3), 471-481.
- Brückner, H. and Westhauser, T.** (2003) Chromatographic determination of L- and D-amino acids in plants. *Amino Acids*, **24**(1-2), 43-55.
- Burow, M., Zhang, Z. Y., Ober, J. A., Lambrix, V. M., Wittstock, U., Gershenzon, J. and Kliebenstein, D. J.** (2008) ESP and ESM1 mediate indol-3-acetonitrile production from indol-3-ylmethyl glucosinolate in *Arabidopsis*. *Phytochemistry*, **69**(3), 663-671.
- Cao, Z., Ma, Y., Chen, M., Mou, R. and Hu, X.** (2011) Analysis of auxins and their amino acid conjugates in rice by liquid chromatography tandem mass spectrometry. *Journal of Instrumental Analysis*, **12**, 018.
- Caplin, S.M. and Steward, F. C.** (1948) Effect of coconut milk on the growth of explants from carrot root. *Science*, **108**(2815), 655-657.

- Catalá, C., Ostin, A., Chamarro, J., Sandberg, G. and Crozier, A.** (1992) Metabolism of indole-3-acetic acid by pericarp discs from immature and mature tomato (*Lycopersicon esculentum* mill). *Plant Physiol.*, **100**(3), 1457-1463.
- Chambers, M.C., Maclean, B., Burke, R., Amodei, D., Ruderman, D. L., Neumann, S., Gatto, L., Fischer, B., Pratt, B. and Egertson, J.** (2012) A cross-platform toolkit for mass spectrometry and proteomics. *Nat. Biotechnol.*, **30**(10), 918-920.
- Chapman, E.J. and Estelle, M.** (2009) Mechanism of auxin-regulated gene expression in plants. *Annu. Rev. Genet.*, **43**, 265-285.
- Chen, K.H., Miller, A. N., Patterson, G. W. and Cohen, J. D.** (1988) A rapid and simple procedure for purification of indole-3-acetic acid prior to GC-SIM-MS analysis. *Plant Physiol.*, **86**(3), 822-825.
- Chen, Q., Zhang, B., Hicks, L. M., Wang, S. and Jez, J. M.** (2009) A liquid chromatography–tandem mass spectrometry-based assay for indole-3-acetic acid–amido synthetase. *Anal. Biochem.*, **390**(2), 149-154.
- Chevolleau, S., Debrauwer, L., Boyer, G. and Tulliez, J.** (2002) Isolation and structure elucidation of a new thermal breakdown product of glucobrassicin, the parent indole glucosinolate. *J. Agric. Food Chem.*, **50**(18), 5185-5190.
- Chevolleau, S., Gasc, N., Rollin, P. and Tulliez, J.** (1997) Enzymatic, chemical, and thermal breakdown of 3H-labeled glucobrassicin, the parent indole glucosinolate. *J. Agric. Food Chem.*, **45**(11), 4290-4296.
- Chisnell, J.R. and Bandurski, R. S.** (1988) Translocation of radiolabeled indole-3-acetic acid and indole-3-acetyl-myoinositol from kernel to shoot of *Zea mays* L. *Plant Physiol.*, **86**(1), 79-84.
- Cholodny, N.** (1935) Über das keimungshormon von gramineen. *Planta*, **23**(3), 289-312.
- Ciesielski, T.** (1872) Untersuchungen über die Abwärtskrümmung der Wurzel. *Beitr. Biol. Pflanzen* **1**, 1–30.
- Cleland, W.W.** (2005) The use of isotope effects to determine enzyme mechanisms. *Arch. Biochem. Biophys.*, **433**(1), 2-12.
- Cohen, J.D.** (1982) Identification and quantitative analysis of indole-3-acetyl-L-aspartate from seeds of *Glycine max* L. *Plant Physiol.*, **70**(3), 749-753.
- Cohen, J.D.** (1981) Synthesis of <sup>14</sup>C-labeled indole-3-acetyl aspartic acid. *J. Labelled Compd. Radiopharmaceut.*, **18**(9), 1393-1396.

- Cohen, J.D. and Bandurski, R. S.** (1982) Chemistry and physiology of the bound auxins. *Annual Review of Plant Physiology*, **33**(1), 403-430.
- Cohen, J.D. and Bandurski, R. S.** (1978) The bound auxins: Protection of indole-3-acetic acid from peroxidase-catalyzed oxidation. *Planta*, **139**(3), 203-208.
- Darwin, C. and Darwin, F.** (1880) *The power of movement in plants* London: John Murray, 593 pp.
- Davies, N.W., Smith, J. A., Molesworth, P. P. and Ross, J. J.** (2010) Hydrogen/deuterium exchange on aromatic rings during atmospheric pressure chemical ionization mass spectrometry. *Rapid Communications in Mass Spectrometry*, **24**(7), 1105-1110.
- Dharmasiri, N., Dharmasiri, S. and Estelle, M.** (2005) The F-box protein TIR1 is an auxin receptor. *Nature*, **435**(7041), 441-445.
- Ding, X., Cao, Y., Huang, L., Zhao, J., Xu, C., Li, X. and Wang, S.** (2008) Activation of the indole-3-acetic acid-amido synthetase GH3-8 suppresses expansin expression and promotes salicylate- and jasmonate-independent basal immunity in rice. *Plant Cell*, **20**(1), 228-240.
- Epstein, E., Baldi, B. G. and Cohen, J. D.** (1986) Identification of indole-3-acetylglutamate from seeds of *Glycine max* L. *Plant Physiol.*, **80**(1), 256-258.
- Epstein, E., Cohen, J. D. and Bandurski, R. S.** (1980) Concentration and metabolic turnover of indoles in germinating kernels of *Zea mays* L. *Plant Physiol.*, **65**(3), 415-421.
- Fukui, H.N., Devries, J. E., Wittwer, S. and Sell, H.** (1957) Ethyl-3-indoleacetate: An artefact in extracts of immature corn kernels. *Nature*, **180**, 1205.
- González-Lamothe, R., El Oirdi, M., Brisson, N. and Bouarab, K.** (2012) The conjugated auxin indole-3-acetic acid-aspartic acid promotes plant disease development. *Plant Cell*, **24**(2), 762-777.
- Gordon, S.A. and Wildman, S. G.** (1943) The conversion of tryptophane to a plant growth substance by conditions of mild alkalinity. *J. Biol. Chem.*, **147**(2), 389-398.
- Gordon, S.A.** (1946) Auxin-protein complexes of the wheat grain. *Am. J. Bot.*, **33**(3), 160-169.
- Gracanin, M., Hawkins, C. L., Pattison, D. I. and Davies, M. J.** (2009) Singlet-oxygen-mediated amino acid and protein oxidation: Formation of tryptophan peroxides and decomposition products. *Free Radical Biol. Med.*, **47**(1), 92-102.

- Hall, P.J.** (1980) Indole-3-acetyl-*myo*-inositol in kernels of *Oryza sativa*. *Phytochemistry*, **19**(10), 2121-2123.
- Hamilton, R.H.** (1961) Isolation of indole-3-acetic acid from corn kernels & etiolated corn seedlings. *Plant Physiol.*, **36**(3), 354-359.
- Huttlin, E.L., Hegeman, A. D., Harms, A. C. and Sussman, M. R.** (2007) Comparison of full versus partial metabolic labeling for quantitative proteomics analysis in *Arabidopsis thaliana*. *Mol. Cell. Proteomics*, **6**(5), 860-881.
- Ilić, N., Normanly, J. and Cohen, J. D.** (1996) Quantification of free plus conjugated indoleacetic acid in *Arabidopsis* requires correction for the nonenzymatic conversion of indolic nitriles. *Plant Physiol.*, **111**(3), 781-788.
- Ishimaru, K., Hirotsu, N., Madoka, Y., Murakami, N., Hara, N., Onodera, H., Kashiwagi, T., Ujiie, K., Shimizu, B. and Onishi, A.** (2013) Loss of function of the IAA-glucose hydrolase gene TGW6 enhances rice grain weight and increases yield. *Nat. Genet.*, **45**, 707-711.
- Iyer, M., Slovin, J.P., Epstein, E., Cohen, J.D.** (2005) Transgenic tomato plants with a modified ability to synthesize indole-3-acetyl-beta-1-O-D-glucose. *J Plant Growth Regul* **24**:142-152
- Kai, K., Horita, J., Wakasa, K. and Miyagawa, H.** (2007a) Three oxidative metabolites of indole-3-acetic acid from *Arabidopsis thaliana*. *Phytochemistry*, **68**(12), 1651-1663.
- Kai, K., Wakasa, K. and Miyagawa, H.** (2007b) Metabolism of indole-3-acetic acid in rice: Identification and characterization of *N*- $\beta$ -D-glucopyranosyl indole-3-acetic acid and its conjugates. *Phytochemistry*, **68**(20), 2512-2522.
- Kawai, Y., Ono, E. and Mizutani, M.** (2014) Evolution and diversity of the 2-oxoglutarate-dependent dioxygenase superfamily in plants. *Plant Journal*, **78**(2), 328-343.
- Kepinski, S. and Leyser, O.** (2005) The *Arabidopsis* F-box protein TIR1 is an auxin receptor. *Nature*, **435**(7041), 446-451.
- Klarskov, K., Johnson, K., Benson, L., Gleich, G. and Naylor, S.** (1999) Eosinophilia-myalgia syndrome case-associated contaminants in commercially available 5-hydroxytryptophan. In *Tryptophan, Serotonin, and Melatonin* (G. Huether, W. Kochen, T.J. Simat and H. Steinhart, eds) New York: Springer, pp 461-468
- Kögl, F., Haagen-Smit, A. and Erxleben, H.** (1934) Über ein neues auxin ("hetero-auxin") aus harn. *Zeitschrift Fur Physiologische Chemie*, **228**(1-2), 90-103.

- Komoszynski, M. and Bandurski, R. S.** (1986) Transport and metabolism of indole-3-acetyl-*myo*-inositol-galactoside in seedlings of *Zea mays*. *Plant Physiol.*, **80**(4), 961-964.
- Korasick, D.A., Enders, T. A. and Strader, L. C.** (2013) Auxin biosynthesis and storage forms. *J. Exp. Bot.*, **64**(9), 2541-2555.
- Kowalczyk, M. and Sandberg, G.** (2001) Quantitative analysis of indole-3-acetic acid metabolites in *Arabidopsis*. *Plant Physiol.*, **127**(4), 1845-1853.
- Labarca, C., Nicholls, P. and Bandurski, R. S.** (1965) A partial characterization of indoleacetylinositols from *Zea mays*. *Biochem. Biophys. Res. Commun.*, **20**(5), 641-646.
- Law, D.M.** (1987) Gibberellin-enhanced indole-3-acetic acid biosynthesis: D-Tryptophan as the precursor of indole-3-acetic acid. *Physiol. Plantarum*, **70**(4), 626-632.
- Leighty, R.W. and Antoniewicz, M. R.** (2011) Dynamic metabolic flux analysis (DMFA): A framework for determining fluxes at metabolic non-steady state. *MeTable Eng.*, **13**(6), 745-755.
- Leverone, L.A., Kossenjans, W., Jayasimihulu, K. and Caruso, J. L.** (1991) Evidence of zein-bound indoleacetic acid using gas chromatography-selected ion monitoring-mass spectrometry analysis and immunogold labeling. *Plant Physiol.*, **96**(4), 1070-1075.
- Lewer, P. and Bandurski, R. S.** (1987) Occurrence and metabolism of 7-hydroxy-2-indolinone-3-acetic acid in *Zea mays*. *Phytochemistry*, **26**(5), 1247-1250.
- Lincoln, C., Britton, J. H. and Estelle, M.** (1990) Growth and development of the *axr1* mutants of *Arabidopsis*. *Plant Cell*, **2**(11), 1071-1080.
- Liu, X., Hegeman, A. D., Gardner, G. and Cohen, J. D.** (2012) Protocol: High-throughput and quantitative assays of auxin and auxin precursors from minute tissue samples. *Plant Methods*, **8**(1), 31.
- Ljung, K., Hull, A. K., Kowalczyk, M., Marchant, A., Celenza, J., Cohen, J. D. and Sandberg, G.** (2002) Biosynthesis, conjugation, catabolism and homeostasis of indole-3-acetic acid in *Arabidopsis thaliana*. *Plant Mol. Biol.*, **50**(2), 309-332.
- Ljung, K.** (2013) Auxin metabolism and homeostasis during plant development. *Development*, **140**(5), 943-950.
- Ljung, K., Hull, A. K., Kowalczyk, M., Marchant, A., Celenza, J., Cohen, J. D. and Sandberg, G.** (2002) Biosynthesis, conjugation, catabolism and homeostasis of indole-3-acetic acid in *Arabidopsis thaliana*. *Plant Mol. Biol.*, **50**(2), 309-332.

- Ljung, K., Ostin, A., Lioussanne, L. and Sandberg, G.** (2001) Developmental regulation of indole-3-acetic acid turnover in Scots pine seedlings. *Plant Physiol.*, **125**(1), 464-475.
- Lorenz, P., Stermitz, F. R. and Beck, J. J.** (1998) On the reaction of (S)-trifluoroacetoxysuccinic anhydride with amines to produce hydroxysuccinamic (malamic) acid derivatives. *Journal Für Praktische Chemie/Chemiker-Zeitung*, **340**(8), 733-737.
- Ludwig-Müller, J.** (2011) Auxin conjugates: Their role for plant development and in the evolution of land plants. *J. Exp. Bot.*, **62**(6), 1757-1773.
- Ludwig-Müller, J. and Hilgenberg, W.** (1989) *N*-malonyltryptophan metabolism by seedlings of Chinese cabbage. *Phytochemistry*, **28**(10), 2571-2575.
- MacCoss, M.J., Wu, C. C., Liu, H., Sadygov, R. and Yates, J. R.** (2003) A correlation algorithm for the automated quantitative analysis of shotgun proteomics data. *Anal. Chem.*, **75**(24), 6912-6921.
- Maltese, F., Kooy, F. and Verpoorte, R.** (2009) Solvent derived artifacts in natural products chemistry. *Natural Product Communications*, **4**(3), 447-454.
- Mansfield, S. and Briarty, L.** (1992) Cotyledon cell development in *Arabidopsis thaliana* during reserve deposition. *Canadian Journal of Botany*, **70**(1), 151-164.
- Markova, T.A. and Gamburg, K. Z.** (1997) Stereoconfiguration of endogenous *N*-malonyltryptophan in plants. *Plant Science*, **122**(2), 119-124.
- Marx, M. and Djerassi, C.** (1968) Mass spectrometry in structural and stereochemical problems. CXLIX. Question of ring expansion in the fragmentation of carbon-13 nitrogen heterocycles. *J. Am. Chem. Soc.*, **90**(3), 678-681.
- Mashiguchi, K., Tanaka, K., Sakai, T., Sugawara, S., Kawaide, H., Natsume, M., Hanada, A., Yaeno, T., Shirasu, K., Yao, H., McSteen, P., Zhao, Y., Hayashi, K., Kamiya, Y. and Kasahara, H.** (2011) The main auxin biosynthesis pathway in *Arabidopsis*. *Proc. Natl. Acad. Sci. U. S. A.*, **108**(45), 18512-18517.
- Matsuda, F., Miyazawa, H., Wakasa, K. and Miyagawa, H.** (2005) Quantification of indole-3-acetic acid and amino acid conjugates in rice by liquid chromatography-electrospray ionization-tandem mass spectrometry. *Biosci. Biotechnol. Biochem.*, **69**(4), 778-783.
- Michalski, A., Damoc, E., Hauschild, J., Lange, O., Wiegand, A., Makarov, A., Nagaraj, N., Cox, J., Mann, M. and Horning, S.** (2011) Mass spectrometry-based proteomics using Q exactive, a high-performance benchtop quadrupole orbitrap mass spectrometer. *Molecular & Cellular Proteomics*, **10**(9).

- Mounet, F., Moing, A., Kowalczyk, M., Rohrmann, J., Petit, J., Garcia, V., Maucourt, M., Yano, K., Deborde, C., Aoki, K., Berges, H., Granell, A., Fernie, A. R., Bellini, C., Rothan, C. and Lemaire-Chamley, M.** (2012) Down-regulation of a single auxin efflux transport protein in tomato induces precocious fruit development. *J. Exp. Bot.*, **63**(13), 4901-4917.
- Murashige, T. and Skoog, F.** (1962) A revised medium for rapid growth and bio assays with tobacco tissue cultures. *Physiol. Plantarum*, **15**(3), 473-497.
- Nakagawa, M., Yokoyama, Y., Kato, S. and Hino, T.** (1985) Dye-sensitized photo-oxygenation of tryptophan. *Tetrahedron*, **41**(11), 2125-2132.
- Nonhebel, H.M. and Bandurski, R. S.** (1984) Oxidation of indole-3-acetic acid and oxindole-3-acetic acid to 2,3-dihydro-7-hydroxy-2-oxo-1H indole-3-acetic acid-7'-O-beta-D-glucopyranoside in *Zea mays* seedlings. *Plant Physiol.*, **76**, 979-983.
- Normanly, J., Cohen, J. D. and Fink, G. R.** (1993) *Arabidopsis thaliana* auxotrophs reveal a tryptophan-independent biosynthetic pathway for indole-3-acetic acid. *Proc. Natl. Acad. Sci. U. S. A.*, **90**(21), 10355-10359.
- Normanly, J., Slovin, J. and Cohen, J.** (2010) Auxin biosynthesis and metabolism. In: *Plant Hormones: Biosynthesis, Signal Transduction, Action!* (3rd edition, revised), (P.J. Davies, ed.) Kluwer Academic Publ., Dordrecht, pp. 36-62
- Novák, O., Hényková, E., Sairanen, I., Kowalczyk, M., Pospíšil, T. and Ljung, K.** (2012) Tissue-specific profiling of the *Arabidopsis thaliana* auxin metabolome. *Plant Journal*, **72**(3), 523-536.
- Nowacki, J. and Bandurski, R. S.** (1980) Myo-inositol esters of indole-3-acetic acid as seed auxin precursors of *Zea mays* L. *Plant Physiol.*, **65**(3), 422-427.
- Oetiker, J.H. and Aeschbacher, G.** (1997) Temperature-sensitive plant cells with shunted indole-3-acetic acid conjugation. *Plant Physiol.*, **114**(4), 1385-1395.
- Östin, A., Catalá, C., Chamarro, J. and Sandberg, G.** (1995) Identification of glucopyranosyl- $\beta$ -1, 4-glucopyranosyl- $\beta$ -1-N-oxindole-3-acetyl-N-aspartic acid, a new IAA catabolite, by liquid chromatography/tandem mass spectrometry. *Journal of Mass Spectrometry*, **30**(7), 1007-1017.
- Östin, A., Ilić, N. and Cohen, J. D.** (1999) An *in vitro* system from maize seedlings for tryptophan-independent indole-3-acetic acid biosynthesis. *Plant Physiol.*, **119**(1), 173-178.
- Östin, A., Kowalczyk, M., Bhalerao, R. P. and Sandberg, G.** (1998) Metabolism of indole-3-acetic acid in *Arabidopsis*. *Plant Physiol.*, **118**(1), 285-296.

- Ouyang, J., Shao, X. and Li, J.** (2000) Indole-3-glycerol phosphate, a branchpoint of indole-3-acetic acid biosynthesis from the tryptophan biosynthetic pathway in *Arabidopsis thaliana*. *Plant Journal*, **24**(3), 327-334.
- Paque, S., Mouille, G., Grandont, L., Alabadi, D., Gaertner, C., Goyallon, A., Muller, P., Primard-Brisset, C., Sormani, R., Blazquez, M. A. and Perrot-Rechenmann, C.** (2014) AUXIN BINDING PROTEIN1 links cell wall remodeling, auxin signaling, and cell expansion in *Arabidopsis*. *Plant Cell*, **26**(1), 280-295.
- Park, S., Cohen, J. D. and Slovin, J. P.** (2006) Strawberry fruit protein with a novel indole-acyl modification. *Planta*, **224**(5), 1015-1022.
- Park, S., Ozga, J. A., Cohen, J. D. and Reinecke, D. M.** (2010) Evidence of 4-Cl-IAA and IAA bound to proteins in pea fruit and seeds. *J. Plant Growth Regul.*, **29**(2), 184-193.
- Pencík, A., Rolcík, J., Novák, O., Magnus, V., Barták, P., Buchtík, R., Salopek-Sondi, B. and Strnad, M.** (2009) Isolation of novel indole-3-acetic acid conjugates by immunoaffinity extraction. *Talanta*, **80**(2), 651-655.
- Percival, F.W. and Bandurski, R. S.** (1976) Esters of indole-3-acetic acid from *Avena* seeds. *Plant Physiol.*, **58**(1), 60-67.
- Phillips, K.A., Skirpan, A. L., Liu, X., Christensen, A., Slewinski, T. L., Hudson, C., Barazesh, S., Cohen, J. D., Malcomber, S. and McSteen, P.** (2011) *Vanishing tassel2* encodes a grass-specific tryptophan aminotransferase required for vegetative and reproductive development in maize. *Plant Cell*, **23**(2), 550-556
- Rampey, R.A., LeClere, S., Kowalczyk, M., Ljung, K., Sandberg, G. and Bartel, B.** (2004) A family of auxin-conjugate hydrolases that contributes to free indole-3-acetic acid levels during *Arabidopsis* germination. *Plant Physiol.*, **135**(2), 978-988.
- Reinecke, D.M. and Bandurski, R. S.** (1981) Metabolic conversion of <sup>14</sup>C-indole-3-acetic acid to <sup>14</sup>C-oxindole-3-acetic acid. *Biochem. Biophys. Res. Commun.*, **103**(2), 429-433.
- Reinecke, D.M. and Bandurski, R. S.** (1988) Oxidation of indole-3-acetic acid to oxindole-3-acetic acid by an enzyme preparation from *Zea mays*. *Plant Physiol.*, **86**, 868-872.
- Rekoslavskaya, N.I.** (1986) Possible role of N-malonyl-D-tryptophan as an auxin precursor. *Biol. Plant.*, **28**(1), 62-67.
- Rekoslavskaya, N. and Gamburg, K. Z.** (1983) Do tomato plants contain endogenous indoleacetylsartpic acid? *Biol. Plant.*, **25**(3), 166-172.

- Rittenberg, D. and Foster, G. L.** (1940) A new procedure for quantitative analysis by isotope dilution, with application to the determination of amino acids and fatty acids. *J. Biol. Chem.*, **133**, 737-744.
- Ronsein, G.E., de Oliveira, Mauricio Cesar Bof, de Medeiros, Marisa Helena Gennari and Di Mascio, P.** (2009) Characterization of O<sub>2</sub> (1Δg)-derived oxidation products of tryptophan: A combination of tandem mass spectrometry analyses and isotopic labeling studies. *J. Am. Soc. Mass Spectrom.*, **20**(2), 188-197.
- Row, V.V., Sanford, W. M. and Hitchcock, A. E.** (1961) Indole-3-acetyl-D,L-aspartic acid as a naturally-occurring indole compound in tomato seedlings. *Contrib. Boyce Thompson Inst.*, **61**, 1-10.
- Sakagami, Y., HONG, T., Manabe, K., Higashi, M. and Marumo, S.** (1995) Reassignment of the absolute stereochemistry of N-malonyl-tryptophan in higher plants. *Biosci. Biotechnol. Biochem.*, **59**(7), 1362-1363.
- Sakagami, Y., Manabe, K., Aitani, T., Thiruvikraman, S. and Marumo, S.** (1993) 1-4-chlorotryptophan from immatum of *Pisum sativum* and reassignment of the absolute stereochemistry of N-malonyl-4-chlorotryptophan. *Tetrahedron Lett.*, **34**(6), 1057-1060.
- Sakai, A., Xiang, D. F., Xu, C., Song, L., Yew, W. S., Raushel, F. M. and Gerlt, J. A.** (2006) Evolution of enzymatic activities in the enolase superfamily: N-succinylamino acid racemase and a new pathway for the irreversible conversion of D-to L-amino acids. *Biochemistry (N. Y.)*, **45**(14), 4455-4462.
- Schenck, D., Christian, M., Jones, A. and Luthen, H.** (2010) Rapid auxin-induced cell expansion and gene expression: A four-decade-old question revisited. *Plant Physiol.*, **152**(3), 1183-1185.
- Schocken, V.** (1949) The genesis of auxin during the decomposition of proteins. *Arch. Biochem.*, **23**(2), 198-204.
- Seidel, C., Walz, A., Park, S., Cohen, J. and Ludwig-Müller, J.** (2006) Indole-3-acetic acid protein conjugates: Novel players in auxin homeostasis. *Plant Biol (Stuttg)*, **8**, 340-345.
- Serrano, P., Casas, J., Llebaria, A., Zucco, M., Emeric, G. and Delgado, A.** (2007) Parallel synthesis and yeast growth inhibition screening of succinamic acid libraries. *J. Comb. Chem.*, **9**(4), 635-643.
- Slominski, B.A. and Campbell, L. D.** (1989) Indoleacetonitriles—Thermal degradation products of indole glucosinolates in commercial rapeseed (*Brassica napus*) meal. *J. Sci. Food Agric.*, **47**(1), 75-84.

- Slovin, J.P., Bandurski, R. S. and Cohen, J. D.** (1999) Auxin. In *Biochemistry and Molecular Biology of Plant Hormones* (P.J.J. Hooykaas, M.A. Hall and K.R. Libbenga, eds) Amsterdam: Elsevier. pp. 115–140.
- Smith, C.A., Want, E. J., O'Maille, G., Abagyan, R. and Siuzdak, G.** (2006) XCMS: Processing mass spectrometry data for metabolite profiling using nonlinear peak alignment, matching, and identification. *Anal. Chem.*, **78**(3), 779-787.
- Staswick, P.E.** (2009) The tryptophan conjugates of jasmonic and indole-3-acetic acids are endogenous auxin inhibitors. *Plant Physiol.*, **150**(3), 1310-1321.
- Sumida, Y., Iwai, S., Nishiya, Y. And Kumagai, S.** (2012) Modified D-succinylase having improved D-form selectivity for N-succinyl-DL-amino acid. *JP Patent* 055409.
- Sztein, A.E., Cohen, J. D. and Cooke, T. J.** (2000) Evolutionary patterns in the auxin metabolism of green plants. *Int. J. Plant Sci.*, **161**(6), 849-859.
- Tam, Y.Y., Epstein, E. and Normanly, J.** (2000) Characterization of auxin conjugates in Arabidopsis. low steady-state levels of indole-3-acetyl-aspartate, indole-3-acetyl-glutamate, and indole-3-acetyl-glucose. *Plant Physiol.*, **123**(2), 589-595.
- Tam, Y.Y., Slovin, J. P. and Cohen, J. D.** (1995) Selection and characterization of [alpha]-methyltryptophan-resistant lines of *Lemna gibba* showing a rapid rate of indole-3-acetic acid turnover. *Plant Physiol.*, **107**(1), 77-85.
- Tateishi, K. and Yamashita, S.** (1998) Isolation of four new indole-3-acetic acid (IAA) oxidative metabolites, a pair of diastereomers 5-O-beta-D-glucopyranosyl 3,5-dihydroxy-2-indolinone-3-acetic acid and 5-O-beta-D-cellobiosyl 3,5-dihydroxy-2-indolinone-3-acetic acid from rice bran. *Biosci. Biotechnol. Biochem.*, **62**(10), 1870-1874.
- Tatsis, E.C., Eylert, E., Maddula, R. K., Ostrozhenkova, E., Svatos, A., Eisenreich, W. and Schneider, B.** (2014) Biosynthesis of nudicaulins: A (13)CO<sub>2</sub>-Pulse/Chase labeling study with *Papaver nudicaule*. *Chembiochem : A European Journal of Chemical Biology*, **15**(11), 1645-1650.
- Thimann, K.V.** (1935) On the plant growth hormone produced by *Rhizopus suinus*. *J. Biol. Chem.*, **109**(1), 279-291.
- Tivendale, N.D., Ross, J. J. and Cohen, J. D.** (2014) The shifting paradigms of auxin biosynthesis. *Trends Plant Sci.*, **19**(1), 44-51.
- Tsurumi, S. and Wada, S.** (1986) Dioxindole-3-acetic acid conjugates formation from indole-3-acetylaspatic acid in *Vicia* seedlings. *Plant and Cell Physiology*, **27**(8), 1513-1522.

- Ueda, M. and Bandurski, R. S.** (1969) A quantitative estimation of alkali-labile indole-3-acetic acid compounds in dormant and germinating maize kernels. *Plant Physiol.*, **44**(8), 1175-1181.
- U.S. Department of Agriculture, Agricultural Research Service.** (2013) USDA National Nutrient Database for Standard Reference, Release 26. Nutrient Data Laboratory Home Page, <http://www.ars.usda.gov/ba/bhnrc/ndl>
- Villalobos, Luz Irina A Calderón, Lee, S., De Oliveira, C., Ivetac, A., Brandt, W., Armitage, L., Sheard, L. B., Tan, X., Parry, G. and Mao, H.** (2012) A combinatorial TIR1/AFB–Aux/IAA co-receptor system for differential sensing of auxin. *Nature Chemical Biology*, **8**(5), 477-485.
- Vlitos, A.J. and Meudt, W.** (1953) The role of auxin in plant flowering. I. A quantitative method based on paper chromatography for the determination of indole compounds & IAA in plant tissue. *Contrib. Boyce Thompson Inst.*, **17**, 197-202.
- Walz, A., Seidel, C., Rusak, G., Park, S., Cohen, J. D. and Ludwig-Müller, J.** (2008) Heterologous expression of IAP1, a seed protein from bean modified by indole-3-acetic acid, in *Arabidopsis thaliana* and *Medicago truncatula*. *Planta*, **227**(5), 1047-1061.
- Walz, A., Park, S., Slovin, J. P., Ludwig-Müller, J., Momonoki, Y. S. and Cohen, J. D.** (2002) A gene encoding a protein modified by the phytohormone indoleacetic acid. *Proc. Natl. Acad. Sci. U. S. A.*, **99**(3), 1718-1723.
- Wenefrida, I., Utomo, H. S. and Linscombe, S. D.** (2013) Mutational breeding and genetic engineering in the development of high grain protein content. *J. Agric. Food Chem.*, **61**(48), 11702-11710.
- Werner, R.A. and Schmidt, H.** (2002) The *in vivo* nitrogen isotope discrimination among organicplant compounds. *Phytochemistry*, **61**(5), 465-484.
- Wille, J.J. and Berhow, M. A.** (2011) Bioactives derived from ripe corn tassels: A possible new natural skin whitener, 4-hydroxy-1-oxindole-3-acetic acid. *Current Bioactive Compounds*, **7**(2), 126-134.
- Won, C., Shen, X., Mashiguchi, K., Zheng, Z., Dai, X., Cheng, Y., Kasahara, H., Kamiya, Y., Chory, J. and Zhao, Y.** (2011) Conversion of tryptophan to indole-3-acetic acid by TRYPTOPHAN AMINOTRANSFERASES OF ARABIDOPSIS and YUCCAs in *Arabidopsis*. *Proceedings of the National Academy of Sciences*, .
- Woodward, A.W. and Bartel, B.** (2005) Auxin: Regulation, action, and interaction. *Annals of Botany*, **95**(5), 707-735.

- Wright, A.D., Sampson, M. B., Neuffer, M. G., Michalczuk, L., Slovin, J. P. and Cohen, J. D.** (1991) Indole-3-acetic acid biosynthesis in the mutant maize Orange Pericarp, a tryptophan auxotroph. *Science*, **254**(5034), 998.
- Wu, T., Liang, Y., Zhu, X., Zhao, M. and Liu, H.** (2014) Separation and quantification of four isomers of indole-3-acetyl-myoinositol in plant tissues using high-performance liquid chromatography coupled with quadrupole time-of-flight tandem mass spectrometry. *Analytical and Bioanalytical Chemistry*, **406**(13), 3239-3247.
- Yu, P., Hegeman, A. D. and Cohen, J. D.** (2014) A facile means for the identification of indolic compounds from plant tissues. *Plant Journal*, doi: 10.1111/tpj.12607
- Yuan, J., Bennett, B. D. and Rabinowitz, J. D.** (2008) Kinetic flux profiling for quantitation of cellular metabolic fluxes. *Nature Protocols*, **3**(8), 1328-1340.
- Zhang, R., Wang, B., Ouyang, J., Li, J. and Wang, Y.** (2008) *Arabidopsis* indole synthase, a homolog of tryptophan synthase alpha, is an enzyme involved in the Trp-independent indole-containing metabolite biosynthesis. *Journal of Integrative Plant Biology*, **50**(9), 1070-1077.
- Zhao, Z., Zhang, Y., Liu, X., Zhang, X., Liu, S., Yu, X., Ren, Y., Zheng, X., Zhou, K. and Jiang, L.** (2013) A role for a dioxygenase in auxin metabolism and reproductive development in rice. *Developmental Cell*, **27**(1), 113-122.

## **Appendix**

The plant hormone auxin is involved in many aspects of plant growth and development. I have collaborated with many colleagues including Drs. Bill Gray, Elliot Meyerowitz, and Bethany Zolman's groups to investigate specific roles auxin plays in different physiological environments. Some of the work have been published and attached as appendix. Representative figures are presented here. They all contributed a better understanding of the action of auxin.

**A.**  
**PHYTOCHROME-INTERACTING FACTOR 4 (PIF4) regulates auxin biosynthesis at high temperature**

Keara A. Franklin, Sang Ho Lee, Dhaval Patel, S. Vinod Kumar, Angela K. Spartz, Chen Gu, Songqing Ye, Peng Yu, Gordon Breen, Jerry D. Cohen, Philip A. Wigge, and William M. Gray

Published in Proceedings of the National Academy of Sciences of the United States of America. Dec 13, 2011; **108**(50): 20231–20235

**Abstract**

At high ambient temperature, plants display dramatic stem elongation in an adaptive response to heat. This response is mediated by elevated levels of the phytohormone auxin and requires auxin biosynthesis, signaling, and transport pathways. The mechanisms by which higher temperature results in greater auxin accumulation are unknown, however. A basic helix-loop-helix transcription factor, PHYTOCHROME-INTERACTING FACTOR 4 (PIF4), is also required for hypocotyl elongation in response to high temperature. PIF4 also acts redundantly with its homolog, PIF5, to regulate diurnal growth rhythms and elongation responses to the threat of vegetative shade. PIF4 activity is reportedly limited in part by binding to both the basic helix-loop-helix protein LONG HYPOCOTYL IN FAR RED 1 and the DELLA family of growth-repressing proteins. Despite the importance of PIF4 in integrating multiple environmental signals, the mechanisms by which PIF4 controls growth are unknown. Here we demonstrate that PIF4 regulates levels of auxin and the expression of key auxin biosynthesis genes at high temperature. We also identify a family of SMALL AUXIN UP RNA (SAUR) genes that are expressed at high temperature in a PIF4-dependent manner and promote elongation growth. Taken together, our results demonstrate direct molecular links among PIF4, auxin, and elongation growth at high temperature.

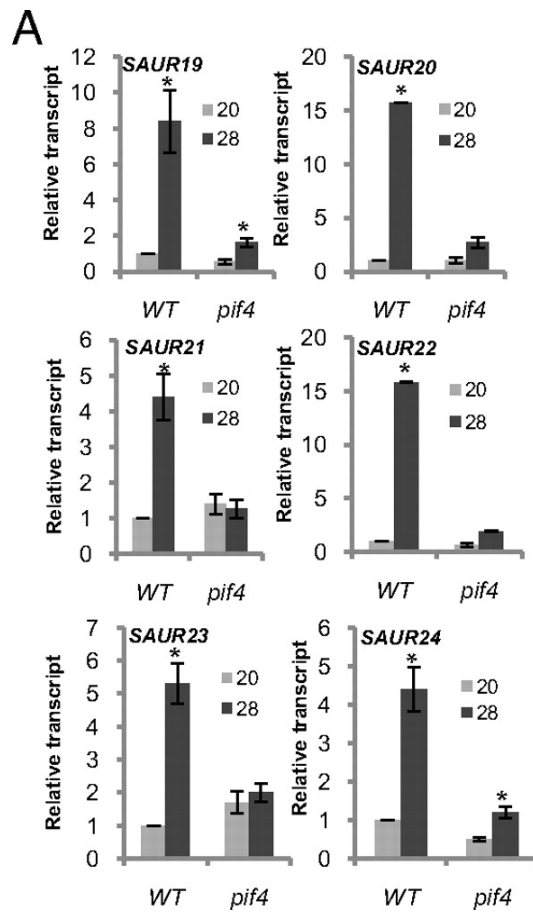


**Figure A- 1 PIF4 regulates expression of the SAUR19–24 subfamily at high temperature.** (A) Relative transcript abundance of SAUR genes 19–24 in 6-d-old Col-0 and *pif4*-101 seedlings grown continuously at 20 °C (20) or grown at 20 °C and shifted to 28 °C for 6 h (28). Data represent the means of three biological repeats. SE values are shown.  $P < 0.05$ .

**B.**

**LEAFY Controls Auxin Response Pathways in Floral Primordium Formation**

Wuxing Li, Yun Zhou, Xing Liu, Peng Yu, Jerry D. Cohen, and Elliot M. Meyerowitz

Published in Science Signaling, 9 April 2013, Vol. 6, Issue 270, p. ra23

**Abstract**

The transcription factor LEAFY is a master regulator of flowering and of flower development. It acts as a component of a switch that mediates the transition from the vegetative to the reproductive phase of plant development. Auxin is a plant hormone with many different roles in plant growth, including the induction of new primordia of both leaves and flowers at the shoot apex. We report that LEAFY acts in part by controlling the auxin response pathway in new primordia. Therefore, regulation of flower development by transcriptional master regulators and hormonal control of morphogenesis appear to be interacting processes. We found that hormone perception not only controls but is also controlled by the transcriptional signals that create plant form.

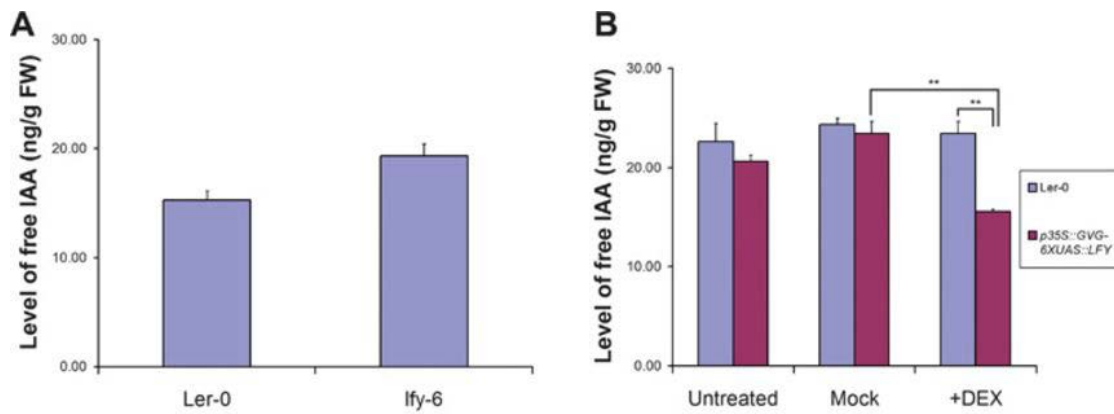


**Figure A- 2 Free IAA amount and expression of auxin biosynthesis genes.** (A) Free IAA quantified from 3 to 8 mg (fresh weight) of inflorescence apices from Ler-0 and lfy-6 plants (n = 5 for each genotype). (B) Free IAA quantified from 8 to 15 mg (fresh weight) of inflorescence apices from Ler-0 and p35S::GVG-6XUAS::LFY transgenic plants in the absence of stimulation, in the presence of DMSO (mock), or 24 hours after the addition of dexamethasone (DEX) (n = 5 for each genotype and condition; P = 0.0079, Wilcoxon test). Data in (A) and (B) are expressed as averages and SEs.

## C

### **Auxin-input pathway disruptions are mitigated by changes in auxin biosynthetic gene expression in *Arabidopsis thaliana***

Gretchen M. Spiess, Amanda Hausman, Peng Yu, Jerry D. Cohen, Rebekah A. Rampey, and Bethany K. Zolman

Published in Plant Physiology, July 2014 vol. **165** no. 3 1092-1104

#### Abstract

Auxin is a phytohormone involved in cell elongation and division. Levels of indole-3-acetic acid (IAA), the primary auxin, are tightly regulated through biosynthesis, degradation, sequestration, and transport. IAA is sequestered in reversible processes by adding amino acids, polyol or simple alcohols, or sugars, forming IAA conjugates, or via a two-carbon elongation forming indole-3-butyric acid (IBA). These sequestered forms of IAA reduce hormone activity. To gain a better understanding of how auxin homeostasis is maintained, we have generated *Arabidopsis thaliana* mutants that combine disruptions in the pathways converting IAA conjugates and IBA to free IAA. These mutants show phenotypes indicative of low auxin levels, including delayed germination, abnormal vein patterning, and decreased apical dominance. Root phenotypes include changes in root length, root branching, and root hair growth. IAA levels are significantly reduced in the cotyledon tissue but not in meristems or hypocotyls. In the combination mutants, auxin biosynthetic gene expression is increased, particularly in the YUCCA/ TAA pathway, providing a feedback mechanism that allows the plant to compensate for changes in IAA-input pathways and maintain cellular homeostasis.

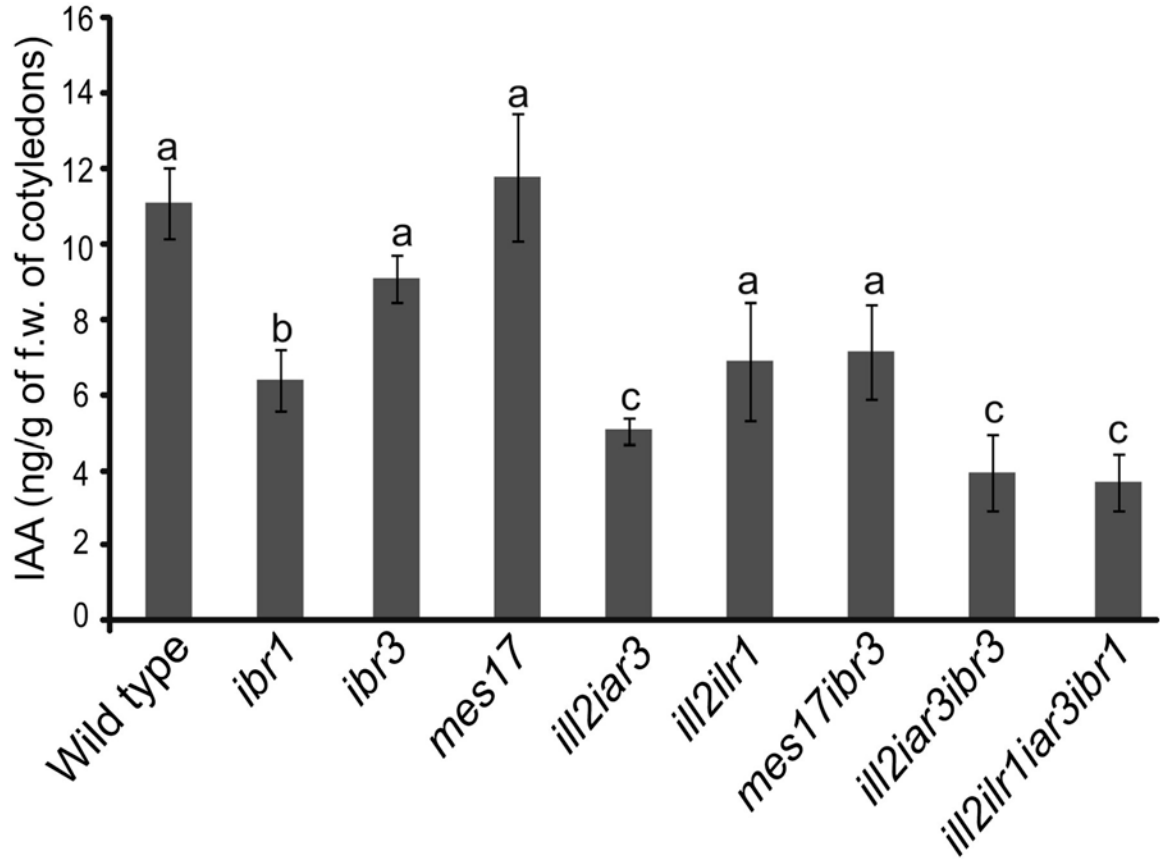


**Figure A- 3 Auxin levels in wide type Arabidopsis and mutants.** Reduced levels of free IAA are seen in combination mutants defective in IBA metabolism and IAA-conjugate hydrolysis; 5-d-old cotyledon tissue was collected, and free IAA levels were measured using gas chromatography-mass spectrometry.  $n \geq 6$ ; error bars represent se. a to c, Significant differences using one-way ANOVA ( $P < 0.05$ ).